MESMAC International Conferences
MES Mampad College (Autonomous)

www.mesmac.in

Collection of selected papers presented in MESMAC International Conference 3

BIO-EPISTEME: AN ANTHOLOGY OF RESEARCH PAPERS IN SCIENCE

People FIRST?

MAN | MACHINE | MILIEU

15 16 17 January 2019

MESMAC INTERNATIONAL CONFERENCES
www.mesmac.in

PEOPLE FIRST?
MAN • MACHINE • MILIEU
2019 January 15 | 16 | 17

MESMAC INTERNATIONAL CONFERENCES

BIO EPISTEME:
AN ANTHOLOGY OF RESEARCH PAPRERS IN SCIENCE

Chief Editor

Dr. P.K. Babu

Associate Editors

Dr. Megha U

Dr.Sajid A Latheef

Publication Division:

Dr. Ghafoor Memorial (ESTED 1965)
M.E.S. MAMPAD COLLEGE
(AUTONOMOUS) Accredited by NAAC with A grade

Mampad College P.O. 676542, Malappuram Dt., Kerala
E-mail: info@mesmampad.org

Bio Episteme:
An Anthology of Research Papers in Science

Editors

Chief Editor
Dr. P.K. Babu

Associate Editors
Dr. Megha U
Dept. of Physics, M.E.S Mampad college

Dr. Sajid A. Latheef
Dept. of English, M.E.S Mampad college

First Edition: January 2019

DGM MES Mampad College
Mampad 676 542

Lay out:
Rajesh monji

ISBN 978-93-5321-814-0

CONTENTS

RECENT ADVANCES IN THEORETICAL AND EXPERIMENTAL PHYSICS

1.

Carbon as photocatalytic promoter in zinc oxide nanotubes

Bhabhina Ninnora Meethal, Sindhu Swaminathan*[1]
Department of Nanoscience and Technology, University of Calicut, Kerala-673635, India
*E-mail: sindhus@uoc.ac.in

Abstract: *Zinc oxide has received much attention for its excellent photocatalytic characteristics. Surface modification of ZnO considerably enhances its photocatalytic activity. Our present study emphasises on the surface modification of oxygen deficient ZnO by incorporating carbon through polymer assistance. Here, a facile sol-gel aqueous mediated synthesis protocol is employed for the preparation of polyaniline-ZnO hybrid nanocomposite. The emeraldine salt of polyaniline (ES) was taken as the polymer matrix but in the composite, polyaniline exists as emeraldine base form. This on calcination, leads to the formation of a grey coloured, carbon doped ZnO, photocatalyst with remarkably efficient and promising characteristics. X-ray photoelectron spectroscopy confirms the presence of carbon and absence of nitrogen in the ZnO nanotubes. The photocatalytic and hydrophilic activities are monitored by dye degradation analysis and contact angle measurements. Carbon embedded ZnO nanotubes are found to be more efficient and super hydrophilic compared to pure ZnO.*

Key words: ZnO, Photocatalyst, Carbon, Super hydrophilic.

1. Introduction

Last few decades witnessed phenomenal increase in water purification and surface cleaning methods employing photocatalysts [1, 2]. Metal oxides such as zinc oxides, with their surface adsorbing property, can remove the soluble pollutants from water utilizing solar energy [3]. Photo-oxidation and photoinduced hydrophilicity are the notable processes occurring on the surface of zinc oxides during photocatalysis. The properties of pure zinc oxide systems can be enhanced by incorporating some foreign ingredients such as metals, nonmetals, polymers etc [4, 5]. The nature and properties of the chosen foreign atoms are decisive in improving the photocatalytic performance of pristine systems. The presence of foreign impurities introduces mid gap energy levels which in turn inhibit the easy recombination of photogenerated electron-hole pairs to some extent [6]. Among various synthesis methods of nanocomposites, polymer associated ZnO nanocomposite formation is easy as the synergetic and complementary performance between polymers and metal oxides makes a significant improvement in the properties of these hybrids.

Hydrophilicity of the material considerably influences the surface chemical compositions and on achieving super hydrophilicity, that material can be effectively used for self-cleaning surfaces [7]. So far, a plethora of methods have been experimented with so as to improve the photocatalytic behavior of pure zinc oxide. The effective methods to implant surface defects are either forming surface oxygen vacancies in pristine system or forming hybrids by adding some foreign impurities [8]. Here our synthesized material encompasses both these properties and exhibit enhanced photocatalytic activity compared to pristine system.

In the present work, hybrid nanocomposite of polyaniline-ZnO was synthesized from one-pot sol-precipitation method. Carbon mid-gap energy levels are incorporated into ZnO matrix by calcination process. The prepared material possesses sufficient surface oxygen

vacancies and mid gap energy levels to trap photoexcited electrons which in turn ensures better photocatalytic activity.

2. Experimental

2.1. Chemicals and Instruments used for the study

The chemicals used for synthesis are Zinc acetate dihydrate $(CH_3COO)_2$ Zn. $2H_2O$, Ethane-1, 2-diamine ($C_2H_4(NH_2)$), methanol (CH_3OH) and dimethylsulfoxide (DMSO) and Polyaniline emeraldine salt (Average mol.wt > 15,000 and particle size 3-100μm). These chemicals were purchased from Merck chemicals and Sigma Aldrich. Double distilled water filtered from Heal force super easy series purification system was used throughout for synthesis and washing process.

X-ray diffraction (XRD) of all synthesized nanomaterials was obtained by Rigaku Miniplex X-ray Diffractometer (Cu Kα, λ= 0.15496 nm). Absorbance of the hybrid samples were investigated with Avantes spectrophotometer (Avaspec-2048) in the form of powder. Surface morphology of the air dried materials was predicted by observing images of Scanning Electron Microscope Zeis Gemini SEM 300. The mapping of constituent elements (Zn, O and C) is obtained from EDS analysis. The emission behaviours of all the prepared samples were recorded from Perkin Elmer LS 45/55 luminescence spectrometer. The FTIR spectra were studied in the form of KBr pellets using Perkin Elmer FTIR Spectrum II spectrophotometer. The X-ray photoelectron spectroscopy (XPS) spectra of the samples were analysed from Axis supra instrument with Monochromatic (AlKα) 600 W X-ray source. Binding energies of carbon were corrected at 284.7 eV. Raman spectra were recorded with JASCO instrument with 532 nm laser wavelength.

2.2 Synthesis

For synthesis, initially a hybrid nanocomposite, PNZ was synthesized by taking ZnO and polyaniline. A precursor solution of zinc acetate in double distilled water (0.015M) was made with heating and stirring. When the temperature reached 60 °C, equimolar concentration of Ethane-1, 2-diamine was injected into the solution using micropipette. After an hour, 0.1 wt% polyaniline emeraldine salts (Average mol.wt > 15,000 and particle size 3-100μm) in dimethyl sulfoxide was added to the reaction mixture, followed by six hours of continuous heating at 60 °C and stirring at 900 rpm, gives a dark blue hybrid precipitate named PNZ. The precipitate was collected after centrifuged at 12000 rpm. The composite PNZ, after heat treatment at 400 °C for one hour resulted in the formation of carbon incorporated ZnO nanotubes (CPNZ) and this grey coloured precipitate was kept for further analyzes.

2.3 Photocatalysis

To examine the activity of CPNZ photocatalyst, 0.002 wt% aqueous methylene blue dye solution was taken as the model system and the degradation of the dye was monitored periodically. 50 mg photocatalyst was added in to 50 ml of dye solution. This suspension was kept under dark for 30 minutes with stirring to avoid any error due to initial adsorption effect. The stirring in darkness also helps dye adsorption on the surface of the photocatalyst to establish adsorption-desorption equilibrium. After dark analysis, the dye solution was placed inside a photocatalytic reactor under 300W Xenon lamp. At 15 minutes of periodic exposure, 5ml aliquots were taken to monitor the dye degradation. The Uv-visible absorption spectra were recorded after centrifuging at 10000 rpm for 10 minutes to avoid any scattering effect.

The recyclability and stability performances of CPNZ were also studied for five consecutive steps by recurrent use of the photocatalyst at each time.

2.4 Estimation of hydroxyl radicals

The reactive oxygen species generated from the photocatalysts were experimentally confirmed and quantified with respect to its photocatalytic properties. Hydroxyl radicals generated from CPVZ is measured and compared with that of pure ZnO. Terephthalic acid (TTA) probe molecules were used to estimate the OH° released from the photocatalysts experimentally by a fluorimeter. For the analysis, $5x10^{-4}$ M TTA solution was prepared with NaOH solution for the complete dissolution of TTA. Then, 5 mg of photocatalysts were dispersed in 50 ml of the prepared solution and placed under light irradiation with continuous stirring for 10 minutes. After light exposure, the solution was centrifuged and the photoluminescence spectra were taken to measure the intensity of the fluorescence.

3. Results and discussions

The schematic of the synthesis procedure is represented below in Figure 1. Polyaniline is completely soluble in DMSO through the formation of hydrogen bonding [9]. This polyaniline-DMSO solution when added to zinc acetate- Ethane-1, 2-diamine mixture, the alkaline mixture deprotonates ES to emeraldine base. With the assistance of mild temperature, polyaniline in its emeraldine base structure interact with ZnO and lead the formation of hybrid nanocomposite PNZ. The composite PNZ, after heat treatment at 400 °C for one hour resulted in the formation of grey coloured, carbon incorporated ZnO and the sample is coded as CPNZ.

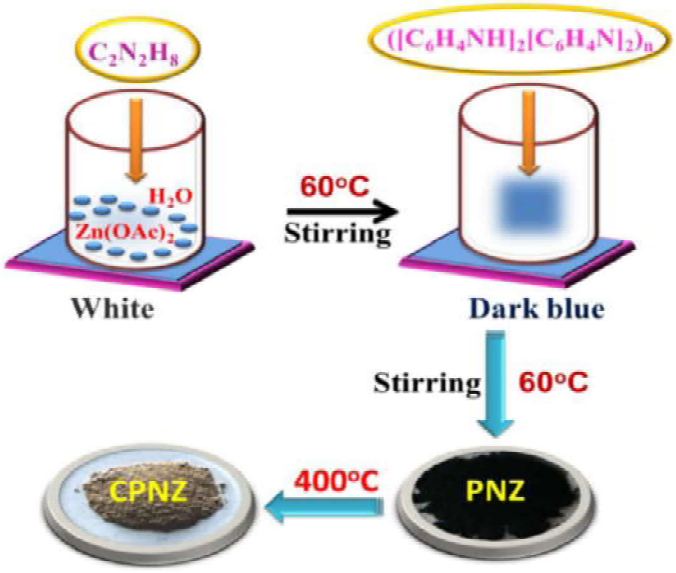

Figure 1 Schematic showing the synthesis procedure of CPNZ

The FESEM images reveal the morphological idea as observed from Figure 2. ES resembles extended fibers. CPNZ are found to have destructive tubular structure similar to pure ZnO with high rate of etching on surface. On temperature treatment, the surface of CPNZ becomes rough because the organic polymer (polyaniline) is detached from its surface. Figure 3 is the elemental mapping obtained from EDS spectrum of CPNZ, which contain Zinc, Oxygen and Carbon only.

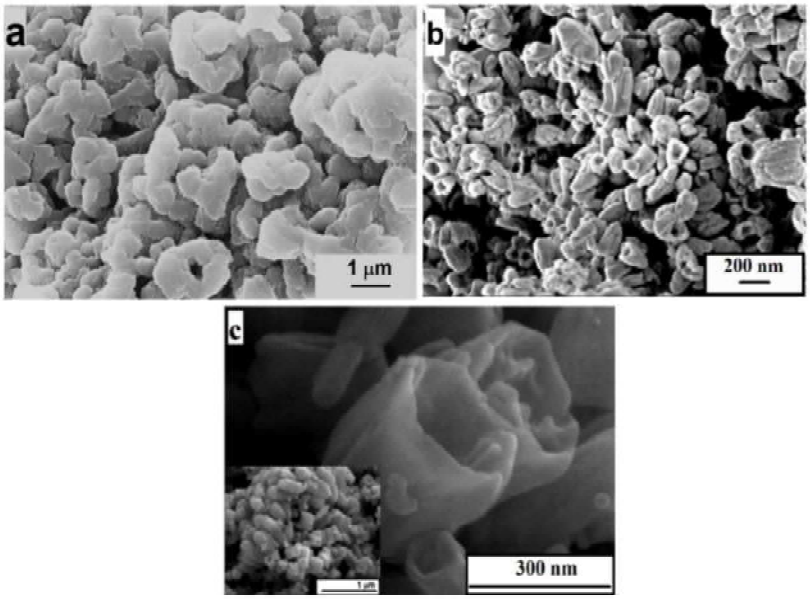

Figure 2. FESEM images of (a) ES, (b) CPNZ and (c) pure ZnO

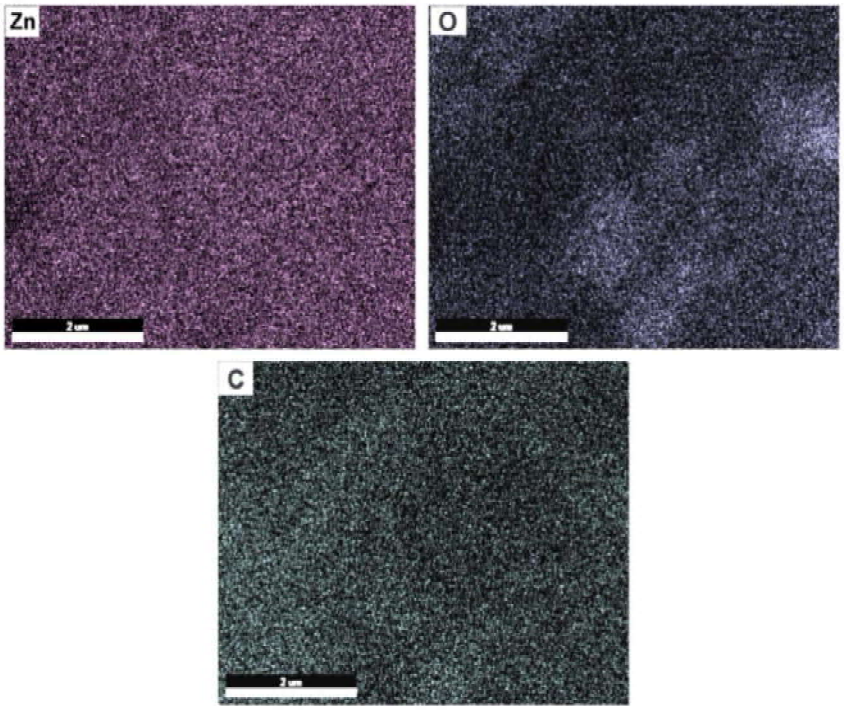

Figure 3. Mapping of Zinc, Oxygen and Carbon elements of CPNZ

The crystallinity and phase purity of the nanocomposites were analyzed from XRD pattern (Figure 4). Commercially available green colored emeraldine salt of polyaniline (ES) is in fully amorphous form whereas CPNZ is crystalline and similar to pure ZnO (JCPDS - 89-0510), indicating that the crystal structure of ZnO is well maintained its wurtzite structure even after the treatment of polyaniline [10]. A gradual shift in the peaks towards lower two theta value with decrease in peak intensity is observed for CPNZ with respect to pure ZnO as seen in Figure 4. The incorporation of carbon decreased the intensity of the CPNZ than pure ZnO.

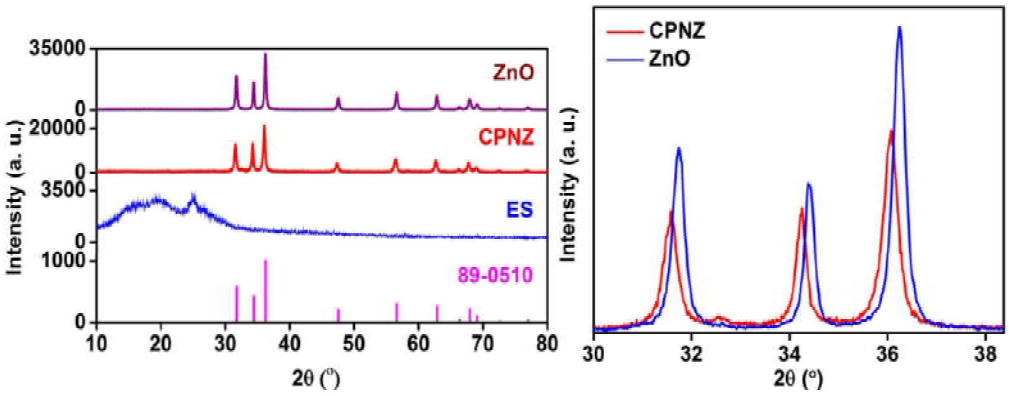

Figure. 4 (a) XRD pattern of ES, CPNZ and pure ZnO compared with standard JCPDS (b) Enlarged image of XRD peaks

FTIR spectra (Figure 5) provide ample evidence about the formation of hybrids compared to their polymer matrix. Intermolecular (3450 cm^{-1} / 3406 cm^{-1}) and intramolecular (2933 cm^{-1}) hydrogen bondings are present in ES, PNZ and CPNZ [11]. The formed PNZ attains an emeraldine base structrure in the presence of alkali during synthesis [12]. The structure of emeraldine salts depicts only benzenoid rings whereas that of emeraldine base features both benzenoid and quinoid rings. C=C stretching band in both quinoid (1585 cm^{-1}) [13] and benzenoid (1486 cm^{-1}) [14] are present in PNZ. Zn-O stretching (500 cm^{-1}) is also seen in PNZ [15]. As vibrational frequency increases in accordance with the bond order, C-N stretching frequency in quinoid (1303 cm^{-1}) [16] is found to be higher in PNZ and that attributes the formation of EB. The peaks at 1120 cm^{-1} and 820 cm^{-1} in PNZ attributes aromatic C-H group in plane and the out of plane deformation for the 1,4-disubsituted benzene. These two peaks are more intense in PNZ than ES due to the change of chemical environment [17]. These observations indicate that the ZnO crystals are associated with the polyaniline by strong coulombic interaction with positively charged backbone [18]. Besides, a hydrogen bonding between imine group of polyaniline and surface hydroxyl grops of ZnO nanomaterials is observed [19]. In CPNZ, a small peak at 2348 cm^{-1} indicate O=C=O asymmetric stretching [20] and peak at 1639 cm^{-1} indicate C=O stretching mode [21]. Peak at 1120 cm^{-1} is also an evidence for the presence of carbon in CPNZ [22]. The peak at 500 cm^{-1} indicates ZnO.

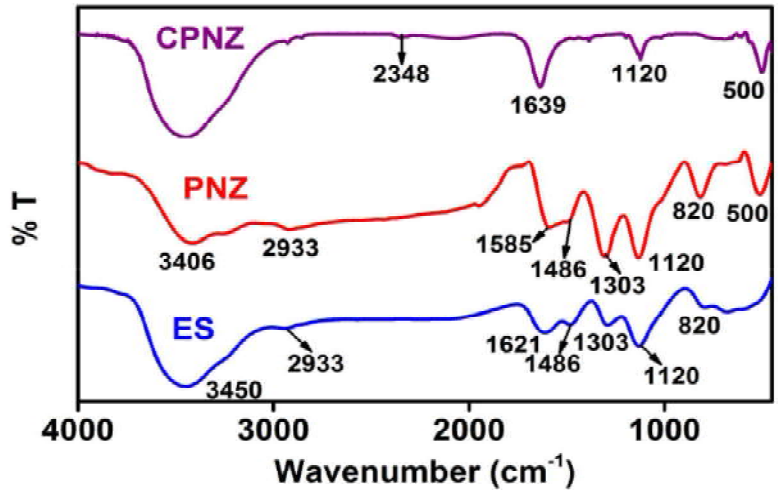

Figure. 5. FTIR spectra of ES, PNZ and CPNZ

A detailed study on the surface composition of CPNZ was predicted from binding energies derived from X-ray photoelectron spectroscopy, the spectra corresponding to Zn 2p, O 1s, C 1s and N 1s are shown in Figure 6. Valence and conduction band alignment are also determined using this spectroscopic technique. Oxygen 1s peak appears as doublet due to the presence of surface oxygen defects [23]. Gaussian fitted peak at 532.6 eV indicate presence of C-OH groups corresponds to oxygen vacancies or defects [24]. Peaks at 530.8 eV and 530.6 eV are attributed to Zn-O binding and lattice oxygen respectively [25, 26]. In the case of Zn 2p, the result shows two main peaks centered at 1022.3 eV and 1045.4 eV corresponds to Zn $2p_{3/2}$ and Zn $2p_{1/2}$ in the ZnO phase respectively. Spin separation of 23.1 eV is same as the previously reported value in the literature [27].

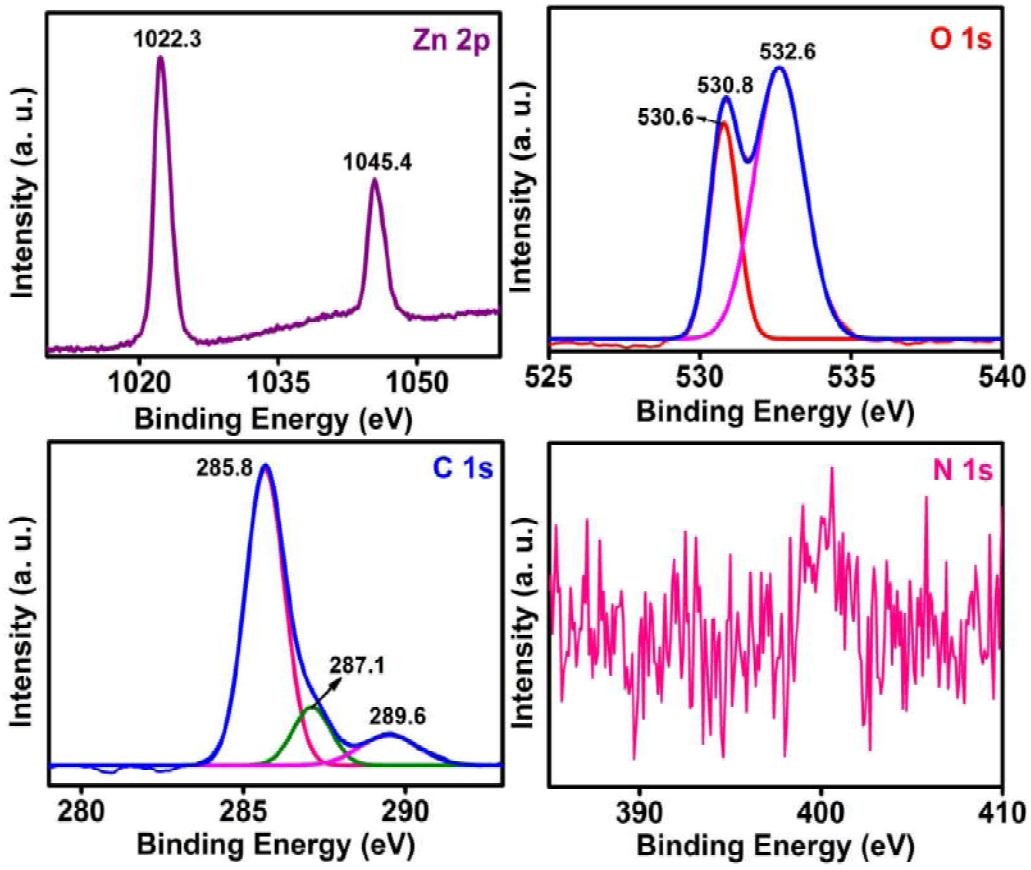

Figure 6. XPS spectra of Zn 2p, O 1s, C 1s and N 1s in CPNZ

Carbon 1s peaks are located at 285.8 eV, 289.6 eV and 287.1 eV and these peaks are corresponds to Zn-O-C, C-O and O-C-O bonds [28]. The absence of nitrogen in the sample also confirmed from the spectral information. Deconvoluted O1s spectrum of pure ZnO is shown in Figure 7 and the peaks obtained from CPNZ are different from that of pure ZnO attributes the presence of carbon atoms in the ZnO lattice. Pure ZnO gives three peaks at 529.3 eV, 531.4 eV and 530.4 eV. Peaks at 529.3 eV and 531.4 eV indicate oxygen deficient regions [29] whereas the peak at 530.4 indicates oxygen in the wurtzite ZnO crystal [30].

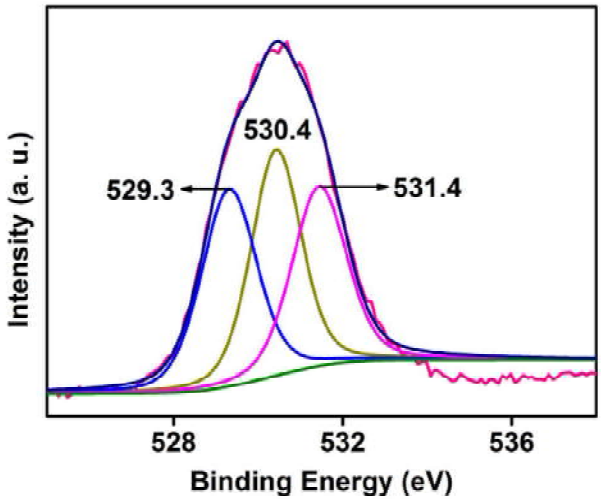

Figure 7. XPS spectra of O 1s of pure ZnO

The absorption spectra of ES, PNZ and CPNZ are depicted in Figure 8. Both ES and PNZ shows a peak at 330 nm attributed to the pi-pi* transition of benzenoid ring [31] and in ES this band appeared broad between 280 to 460 nm as it contain only benzenoid rings. In PNZ, the broad peak at 280-400 nm gives the indication of the incorporation of ZnO. The absorption spectra of ES show high intensity absorption at 635 nm, due to the delocalization of polarons [31]. Polarons are conduction electrons present in polar organic semiconductors. Presence of polarons helps for the conduction of ES. But in PNZ this absorption peak is fully diminished indicating the conversion of ES to EB. During the formation of EB, ES combine with ZnO-1, 2-diaminoethane resulted in the destruction of amine associated polarons. The near IR peak at 1082 nm present in ES and PNZ attribute to the existence of polarons in amine and imine nitrogens respectively [32]. In CPNZ the band edge slightly shifted towards visible region. According to Sandesh *et al*, the red shift observed in absorbance is the indication of oxygen vacancies present in the sample [33].

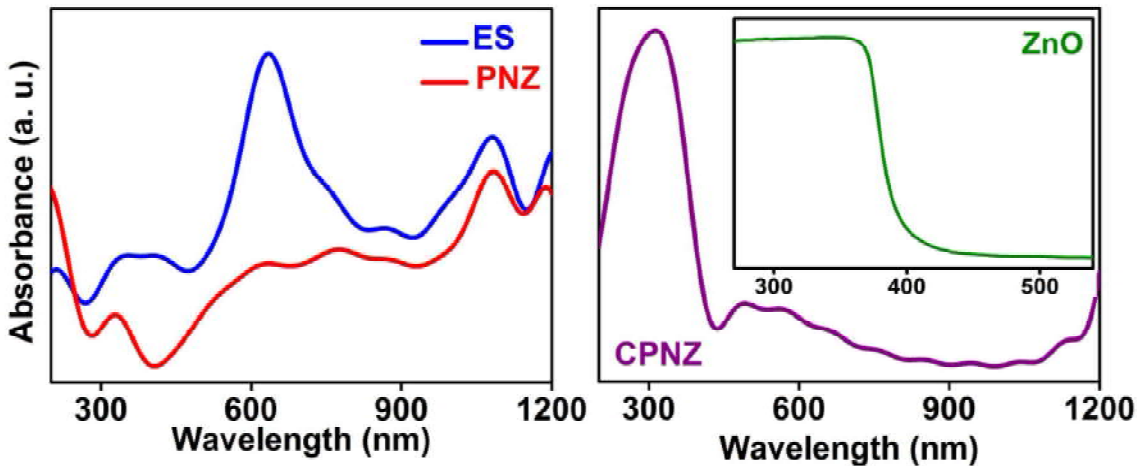

Figure 8. Absorption spectra of (a) ES and PNZ (b) CPNZ and pure ZnO (inset)

The photoluminescence spectra are depicted in Figure 9. The PL spectra are taken by exciting the samples at 320 nm. Emission peaks of CPNZ spans over ES and PNZ. Incorporation of ZnO intensifies emission of PNZ compared to ES attributes extended conjugation present along benzenoid and quinoid rings, which helps delocalization of excitons [15]. The emission peaks in CPNZ mainly attributes to band edge emission and

defect emissions [34, 35].

The band gap observed for CPNZ is 3.12 eV. The valence band maximum is found to be at 3.11 eV from valence band spectra. By considering these two values, the density of states of CPNZ is being predicted as shown in Figure 10. There will be an existence of midgap states due to the incorporation of carbon in the nanotubes and this will influence the density of states by generating a small tailing effect in valence band [36]. The conduction band minimum was calculated as -0.01 eV. Conduction band tail can be anticipated just like valence band tail because of the presence of crystal defects [37].

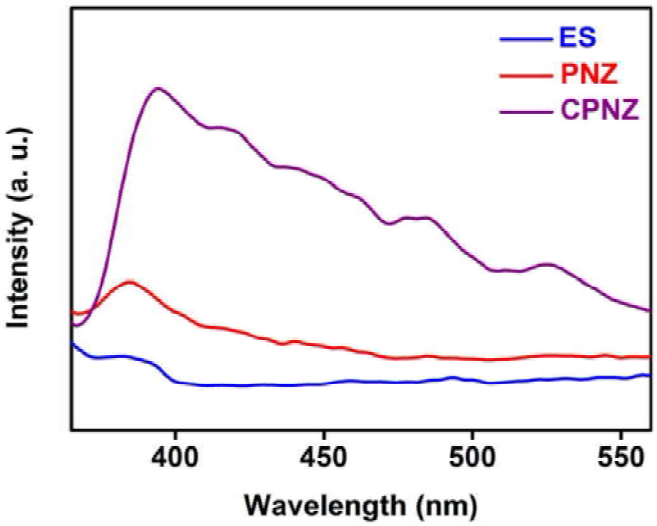

Figure 9. Photoluminescence spectra of ES, PNZ and CPNZ

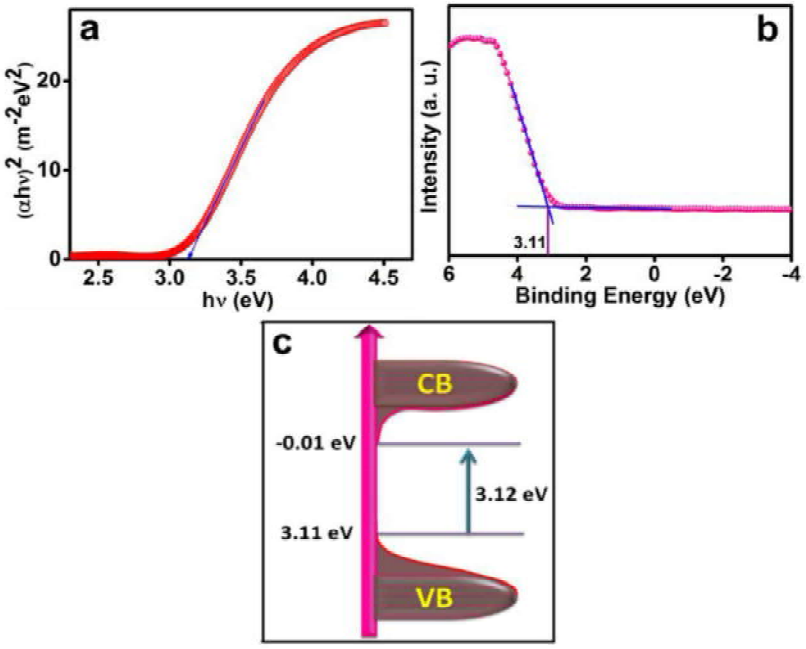

Figure 10. (a) Tauc plot (b) Valence band XPS and (c) Density of states of CPNZ

The degradation of methylene blue in presence of CPNZ is shown in Figure 11 (a). CPNZ completely cleared the dye solution within 57 minutes whereas pristine ZnO takes 60 minutes for the same. The recyclability and stability performances of CPNZ were also studied for five consecutive steps and the material exhibit stability and recyclability very well. The graph showing stability performance of CPNZ is as depicted in Figure 11 (b). The generation of hydroxyl radicals is mainly responsible for the photocatalytic activity of CPNZ. Hydroxyl radicals generated from CPNZ is estimated using terephthalic acid (TTA) probe. The fluorescent intensity obtained from hydroxyl terephthalic acid (HTTA) is depicted in Figure 11 (c). CPNZ releases more reactive oxygen species compared to pure ZnO which are responsible for the higher photocatalytic activity of CPNZ.

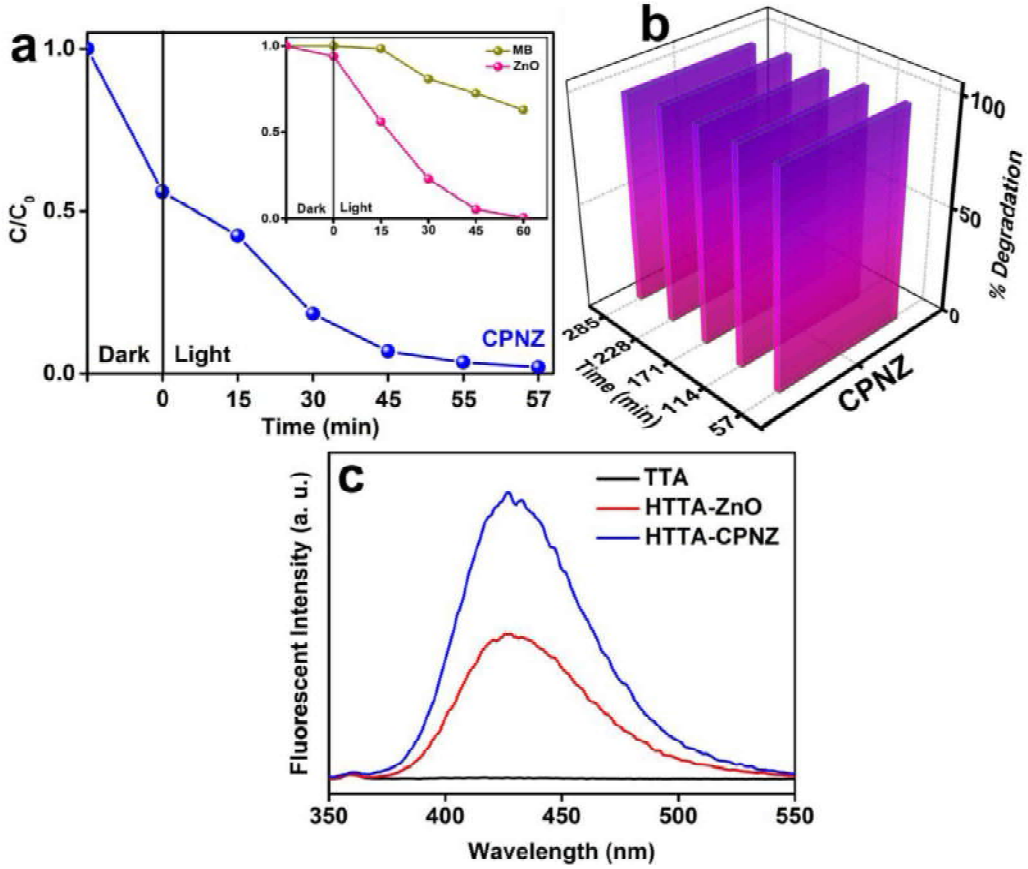

Figure 11 (a) Photodegradation of MB in presence of CPNZ and (b) Photocatalytic stability of CPNZ (c) Fluorescence spectra of TTA before and after light exposure in presence of pristine ZnO and CPNZ.

The carbon induced mid-gap energy levels trap photogenerated electrons and holes thus these excitons are easily available for executing photocatalysis. Moreover the incorporation of carbon and oxygen vacancies increases the Lewis acidity of CPNZ thereby a Lewis base, MB, can easily adsorbs on CPNZ surface [38]. All these factors contribute higher photocatalytic activity of CPNZ compared to pure ZnO.

Antifogging activity of CPNZ coated glass surface is checked from contact angle measurements. The wettability images obtained from dynamic contact angle measurements

are displayed in Figure 12. When subjected to CPNZ coated glass substrate for dynamic contact angle measurements, water was making 19.9° contact angle with the surface. Within hundred seconds the film attains super hydrophilicity and the angle reaches to almost zero. Here the growth of zinc oxide nanotubes happened through oxygen terminated zinc polar surfaces. According to *M. Miyauchi et al,* terminated oxygen ions on the surface of metal oxides are the reactive sites for hydrophilicity. Photoinduced superhydrophilicity originates in CPNZ from the increasing hydroxyl groups of its surface attributes higher crystal defects [39].

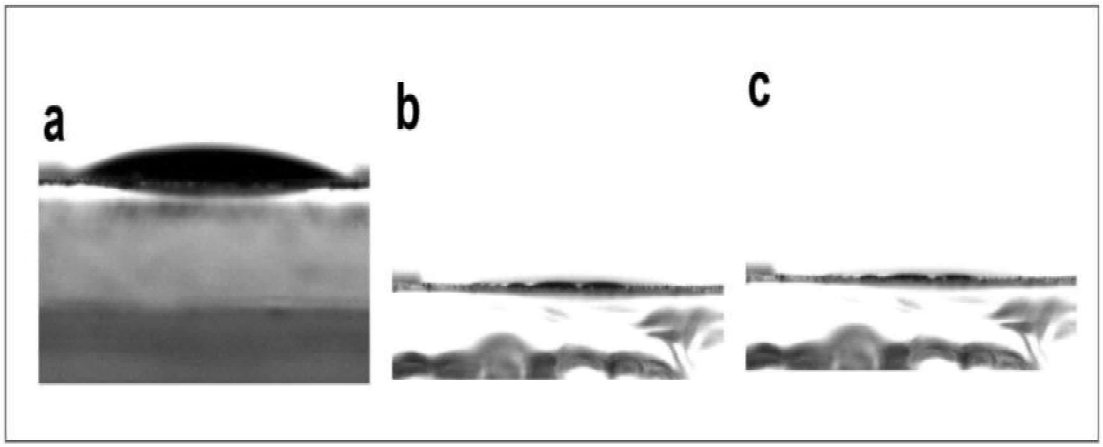

Figure 12. Photographs of water contact angle measurements on CPNZ surface (a) initial (b) after 100 seconds (c) after 120 seconds with illumination

Conclusion

Carbon incorporated ZnO nanostructure with the assistance of polyaniline was synthesized by a template free sol-precipitation method. ZnO-Polyaniline interactions were confirmed from various analysis techniques such as XRD, FTIR and UV. After heat treatment, the presence of carbon and absence of nitrogen in CPNZ were confirmed from XPS. The carbon embedded system shows better photocatalytic performance than pure zinc oxide. The synergetic effect of mid-gap levels combined with oxygen deficiency in carbon incorporated ZnO attributes better photocatalytic activity and can be considered as a promising material for effective water and surface treatments.

Acknowledgements

Author Bhabhina acknowledges Council of Scientific and Industrial Research (CSIR) for the Senior Research Fellowship (SRF). Author Sindhu acknowledges Council for Scientific and Industrial research (CSIR), Government of India for the financial support received in the form of research grant (No. 03(1285)/13/EMR-II). Central Sophisticated Instrumentation Facility (CSIF) of University of Calicut is greatly acknowledged for SEM analysis.

References

[1] F. Parrino, M. Bellardita, E.I. García-López, G. Marcì, V. Loddo, L. Palmisano, ACS Catal., 2018, 8, 11191-11225.
[2] M. J. Limo, A. S. Rabada, E. Boix, V. Thota, Z. C. Westcott, V. Puddu, C. C. Perry, Chem. Rev., 2018, 118, 11118−11193.
[3] M. Liu, L. Feng, X. Zhang, Y. Hua, Y. Wan, C. Fan, X. Lv, H. Wang, ACS Appl. Mater. Interfaces, 2018, 10 (38), 32038–32046.
[4] J. F. S. Fernando, M. P. Shortell, K. L. Firestien, C. Zhang, K. V. Larionov, Z. I. Popov, P. B. Sorokin, L. Bourgeois, E. R. Waclawik, D. V. Golberg, Langmuir, 2018, 34, 7334−7345.
[5] L. Zhu, H. Li, Z. Liu, P. Xia, Y. Xie, D. Xiong, J. Phys. Chem. C, 2018, 122 (17), 9531–9539.
[6] A. B. Lavand, Y. S. Malghe, Int. J. Photochem. 2015 (2014), 1- 9.
[7] Z. Zhang, X. Cheng, Z. Huang, Q. Wang, P. Dong, Y. Chen, X. Zhang, RSC Adv., 2015, 5, 97702.
[8] J. Yang, Y. Guo, R. Jiang, F. Qin, H. Zhang, W. Lu, J. Wang, J. C. Yu, J. Am. Chem. Soc., 2018, 140, 27, 8497-8508.
[9] S-J. Su, N. Kuramoto, Macromolecules **2001**, 34, 7249-7256.
[10] S. Chaturvedi, R. Das, P. Poddar, S. Kulkarni, RSC Adv., 2015, 5, 23563–23568.
[11] N. Parveen, M. O. Ansari, M. H. Cho, Ind. Eng. Chem. Res., 2016, 55, 116–124.
[12] T. Ogoshi, Y. Hasegawa, T. Aoki, Y. Ishimori, S. Inagi, T. Yamagishi, Macromolecules, 2011, 44, 7639–7644.
[13] K. Mallick, M. Witcomb, M. Scurrell, Platin. Met. Rev., 2007, 51, 3–15.
[14] N-A. Rangel-Vazquez, C. Sánchez-lópez, F.R. Felix, Polímeros, 2014, 24, 453–463.
[15] C. Pholnak, C. Sirisathitkul, S. Suwanboon, D.J. Harding, Mater. Res., 2014, 17, 405–411.
[16] V. J. Babu, S. Vempati, S. Ramakrishna, Mater Sci Appl, 2013, 4, 1–10.
[17] Z. Tang, J. Wu, M. Zheng, Q. Tang, Q. Liu, J. Lin, J. Wang, RSC Adv., 2012, 2, 4062-4064.
[18] P. Rajakani, C. Vedhi, Int. J. Ind. Chem., 2015, 6, 247–259.
[19] S. Ameen, M. S. Akhtar, Y. S. Kim, O. B. Yang, H. S. Shin, Colloid Polym. Sci., 2011, 289, 415–421.
[20] D. Sharabi, Y. Paz, Appl. Catal. B: Environmental, 2010, 95,169–178.
[21] P. Muthukumar, C. Rangasami, S. Ganesan, Chalcogenide Letters, 2013, 10 (3), 113 – 119.
[22] V. Ţucureanu, A. Matei, A. M. Avram, Critical reviews in analytical chemistry, 2016, 46 (6), 502–520.
[23] H. Huang, F. Li, H. Wang, X. Zheng, RSC Adv.,**2017**, 7, 50056.
[24] D. H. Wang, Y. Hu, J. J. Zhao, L. L. Zeng, X. M. Tao, W. Chen, J. Mater. Chem., A, 2014, 2, 17415.
[25] M. T. Uddin, Y. Nicolas, C. Olivier, T. Toupance, L. Servant, M. M. Muller, H-J. Kleebe, J. Ziegler, W. Jaegermann, Inorg. Chem., 2012, 51, 7764−7773.
[26] V. L. prasanna, R. Vijayaraghavan, Langmuir, 2015, 31, 9155−9162.
[27] G-H. An, D-Y. Lee, H-J. Ahn, ACS Appl. Mater. Interfaces, 2017, 9, 12478−12485.

[28] D. H. Wang, Y. Hu, J. J. Zhao, L. L. Zeng, X. M. Tao, W. Chen, J. Mater. Chem. A, 2014, 2, 17415.
[29] H. Y. Yang, S. F. Yu, S. P. Lau, T. S. Herng, M. Tanemura, Nanoscale Res Lett., 2010, 5, 247-251.
[30] L. Etgar, J. S. Bendall, V. Laporte, M. E. Welland, M. Graetzel, J. Mater. Chem., 2012, 22, 24463.
[31] J. Gu, S. Kan, Q. Shen, J. Kan, Int. J. Electrochem. Sci., 2014, 9, 6858 – 6869.
[32] J. Laska, Mater. Sci. Eng., B, 1999, 68, 76–79.
[33] S. Y. Sawant, M. H. Cho, RSC Adv., 2016, 6, 70644-70652.
[34] M. Willander, O. Nur, J.R. Sadaf, M.I. Qadir, S. Zaman, A. Zainelabdin, N. Bano, I. Hussain, Materials, 2010, 3, 2643-2667.
[35] H.G. Chen, J.L. Shi, H.R. Chen, J.N. Yan, Y.S. Li, Z.L. Hua, Y. Yang, D.S. Yan, Opt. Mater., 2004, 25, 79–84.
[36] X. Zhang, J. Qin, R. Hao, L. Wang, X. Shen, R. Yu, S. Limpanart, M. Ma, R. Liu, J. Phys. Chem. C, 2015, 119, 20544−20554.
[37] X. Chen, L. Liu, P. Y. Yu, S. S. Mao, Science, 2011, 331,746-750.
[38] B. N. Meethal, R. Ramanarayanan, S. Sindhu, Appl. Nanosci, 2018, 8(6), 1545-1555.
[39] M. Miyauchi, A. Shimai, Y. Tsuru, J. Phys. Chem. B 2005, 109, 13307-13311.

2.

Dosimetric studies on immobilization devices and treatment couch in cancer radiation therapy using medical linear accelerator

Arun Krishnan M P[1,2], Bhagyalakshmi A T[1], Niyas P[2], Ranjith C P[2], Vysakh R[2], Irfad M P[2], Rifa K T[2], Kalidass V[2], Salma K T[2], Velayudham Ramasubramanian[1], Jianping Hu[1*] and M. Ummal Momeen[1*]

[1]School of Advanced Sciences, Vellore Institute of Technology, Vellore- 632014, Tamil Nadu, [2]MVR Cancer Center and Research Institute, Choolur, Kozhikode- 673601, Kerala

*Corresponding authors: ummalmomeen@gmail.com, jianpinghu@hotmail.com

Abstract: *The use of modern treatment techniques such as Intensity Modulated Radiation Therapy (IMRT) demands the accurate and precise treatment plan simulation. The effect of patient positioning device and carbon fiber couch in the treatment plan simulation is studied. The effect of couch in treatment plans was studied from the IMRT plans of a cohort of 100 patients, which included head and neck, lung, brain, liver and pelvis treatment sites. Treatment plans were generated using Monte-Carlo method based Monaco planning system (V5.11.02) with simulated 6MV X ray photon energies from Versa HD medical linear accelerator. Pre-treatment simulation was carried out with a 16 slice Computed Tomography (CT) scanner using a high density couch, which was removed by contouring in planning systems and treatment was carried out in Versa HD linear accelerator with a low density carbon fiber couch. The effect of couch on the dose distribution was studied by generating two different treatment plans; with and without including an existing low density couch from system library. In both cases the actual high density couch used in simulation was not included in dose calculation. Low density immobilization devices were found to have less attenuation in comparison to their high density devices. The percentage of attenuation is ranging from 0.49 to 1.1 for low density, whereas it is 2.5 to 11 for high density immobilization devices. The effect of treatment couch top should also be simulated during treatment planning as it introduces a considerable change in patient skin dose and subsequent depth doses.*

Keywords: Attenuation, immobilisation, radiation therapy, IMRT

Introduction

Cancer refers to any one of a large number of diseases characterized by the development of abnormal cells that divide uncontrollably and have the ability to infiltrate and destroy normal body tissue. Global Cancer Statistics in 2018 shows that worldwide there will be an estimated 18.1 million new cancer cases (17.0 million excluding non-melanoma skin cancer) and 9.6 million cancer deaths (9.5 million excluding non-melanoma skin cancer) in 2018[(1).] According to Indian Council of Medical Research press release on 12th September 2018 the proportional contribution of cancers to the total health loss in India has doubled from 1990 to 2016. [(2)] According to them the number will reach to 17 lakhs new cancer cases by 2020.

Cancer is curable if detected early and treated with proper combination of treatment modalities. Radiation therapy which uses high energy X rays is one among them. Radiation therapy mainly comprises of 3 stages, starting from patient simulation by 3-Dimensional

computed tomography (CT) images followed by treatment simulation in treatment planning system (TPS) and delivery of simulated treatment by Linear Accelerator (LINAC).

Due to the improvement in technology we can accurately deliver the maximum amount of radiation dose to tumour and spare the surrounding normal tissues, thus improving the life quality of cancer patients. One of such high end technology is Intensity Modulated radiation therapy (IMRT).By this technique we can precisely plan and deliver the radiation dose to tumour and hence the accuracy required in this technique is very high.[5] As per International Atomic Energy Agency- Technical Report Series 398(TRS 398) the accuracy of treatment delivery should be of the order of 2%.[6] For accurate radiation delivery every patient should be properly immobilised on a carbon fibre couch. The increasing use of carbon fibre in treatment tables is due to its favourable characteristics such as high beam transmission, physical resistance, low specific density, light weight and high specific strength. These characteristics of carbon fiber make it appropriate to be used in radiotherapy couch.[7] During IMRT radiation will be delivered through multiple beam angles causing radiation to passes through the immobiliser and carbon fibre couch. In this study we are analysing the effect of these immobiliser and carbon fibre couch.

Materials and Methods:

In our centre we have Elekta Synergy LINAC with 6, 10, 15 MV photon energies along with iBEAM evo carbon fibre couch. The iBeam evo couch top manufactured by Medical Intelligence (Schwabmünchen, Germany) consists of two thin carbon fibre plates which is 2 mm thick and it is sandwiched with the 46 mm of foam. The carbon fibre thickness increases to 4.5 mm towards the edges of the couch(.[3])
The patient immobilisation systems are from Orfit Company with high density and low density variables.16 slice Computed Tomography (CT) scanner from General Electric (GE) were used for pre treatment simulation of the patient. Treatment plans were created using Monaco (Version-5.11.02) planning system which uses Monte-Carlo algorithm.

Figure 1:Elekta Synergy Linear Accelerator

Figure 2: PET CT scanner with flat couch

For optimising cost effectiveness, patient set up accuracy and patient workload we simulate the patient with high density immobilisers and carry out treatment with its low density replicas which are transparent to high energy X rays. In this study we measured the attenuation through 19 immobilisation devices including both low and high density and also

the couch top extension. Attenuation was measured using a 30 cm x 30 cm x 30 cm water equivalent solid phantom. The measurement was performed using 0.65 cm^3 Farmer type ionization chamber at a depth of 5 cm for 6, 10 and 15 MV energy X-rays with a source to measurement distance of 100 cm for 10 cm x 10 cm radiation field size using the equation 1.

$$\text{Percentage of Attenuation} = \left(1-\frac{Qm}{Qnm}\right) \times 100\% \quad (1)$$

Qm - charge collected with immobiliser

Qnm - charge collected without immobiliser

The attenuation was studied with respect to change in energy and density. The graph showing percentage attenuation of these devices with energy were plotted. Among these immobilisation devices, it is the carbon fibre couch on which a patient lay down and that is common to all patients and hence a comprehensive study on its attenuation with respect to energy was carried out. The carbon fibre is transparent to radiation with a very minimal attenuation. The effect of this attenuation on skin dose is studied for couch top extension by using Radiation Field Analyser, together with water phantom, (625000 cm^3 volume) using 0.13 cm^3 cylindrical ionization chamber for all the available energies and with 10 cm x 10 cm field size. Depth versus dose curve for all the available photon energies were plotted both with and without couch.

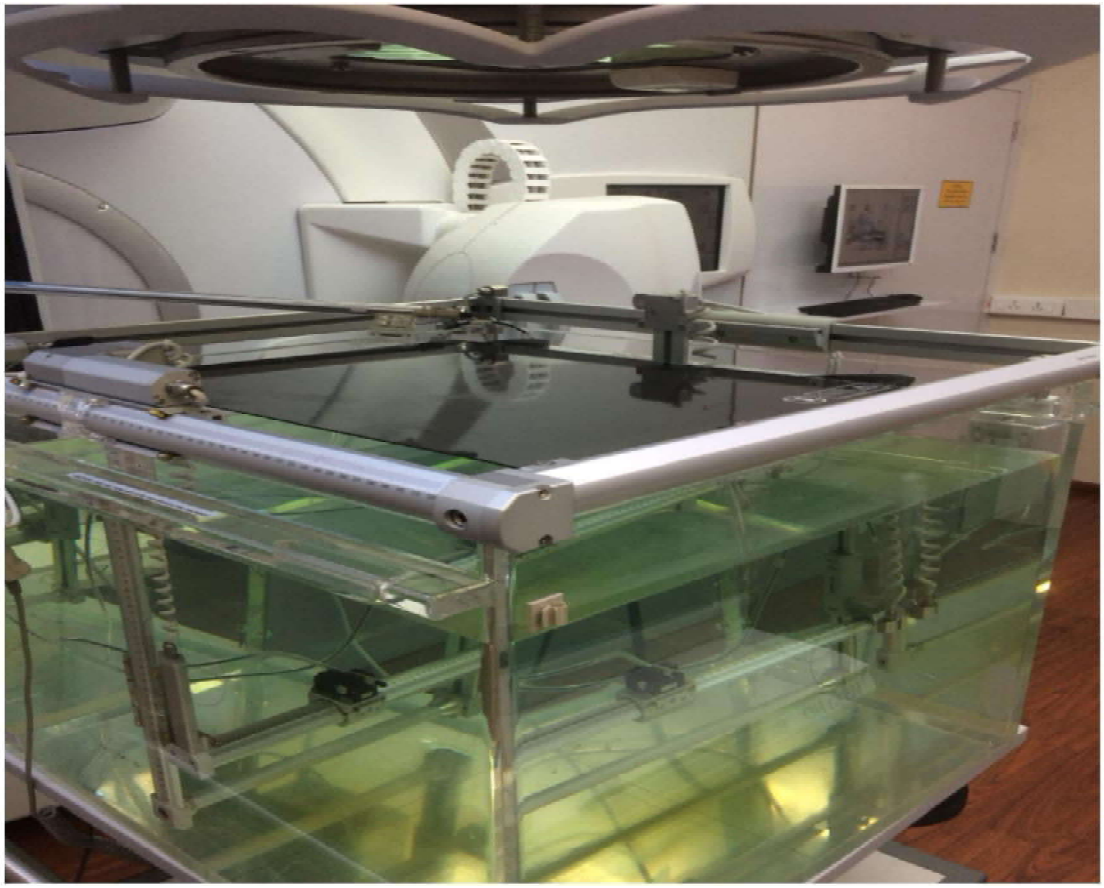

Figure 3: Experimental setup consisting of Radiation Field Analyser and ionisation chambers to measure the depth versus dose curve with and without the inclusion of couch.

To further evaluate the importance of "considering" the effect of couch attenuation we simulated the Volumetric Modulated Arc Therapy (VMAT) plans in MONACO Treatment Planning System (TPS) with and without couch. A total of 46 patients treatment plans were evaluated - 8 patients with lung cancer, 2 patients with brain tumour, 21 patients with Head and Neck cancers, 9 patients undergone liver SBRT and 6 patients with prostate cancer. The target volume coverage and normal structure doses were analysed for individual patients and results were tabulated. Treatment plans were generated in Monte Carlo (MC) based MONACO treatment planning system on three dimensional images from 16 Slice CT scanner with in-house high density couch. All the patients were simulated with a slice thickness 2.5 mm. Both set of plans were generated for 6MV photon without considering the high density in-house couch as it is not used for treatment. Virtually simulated low density couch from plan library was introduced in the treatment planning system separately for creating treatment plans which considers the effect of couch. This couch has an effective electron density of 0.13 g/cm^3 (3) which is used for dose calculation. Second set of plans were generated without considering the effect of couch. For all the plans the resolution for calculation were set as 3mm.Total of 92 VMAT Plans were generated and analysed in terms of PTV coverage and normal organ dose.

Results and Discussion

Attenuation of radiation depends on energy and density of attenuator. As energy increases, penetration will increase and attenuation will decrease. High density materials have a greater attenuation when compared with low density materials for any energy. The observed data shows the same result. Table 1 elaborates the percentage attenuation of various immobilization devices for 6, 10 and 15 MV energies.

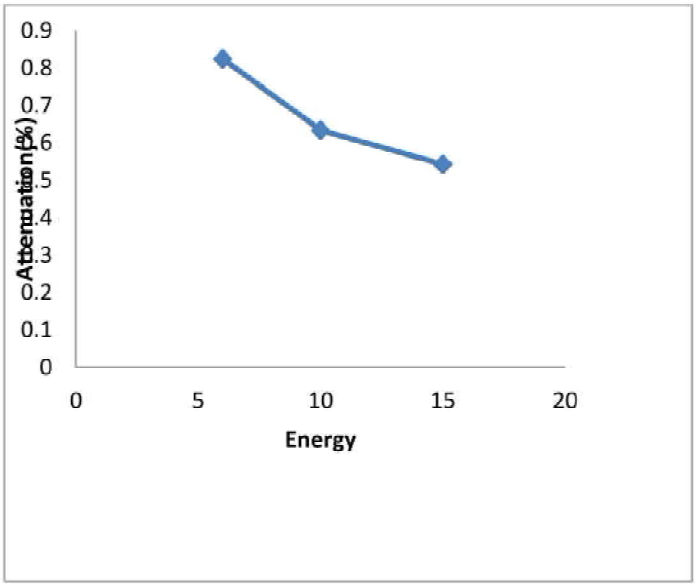

Figure 4. Graph shows the attenuation of the immobilisation device Vaclock with energy

Sl No	Immobiliser	Attenuation For Energy(%)		
		6 MV	10 MV	15 MV
1	Vaclock	0.82368	0.63353	0.54232
2	White thermoplastic Mould	0.61776	0.48733	0.44801
3	Ocean Green thermoplastic Mould	0.90090	0.68226	0.68226
4	Paediatric head rest -with flap	0.66924	0.56043	0.54232
5	Paediatric head rest- without flap	0.72072	0.58480	0.54232
6	Short neck –with flap	0.79794	0.60916	0.58948
7	Long neck –with flap	0.74646	0.68226	0.54232
8	Long neck –without flap	0.74646	0.65789	0.58948
9	Wedge -9’	0.56980	0.61290	0.40332
10	Knee rest	3.96270	3.18706	2.77580
11	Belly board –low density	0.88060	0.75999	0.61684
12	Wedge -18’ low density	0.77700	0.68644	0.56940
13	Wedge-18’ high density	14.01191	11.52243	10.22539
14	All in one board	1.16550	1.02966	0.90154
15	All in one board –high density	3.39290	2.84383	2.53855
16	BRAIN SPACER -5cm	0.51800	0.44128	0.35587
17	SPACER -5cm HIGH DENSITY	12.19891	9.97794	8.89680
18	Breast board	4.48070	3.67737	3.22657
19	Couch Top	1.64736	1.07212	0.99033
20	Couch extension	1.42450	1.34837	1.18624

Table 1. The percentage attenuation of various immobilization devices for 6, 10 and 15 MV energies.

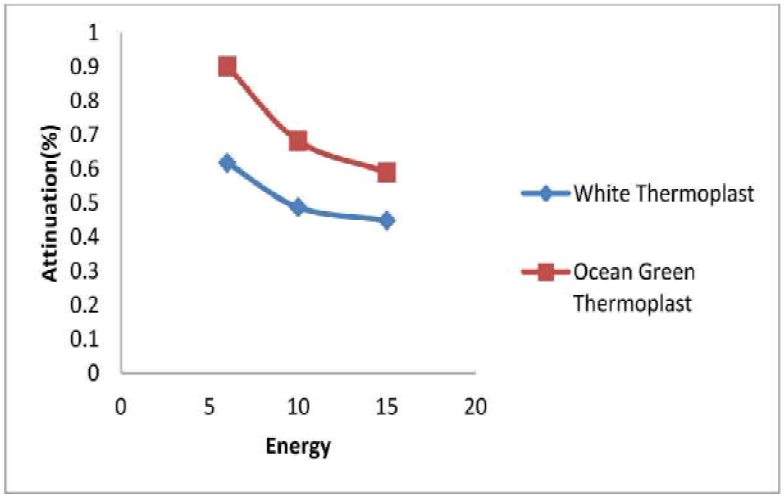

Figure 5. Red line in graph shows the percentage attenuation of Ocean Green Thermoplastic mask with energy and blue line shows the attenuation of white thermoplastic mask with energy.

On considering specific immobilisation devices figure 5 shows that ocean green thermoplastic mask attenuates more in comparison to the white thermoplastic masks and hence enabling the use of white masks for any known radiation sensitive patients, thus reducing toxicity of skin, although both serves the same physical function. Considering all the head rests, they attenuates on an average of 0.736±0.0467, 0.619±0.0505, 0.561±0.0258 for 6MV, 10MV and 15MV respectively (figure 6). All in one base plate are used in between the patient and the treatment couch to position the immobilisation devices rigidly. Low density all in one base plate should be used for treatment and its high density replica is used in simulation which should be removed during treatment planning.

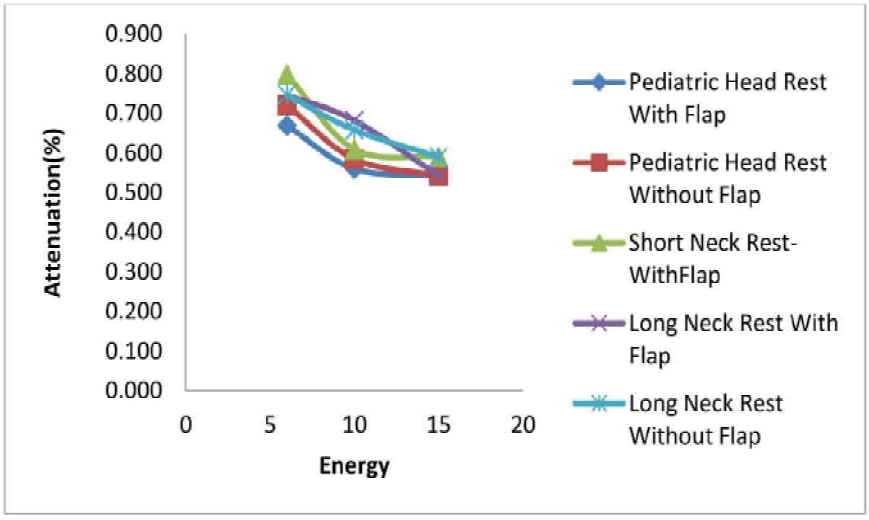

Figure 6. Graph shows the percentage attenuation of various head rests with energy.

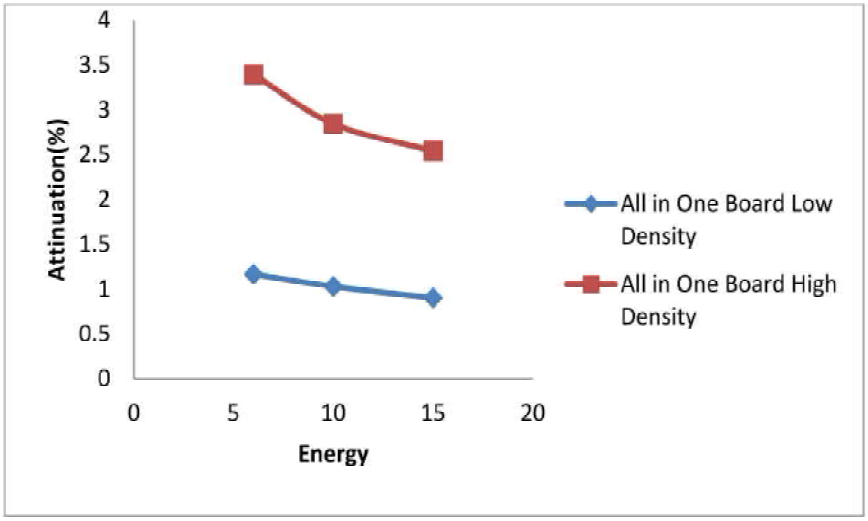

Figure 7. Red line in the graph shows the percentage attenuation of low density all in one base plate with energy and blue line in the graph shows the percentage attenuation of high density all in one base plate with energy.

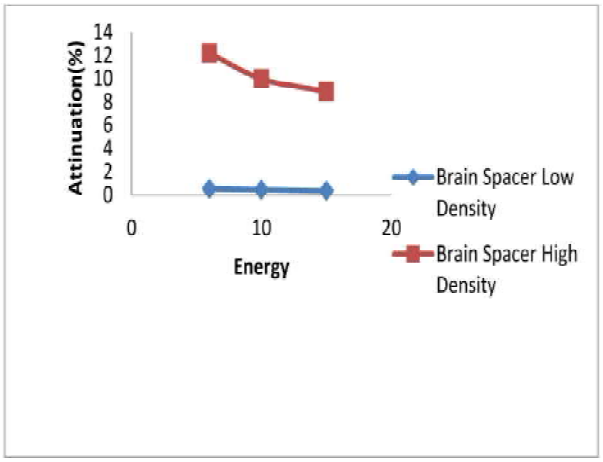

Figure 8. Red line in graph shows the percentage attenuation of high density brain spacers with energy and blue line shows the attenuation of low density brain spacer with energy

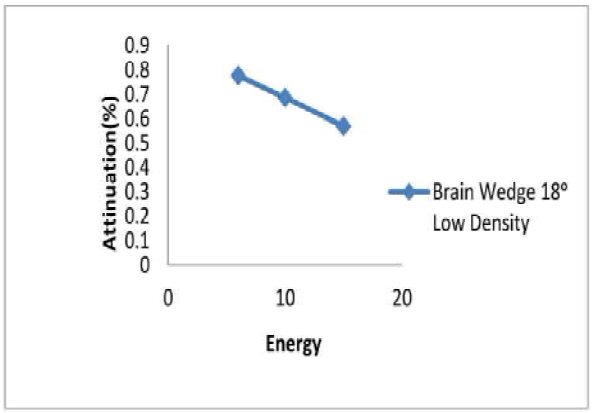

Figure 9. Figure shows percentage attenuation of 18° low density brain wedge

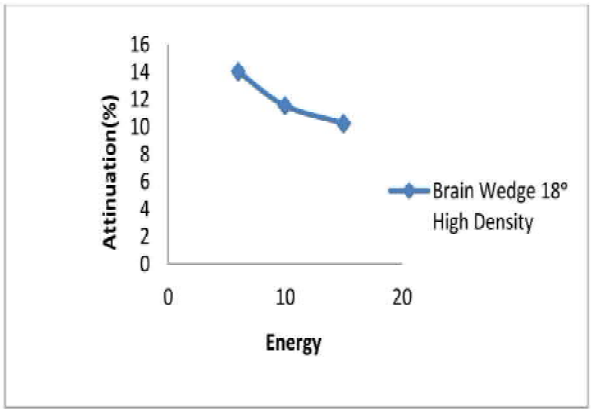

Figure 10. Figure shows percentage attenuation of 18° high density brain wedge

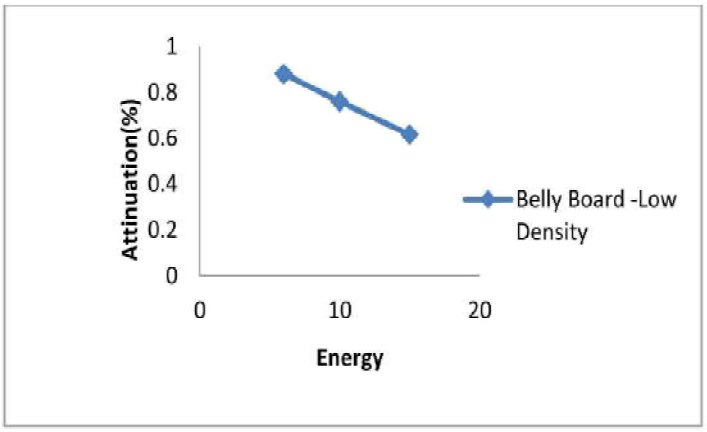

Figure 11. Figure shows percentage attenuation of low density belly board with energy

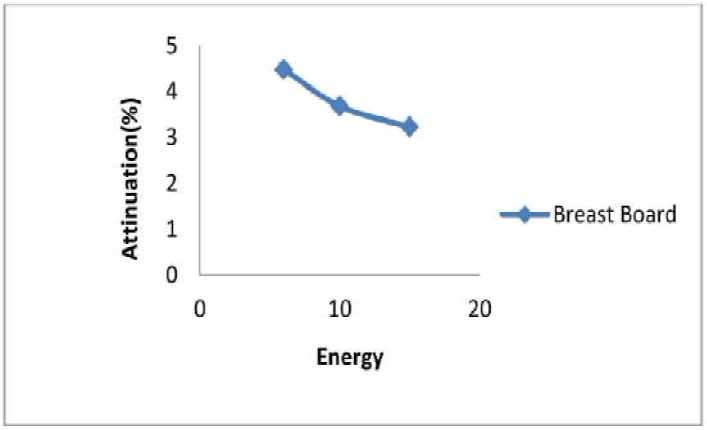

Figure 12. Figure shows percentage attenuation of breast board with energy

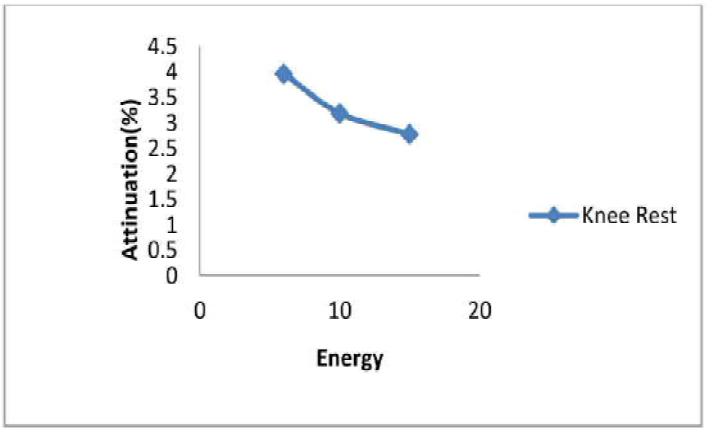

Figure 13. Figure shows percentage attenuation of knee rest with energy

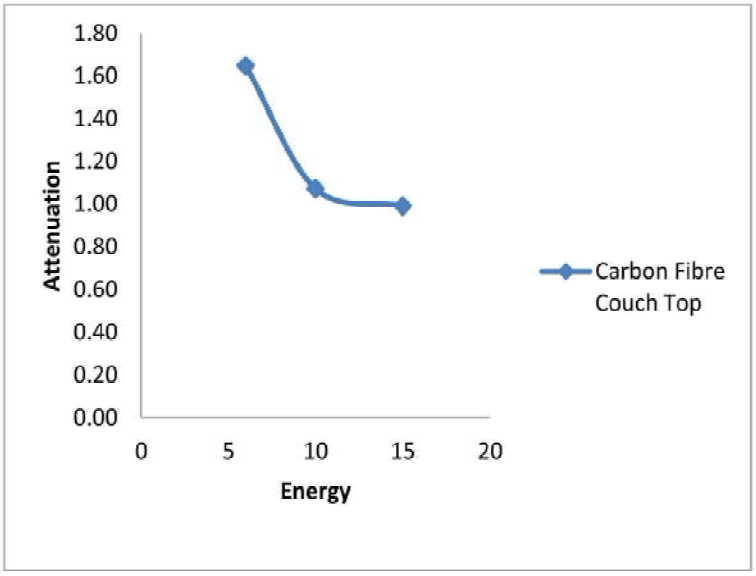

Figure 14. Figure shows percentage attenuation of couch top with energy

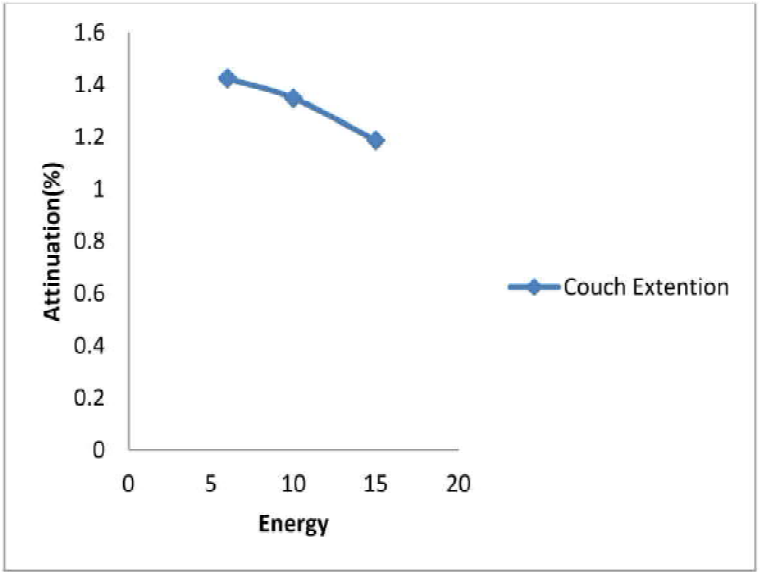

Figure 15. Figure shows percentage attenuation of couch extension with energy

Even though carbon fibre is considered as transparent to high energy X-ray, our study shows a considerable attenuation by Carbon fibre couch and its extension. This added light to the scope of further study. Hence its effect on depth dose curve for all the energies were obtained and it was realised from figure 16 that there was a considerable increase in skin dose when couch was introduced in the path of the beam..

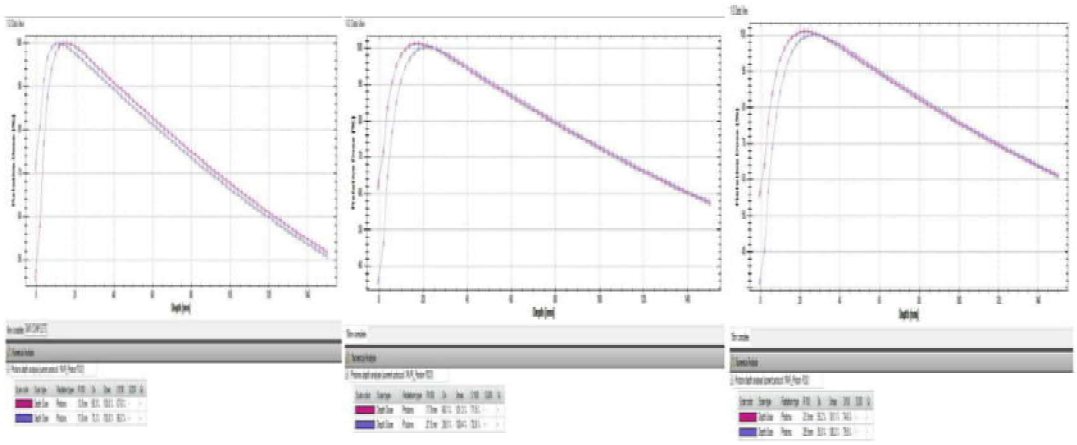

Figure 16. The graph shows the variation of 6 MV, 10MV and 15MV (from left to right) photon beams with the inclusion of couch top in the path of the beam qualitatively. Percentage depth dose id normalised to 100% at the depth of maximum dose

Quantitatively skin dose increased from 50.8% to 75.3%, 39.9% to 66.1% and 35% to 59.2% with the inclusion of couch for 6MV, 10MV and 15MV respectively. Thus, there is an increment of 24.97 (±0.008) % in skin dose with the inclusion of couch during treatment, which is a considerable value and needs to be taken into account during treatment plan simulation.

For this purpose 42 intensity modulated patient plans were analysed with and without couch to estimate the importance of couch inclusion in treatment planning simulation. If we do not consider the carbon fibre couch in treatment plan simulation and treat the patient with carbon fibre couch in machine, there will be an overestimation of dose in simulated planning results compared to the actual treatment delivery. To quantify this effect we made two plans for all the patients under study, one with couch which will simulate the delivery and the other without couch to check the extent of couch effect. For prostrate case we found that during treatment delivery the volume of PTV receiving 100% of prescription dose will be reduced from 0.7% to 7.3%. Similarly the % reduction in doses for various sites is tabulated.

Site	Range of reduction of dose
Lung	0.7% to 12.04%
Brain	0.5 % to 2.4%
head and Neck	1% to 6%
Liver	0.32% to 2.5%
Prostate	0.71% to 7.3%

Conclusion

The attenuation of treatment beam through the low density immobilisation devices is negligible and hence can be excluded vivaciously from the treatment plan simulation. The use of couch inclusion based model improves the accuracy of delivered dose. The couch model provides an accurate calculated dose in the build-up region and hence we can assess the skin

doses correctly, which in turn provides a chance to prevent the skin toxicities during treatment and thus improving the quality of life of patients.

References

1.https://www.icmr.nic.in/. press conference 12 September, 2018
2. Freddie Bray, Jacques Ferlay,Isabelle Soerjomataram,Rebecca L. Siegel,Lindsey A. Torre, Ahmedin Jemal, Global Cancer Statistics 2018: GLOBOCAN Estimates of Incidence and Mortality Worldwide for 36 Cancers in 185 Countries, CA: Cancer J Clin. 2018;68:394-424.
3. iBEAM evo Couch top User Manual, Version 11 of 2007-11-15
4. C. Huertas,H.U. La Paz, C. Ferrer, C. Huerga, I. Mas, A. Serrada Treatment couch modeling in Elekta Monaco treatment planning system, ESTRO 2016; 35: 389-390
5. KY Cheung, PhD. Intensity modulated radiotherapy: advantages, limitations and future developments. Biomedical Journal of Imaging and Intervention. 2006 Jan-Mar; 2(1): e19.
6. IAEA – TRS 398 IAEA TRS-398 Absorbed Dose Determination in External Beam Radiotherapy: An International Code of Practice for Dosimetry based on Standards of Absorbed Dose to Water.
7. Chun-Yen Yu, Wen-Tsae Chou,[1] Yi-Jen Liao et al Impact of radiation attenuation by a carbon fiber couch on patient dose verification. Published online 2017 Feb 27. doi: [10.1038/srep43336]

3.

Room temperature AC impedance studies of Bi and Sr doped $NdCo_{0.6}Fe_{0.4}O_3$ nanosized perovskites

Megha.U[a] ,George Varghese[b], Shijina.K[c]
[a] Department of Physics, DGM MES Mampad College, Malapuram-676542,Kerala,India.
[b] Research Centre, Mar Ivanios College, Thriuvananthapuram-695015, Kerala, India.
[c] Department of Physics, N.S.S. College, Cherthala, Alappuzha -688541, Kerala, India.
Formerly Department of Physics, University of Calicut, Malappuram - 673635, Kerala, India.
meghaunikoth@gmail.com, gv@uoc.ac.in

Abstract *In this communication, the effect of Bi and Sr doping on the structural and electrical properties of $NdCo_{0.6}Fe_{0.4}O_3$ have been investigated. The XRD data reveals that all compounds have orthorhombic crystal structure with pbnm space group and Bi (x =0.2) has the existence of secondary peaks. SEM micrograph confirms the formation of dense nanostructures with well shaped grain boundaries and elemental composition was confirmed from EDAX spectra. The oxidation states of elements present in the compound were analysed using XPS. The existence of highly resistive grain boundaries was evident in impedance studies at room temperature. The presence of relaxation due to the grain and grain boundary effect was established from the combined dielectric and conductivity measurements and was well explained by Maxwell-Wagner Model.*

Keywords: Perovskites, Impedance spectra, Grain boundary effect, Maxwell- Wagner relaxation.

1. Introduction

The rare earth cobalties ($RCoO_3$) with perovskite structure have lot of applications in the field of optoelectronics and spintronics due to the fascinating electrical, magnetic and optical properties. In cobalties there exists a strong inter-relation between spin and orbital degrees of freedom. The cobalt ions in these compounds can exist in three spin states, low spin - LS state (t_{2g}^6 e_g^0), intermediate spin - IS state (t_{2g}^5 e_g^1) and high spin H-S state (t_{2g}^4, e_g^2). The temperature dependent spin transitions of Co^{3+} makes these materials as a potential candidate for many applications such as sensors, substrates, catalytic electrodes and are highly thermoelectric materials[1,2].

$NdCoO_3$ perovskites are reported as a p-type semiconductor and at 275K, Co^{+3} in it can undergo transition from LS to IS state [3]. Morchshakov et.al. studied the heat conductivity and thermopower of $Nd_{1-x}Sr_xCoO_3$ and reported that adjunction of Sr in $NdCoO_3$ changes its magnetic properties and increases transition temperature, T_C [4]. The effect of Ni substitution on $NdCoO_3$ perovskites was studied by Vinod Kumar et al. He reported that Ni substitution enhances the conductivity of the material [5]. The high temperature thermoelectric properties of $LnCo_{1-x}Ni_xO_3$ compounds were reported by Robert et.al [6]. In this work, we report the study of complex impedance spectroscopy of Bi and Sr doped $NdCo_{0.6}Fe_{0.4}O_3$ which was not done so far. It is a non-destructive method for the study of interfacial, grain boundary and bulk grain effects. Combined dielectric and impedance measurements can explain the conduction mechanism and the existence of the grain boundary effects. By Maxwell- Wagner model the relaxation process was successfully explained [7, 8, 9].

2. Experimental

Bi and Sr doped $NdCo_{0.6}Fe_{0.4}O_3$ nanopowders were synthesized by a polymeric precursor method by dissolving $Nd(NO_3)_3$.$6H_2O$, $Co(NO_3)_2$.$6H_2O$, $Fe(NO_3)_3$.$9H_2O$, $Bi(NO_3)_3$.$9H_2O$,

$Sr(NO_3)_2$, citric acid and ethylene glycol (all Sigma Aldrich 99.99 - 99% purity) in concentrated nitric acid and deionised water. The solution was heated to form polymer complex and finally leads to auto-combustion to form ashes. These powders were calcined at 700°C for 6 h and sintered at 900°C for 8 h.

The phase purity and the crystal structure of the synthesized nanopowders were determined by Rigaku Miniflex 600 X-ray Diffractometer, with scan rate 1°/minute and Cu-Kα radiation, λ= 1.5418 Å. The Scanning Electron Microscopy, SEM (Carl *Zeiss Ultra 55* FE-*SEM*) equipped with Energy Dispersive X-ray Spectrometer (EDS) were used for determining the morphology and the elemental composition. The X-ray photoelectron spectra were taken at room temperature using AXIS Ultra DLD Kratos with MgKα source of excitation energy 1253.68eV. The impedance and dielectric studies were done using TFA 2000 ac impedance analyser in the frequency range from $1 < f < 10^6$ Hz equipped with LCR meter.

3. Results and Discussions

The XRD diffraction patterns of $NdCo_{0.6}Fe_{0.4}O_3$ (N0), $Nd_{0.9}Bi_{0.1}Co_{0.6}Fe_{0.4}O_3$ (N1), $Nd_{0.8}Bi_{0.2}Co_{0.6}Fe_{0.4}O_3$ (N2) and $Nd_{0.8}Bi_{0.1}Sr_{0.1}Co_{0.6}Fe_{0.4}O_3$ (N3) were shown in Fig.1.The crystallographic structure belongs to orthorhombic crystal structure of $NdCoO_3$(ICDD No. 01-074-8955) with pbnm space group and Bi (x=0.2) has secondary peaks. The lattice parameters were obtained by PDXL software and the tolerance factor was calculated from Goldschmidt formula Table.1. The crystallite size were calculated using Scherer formula. The samples N1 and N3 obey Vigard's law and for N2 due to the crossing of solubility limit of Bi, has the presence of secondary peaks. The lattice parameter variation with various doping concentrations was shown in Fig.2.

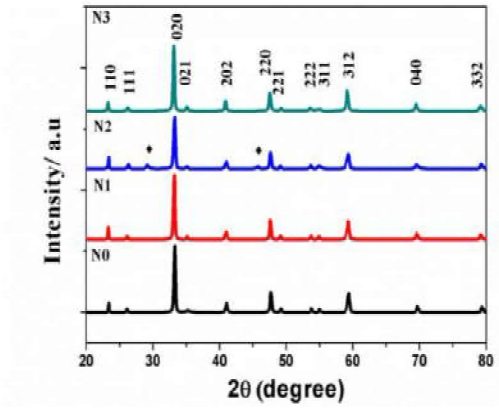

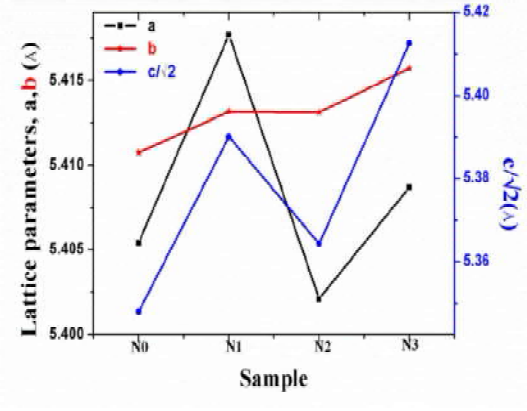

Figure.1.XRD patterns of samples (a)N0 (b)N1(c)N2 and (d)N3.**Figure.2.**Variation of lattice parameters with doping.

Samples	Lattice parameters (Å) ±0.001(Å)			Volume $(Å)^3$	Tolerance Factor	Crystallite Size(nm)
	a	b	c			
$NdCo_{0.6}Fe_{0.4}O_3$ (N0)	5.4054	5.3863	7.5632	305.0843	0.956	38.5
$Nd_{0.9}Bi_{0.1}Co_{0.6}Fe_{0.4}O_3$ (N1)	5.4177	5.3962	7.6228	305.0843	0.947	37.2
$Nd_{0.8}Bi_{0.2}Co_{0.6}Fe_{0.4}O_3$ (N2)	5.4021	5.3965	7.5863	305.0859	0.938	40.7
$Nd_{0.8}Bi_{0.1}Sr_{0.1}Co_{0.6}Fe_{0.4}O_3$ (N3)	5.4087	5.4066	7.6545	305.0843	0.954	30.7

Table.1. Lattice parameters, volume, tolerance factor and the crystallite size of Bi and Sr substituted $NdCo_{0.6}Fe_{0.4}O_3$.

The SEM images and EDS spectra of nanopowders are shown in Fig 3 and 4. Dense nanostructures with well shaped grain boundaries were obtained and it was observed that the grain size decreased with doping of Bi and Sr. At higher temperature due to the high sinterability and the grain growth inhibition offered by Bi reduces the size of grain [10]. The average grain size obtained was in the range from 200 to 400nm.

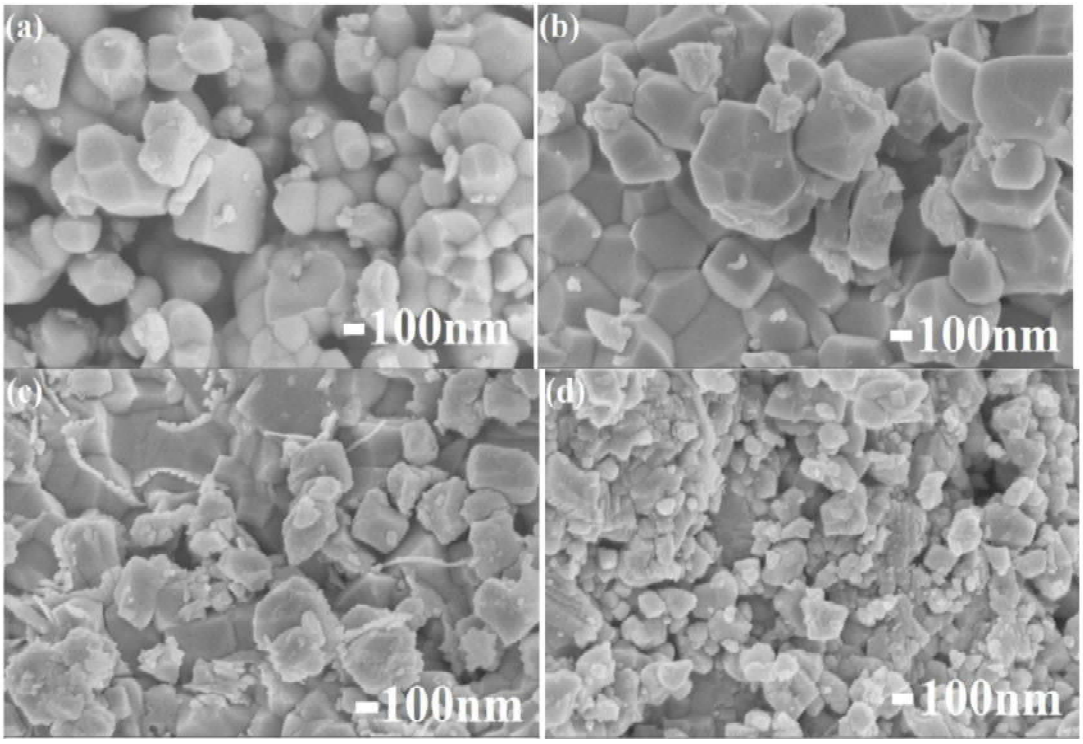

Figure.3. SEM images of (a) N0 (b) N1 (c) N2 and (d) N3

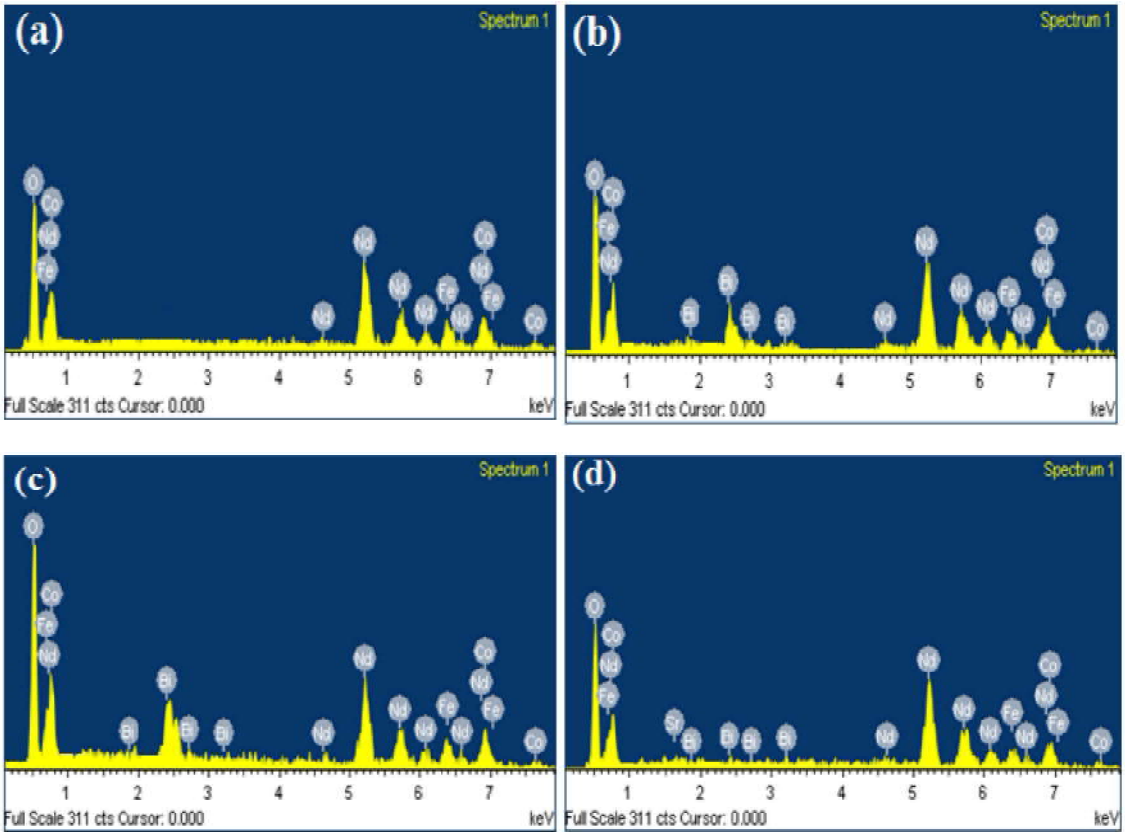

Figure.4. EDAX spectrum of (a) N0 (b) N1 (c) N2 and (d) N3.

Inorder to identify the oxidation states of elements present in N0, N1, N2 and N3, XPS spectra is recorded at room temperature. The peaks of each element are fitted by XPS-PEAKFIT41 software and the carbon 1s peak is considered as standard with a binding energy of 285eV [11-14].

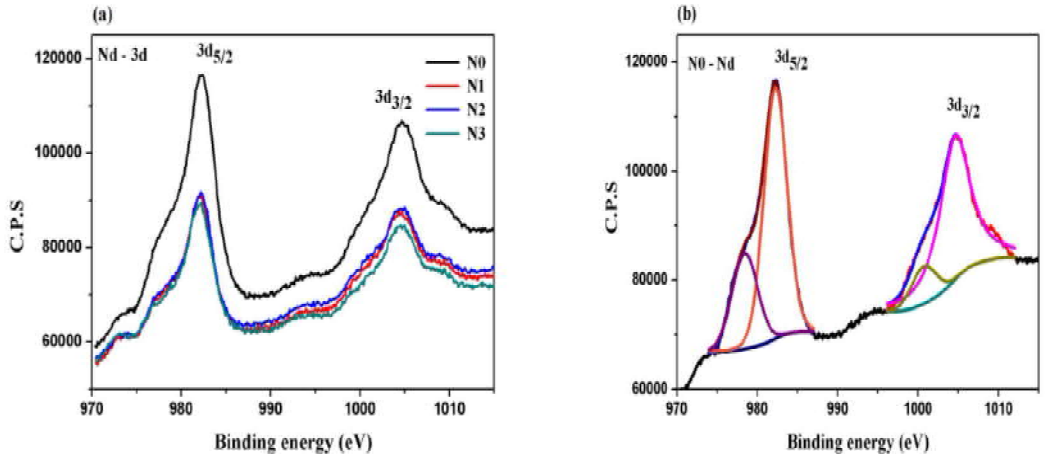

Figure.5. XPS spectra of (a) Nd-3d in N0, N1, N2 and N3 (b) peak fitting of Nd in N0.

Fig.5 shows the narrow scan core level energy spectra of Nd-3d in N0, N1, N2 and N3. The $Nd3d_{3/2}$ has peaks at 1004.6±0.3eV and 1000.7±0.3eV and $Nd3d_{5/2}$ at 982.3±0.3eV and 978.4±0.3eV. The binding energy splitting of 4±0.2eV and an exchange splitting of 22± 0.2eV are obtained [15]. There exists a slight shift in peak positions due to the substitution of Bi and Sr, shows all compounds have similar perovskite structures. All other elements were fitted as in ref.[1]. The Bi, Co and Fe have +3 oxidation states. The Co and Fe spectra have the presence of satellite peaks indicates the presence of Co^{2+} and Fe^{2+} ions. The Sr has +2 oxidation states. The oxygen vacancies are found to be more in Sr doped sample, N3.

Samples	N0	N1	N2	N3
Nd -$3d_{3/2}$	1004.6 1000.7	1004.3 1000.4	1004.5 1000.6	1004.3 1000.3
Nd -$3d_{5/2}$	982.3 978.4	982.1 978.4	982.2 978.6	982.1 978.3
Bi-$4f_{5/2}$		164.8 164.3	164.6 164.2	164.5 164.3
Bi-$4f_{7/2}$		159.5 159	159.4 158.9	159.2 159
Sr–$3d_{3/2}$				134
Sr–$3d_{5/2}$				132.1
Co–$2p_{1/2}$	795.5	795.5	795.5	795.5
Co– $2p_{3/2}$	780.4	780.4	780.4	780.4
Co- satellite	790.3	790.2	790	789.5
Fe –$2p_{1/2}$	724.3	724.4	724.5	724
Fe–$2p_{3/2}$	710.9	710.7	710.7	710.6
Fe-satellite	713.7	714	713.4	714
O–1s	531.5 529.3	531.4 529.4	531.3 529.5	531.4 529.2
O_A/O_L	0.98	0.62	0.56	1.05

Table.2.XPS peak positions (binding energy, eV) of elements

The variation of real (Z') and imaginary part (Z'') of impedance with frequency at room temperature is shown in Fig.6. The value of Z' and Z'' is found to be high in low frequency indicates large effects of polarization and the value decreases monotonically with increase in frequency.

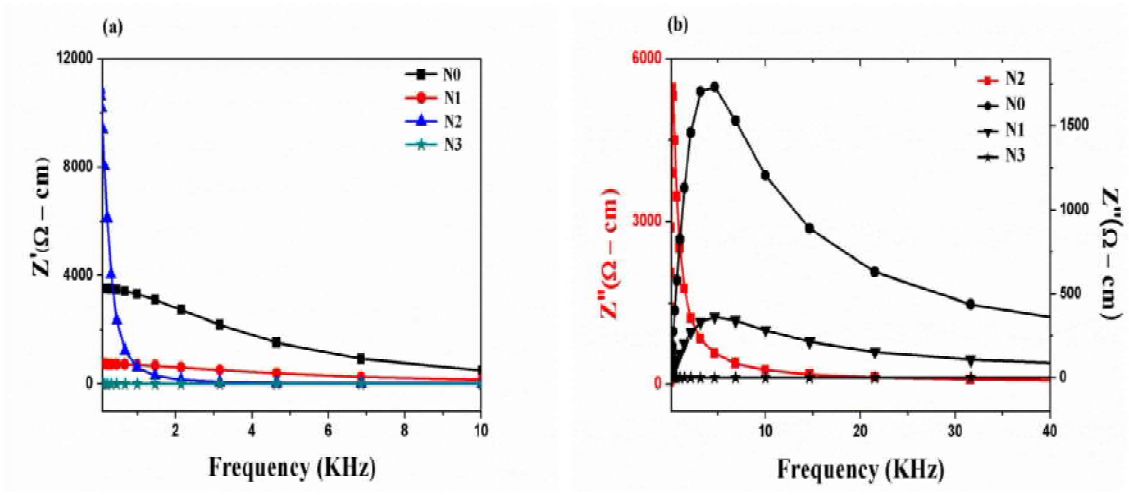

Figure 6 . The variation of (a) *Z'* and (b) *Z''* with frequency at room temperature.

The presence of an asymmetric relaxation is observed in the *Z''* vs frequency plot. The impedance is high for N2 due to the presence of secondary peak of Bi and N3 has no impedance at room temperature.Fig.7 shows the Nyquist plots of samples N0, N1 and N2 at room temperature, with an equivalent circuit inside. The single semicircle in Cole-Cole indicates single relaxation process, since the capacitance is in nanofarad the semicircle represents the behaviour of the grain boundaries. The circuit parameters are obtained from Z-view software and tabulated in Table.5.5 with an error of ±5%. R1 and R2 are the contact resistance and grain boundary resistance, C is the capacitance of grain boundary. The N3 did not show semicircular impedance plot [16]. It was well established in the Cole-Cole that the effect of grain boundaries are found to be dominant than grain at room temperature.

The fitting the curve using Z-view software the circuit parameters are obtained and tabulated in Table.3. R1 is the contact resistance, which is very small compared to the grain boundary resistance (R2) and C is the capacitance of grain boundary. The increase in size of semicircular arcs with doping is attributed by the increase in resistance of the corresponding components in the sample. The P2 has high grain boundary resistance due to the presence secondary peak of Bi. The R-C parallel circuit has a relaxation with time constant τ can obtained using $\tau = R_{g.b} \times C_{g.b}$ and $2\pi f_{max} \tau = 1$

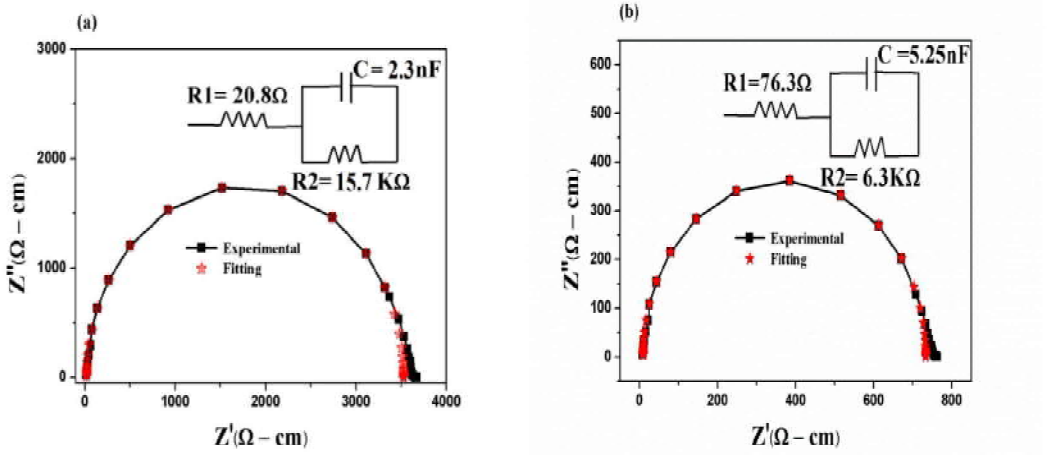

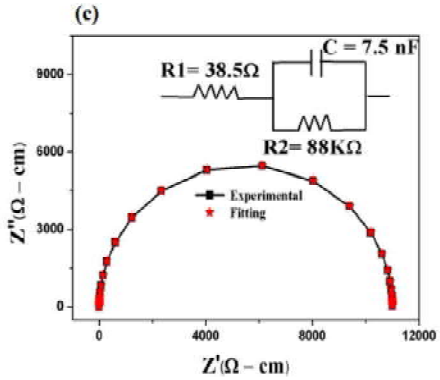

Figure 7. Nyquist plot of (a) N0 (b) N1 and (c) N2 at room temperature with the equivalent circuit inside.

The variation of dielectric constant, dielectric loss tangent and ac conductivity with frequency was shown in Fig.8. At low frequency, the value of dielectric constant and loss coefficient was high. As frequency increases the dielectric constant become frequency independent. The total dielectric constant will be the sum of electronic, atomic/ionic, dipolar and interfacial/surface polarizations at lower frequency. As the frequency increases, only the electronic polarisation can exists which influences the dielectric constant of a material. Due to the large dc conductivity in the sample N1, the value of tanδ is high[9].

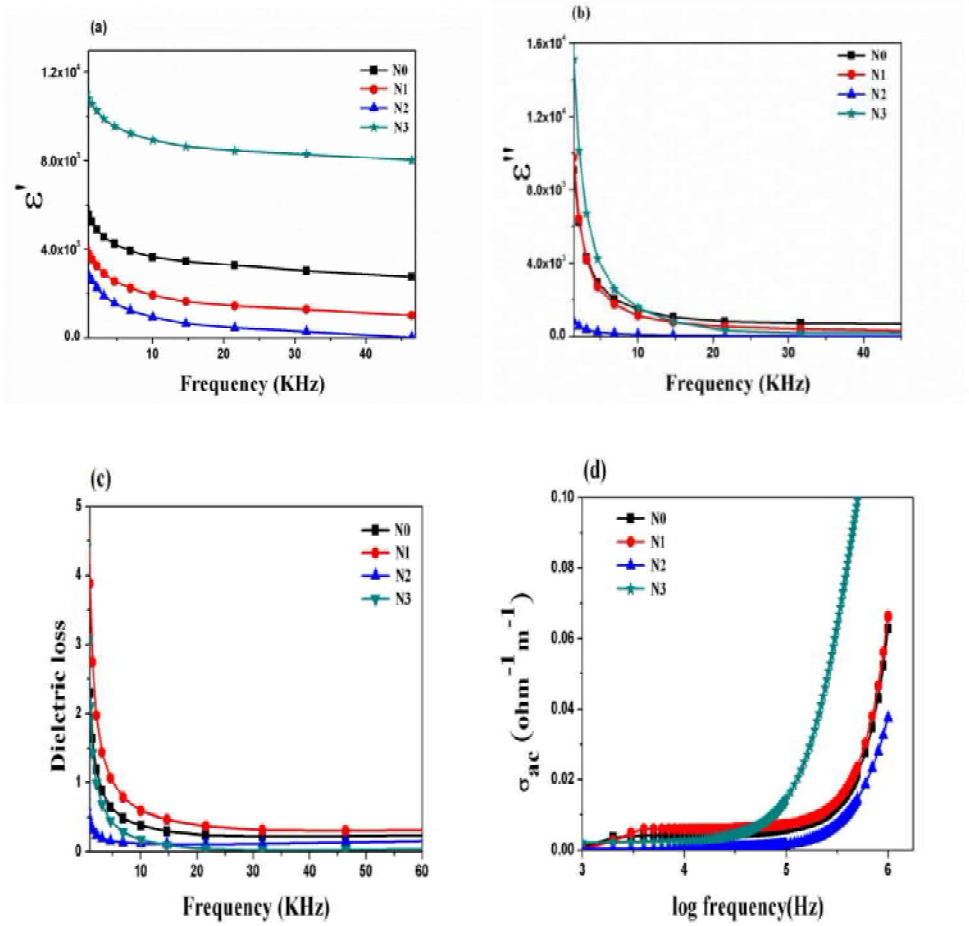

Figure.8.The variation (a) real (b) imaginary part dielectric constant (c) dielectric loss and (d) a.c conductivity of samples N0, N1, N2 and N3

High frequency region of samples shows in Fig.8 has power law behaviour. According to the Jonscher's UDR law (Universal dielectric response), the total electrical conductivity can be written as, $\sigma(\omega) = \sigma_{dc} + \sigma_0 f^s$, $s \leq 1$,where s is the frequency exponent , σ_{dc} is the dc bulk conductivity and σ_0 is a constant. Here up to the frequency of 100 kHz conductivity stayed constant due to the free charge formation and after that the conductivity increases linearly as in the disordered materials. The frequency exponent value was $0 \geq s \leq 1$, from the slope of log σ_{ac} versus log f plot. The Bi(X=0.2) has low conductivity due to the presence of secondary peak and high grain boundary resistance .The Sr doped sample N3 is more conductive material, this result is complementary to the result obtained from impedance spectra[9].

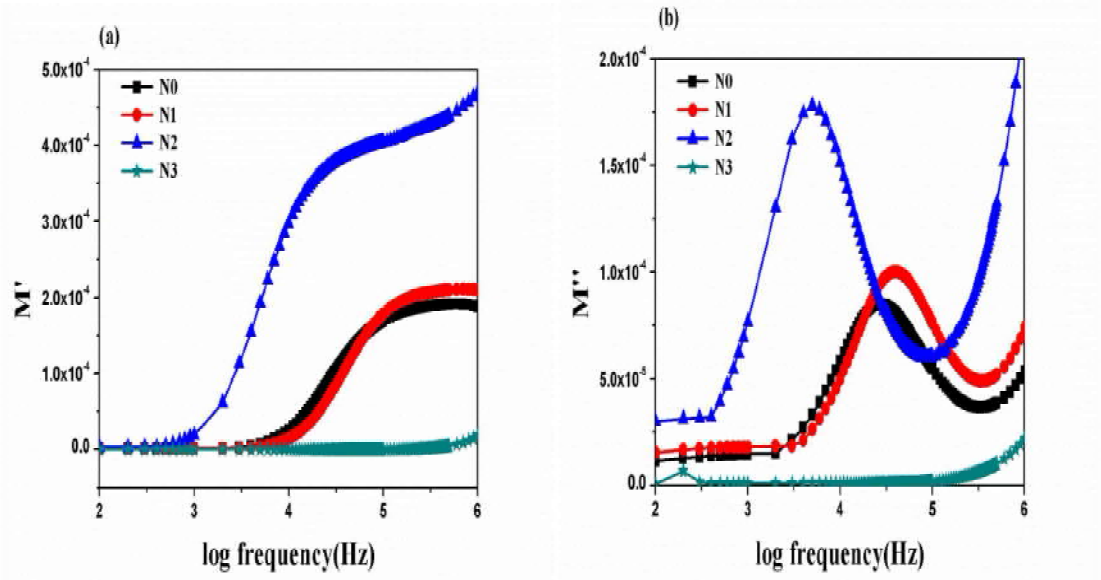

Figure.9. The variation of real and imaginary part of electric modulus with frequency of samples N0, N1, N2 and N3

Inorder to study the relaxation process, we have to introduce a parameter called electrical modulus which is the reciprocal of the complex permittivity Fig.9. At low frequency M' and M" has frequency independent behaviour and above 1 kHz it has frequency dependence. The information about the charge transport mechanism such as electrical transport, conductivity, relaxation etc. can be studied from the electric modulus plot. In imaginary part of electric modulus versus frequency plot a peak was observed which indicates the presence of conductivity relaxation process. The combined dielectric and electric modulus measurements can explains the grain boundary effect and the conduction mechanism in solids. By Maxwell - Wagner Model, the dielectric medium is made of well conducting grains with poorly conducting or resistive grain boundary was responsible for the relaxation process. At low frequency, small conductivity of grain boundary contributed high dielectric constant. The relaxation peak of N2 is shifted to low frequency region due to the presence of the secondary peak of Bi and high grain boundary effect [17] .

Conclusion

The Bi and Sr dopped nanopowders of $NdCo_{0.6}Fe_{0.4}O_3$ multinary perovskites were successfully synthesized by a polymer precursor method. All compounds synthesised have orthorhombic crystal structure with pbnm space group, Bi (x=0.2) shows the existence of secondary peaks. Dense micrographs were obtained from SEM images with an average grain size of the order of hundred nanometres and the grain size were reduced by doping of Bi and Sr. The presence of all elements in the compound was confirmed from EDS spectra. From the impedance and dielectric measurements, it was confirmed that the compound with Bi (x=0.2), N2 has the presence of highly resistive grain boundary wall. The conductivity decreases due to the presence of secondary peaks in N2. Two distinct values for dielectric constant at low and high frequency, and also the asymmetric modulus behaviour indicated the relaxation process. The process of relaxation in these systems was well explained by Maxwell -Wagner model. N3 has less resistive grain boundary wall and are highly conductive materials.

Acknowledgements

Two of the authors Megha.U and Shijina.K acknowledge University Grant Commission, Govt. of India, for the BSR –RFSMS(NO.7-180(BSR)2007 Fellowship.

References

1. Megha U, George Varghese and Shijina K 2016 *Bull. Mater. Sci.* **39** 125-131.
2. Megha U, Shijina K and George Varghese 2014 *Process. Appl. Ceramics* **8** 87-92.
3. Bartolomc F, Kuzmin M D, Bartholonc J, Blasco J and Garcia J 1995 *J. Magn. Magn. Mater.* **140-144** 2159 -2160.
4. Morchshakov V, Haupt L, Barner K, Troyanchuk I O, Rao G H, Ghoshray A and Gmelin E 2004 *J. Alloys. compds*. **372** 17-24.
5. Vinod Kumar, Rajesh Kumar, Shukla D K and Ravi kumar 2013 *J.Alloys. compds*. **574** 316-319.
6. Robert R, Aguirre M H, Hug P, Reller A and Weidenkaff A 2007 *Acta Materialia* **55** 4965-4972.
7. R.W.M.Kwok available from: http://www.phys.cuhk. edu.hk/~surface/ XPSPEAK.
8. D.A.Shirley, Phys. Rev. B. 5; 1972: 4709.
9. Megha.U, George Varghese and Shijina. K 2017 Process. Appl. Ceramics 11[1] 52-59.
10. J .Vegh, J. Electronic Spectrosc. Rel. Phenom. 151; 2006: 159.
11. A.Galenda, M.M.Natile, V.Krishnan, Helmut Bertagnolli, A.Glisenti, Chem. Mater.19; 2007: 2796-2808.
12. Adamczyk M, Ujma Z, Szymczak L, Soszynski A and Koperski J 2007 *Mater. Sci. Eng. B* **136** 170-176.
13. Nadeem M, Akhtar M J, Khan A Y, Shaheen R and Haque M N 2002 *Chem. Phys. Lett.* **366** 433–439.
14. Niranjan Sahu and Panigrahi S, 2013 *Bull. Mater. Sci*. **36** 699–708.
15. Nurdan Demirci Sankir, Erkan Aydin and Mehmet Sankir 2014 *Int. J.Electrochem. Sci.* **9** 3864-3875.
16. Lunkenheimer P, Gotzfried T, Fichtl R, Weber S, Rudolf T, Loidl A, Reller A and Ebbinghaus S G 2006 *J. Solid. State Chem*. **179** 3965-3973.
17. Jianjun Liu, Chun-Gang Duan, Wei-GuoYin, Mei W N and Smith R W 2004 Phys. Rev. B **70** 144106.

4.

Emphasising the role of Silver nanoparticles in the enhancement of photocatalytic efficiency of TiO_2

Rajita Ramanarayanan[a], Sindhu Swaminathan*[b]
[a] S. A. R. B. T. M Goverment College, Koyilandy
[b] Department of Nanoscience & Technology, University of Calicut,
Kerala- 673635, India
email: sindhus@uoc.ac.in

Abstract *The effective utilisation of solar energy to drive catalytic reactions for water purification has received tremendous attention in the recent times. Though semiconductor nanomaterials are being extensively used for photocatalysis, their main drawback lies in their effective utilisation of solar flux due their absorption in UV region. Noble metal incorporated photocatalyst show great promise in this regard by their strong absorption in visible region due to their plasmonic effects. In this work Ag - TiO_2 nanocomposite was synthesized and characterised using Scanning Electron Microscopy (SEM), Energy dispersive X-ray analysis (EDAX), X-ray photoelectron spectroscopy (XPS), Diffuse reflectance spectroscopy (DRS) and photoluminescence (PL) measurements. It was found that the presence of silver nanoparticles in TiO_2 shifted absorbance towards visible region and improved charge transport by suppressing electron-hole recombination. Evaluation of photocatalytic activity by degradation of Methylene Blue dye verified the superior photocatalytic performance of the Ag - TiO_2 nanocomposite over commercial TiO_2.*

Keywords: Photocatalyst, plasmonic, nanocomposite

1. Introduction

Photocatalysis is a promising green technology utilised to tackle environment pollution waste water management. It involves the conversion of light energy from Sun to chemical energy to drive a redox reaction[1]. The semiconductor oxides are the most commonly available photocatalysts because of their band structure. When incident light falls on a photocatalyst the excited electrons move toward the conduction band creating holes simultaneously in the valence band. The electrons react with oxygen molecules to form superoxide radicals and holes react with adsorbed water molecules to form hydroxyl radicals which degrade the organic compounds in water[2].

TiO_2 is one of the most favoured semiconductor photocatalyst because of its stable and non-toxic nature. However TiO_2 suffers limitations due to its limited absorption confining to only UV region which amounts to about 5% of the solar spectrum[3]. Hence the focus of active research since last decade has shifted to doping of TiO_2 to impart colour to the otherwise white TiO_2 thus extending the absorbance to visible region which contributes to about 43% of the spectrum. Noble metal nanostructures due to their surface plasmon resonance are able to concentrate light flux to a small region near its vicinity leading to manifold increase in electric field intensity. In other mechanism charge carriers injected from excited plasmonic-metal nanostructures into the surface of the semiconductor similar to dye sensitization in a dye sensitized solar cell (DSSC). These two mechanisms along with scattering are responsible for light harvesting properties and catalytic behaviour of metal nanostructures[4].These nanostructures in combination with a semiconductor form nano-composite materials which show improved charge separation,significant decrease in electron hole recombination thereby enhancing the overall photocatalytic behaviour[5].In this work Ag-TiO_2 was prepared using an environmentally benign protocol and tested for its

photocatalytic behaviour in the degradation of MB dye under simulated sunlight.

2. Experimental

2.1 Materials

TiO_2 nanoparticles (P25, Sigma Aldrich), Silver nitrate (99.9%) (Merck), distilled water (Millipore System) and ethanol (≥ 99% Sigma Aldrich) were used as reagents and solvents.

2.2 Methods

The leaf extract was prepared by boiling and stirring 3 grams of fresh cleaned guava (Psidiumguajava) leaves for 30 minutes in distilled water using a hotplate(IKA RCT Basic). The extract was cooled and filtered using filter paper and stored at 4 °C for further uses. The extract can be stored for about 2-3 weeks.

For synthesis of silver nanoparticles 1 mL of the extract was added to 20 mL of 1 mM of $AgNO_3$ solution and stirred using pipette to ensure uniform mixing. The colour change of the silver salt solution to pale yellow and then yellowish brown implies the formation of silver nanoparticles. The scheme of the synthesis is depicted in Fig. 1.

The Ag-TiO_2 nanocomposite was prepared by mixing 0.5 gm of commercial TiO_2 in 10 ml of Silver colloid solution and stirred for half hour. The slurry obtained was rinsed with ethanol to remove excess of silver nanoparticles and air-dried at 60 degrees to be used in the experiment.

To study photocatalytic activity, 50 mg of TiO_2 and Ag-TiO_2 was added separately to 50 mL of Methylene Blue (MB) dye of 20 ppm in distilled water. The mixture was stirred under dark condition to reach absorption-desorption equilibrium for 20 minutes. After reaching the equilibrium, about 4 mL of the dye solution was taken and centrifuged for 12,000 rpm for 10 minutes. The solution was studied for decrease in MB concentration by monitoring the principal peak intensity using a UV-Vis Spectrophotometer. Then the mixture is illuminated by 300 W Xenon lamp and the concentration of the dye is monitored after15, 30 and 45 minutes.

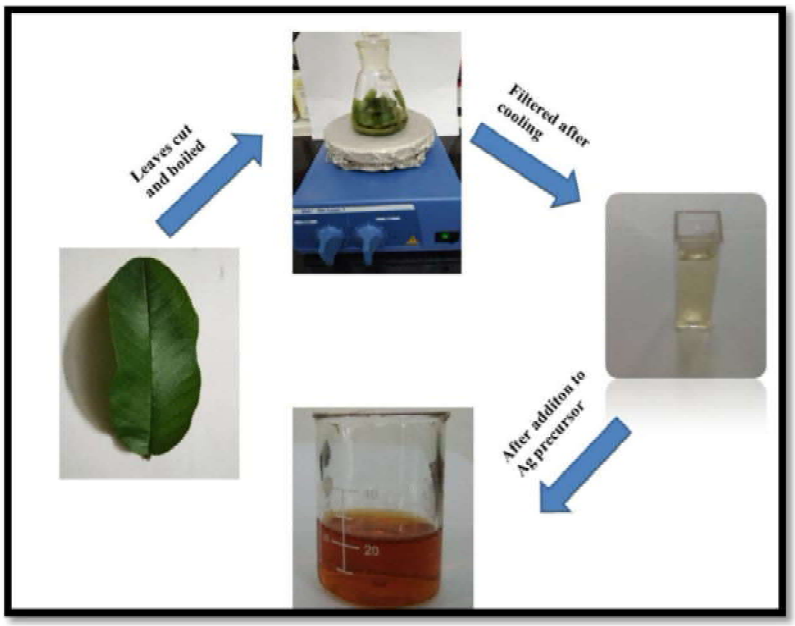

Figure.1 Scheme of synthesis showing formation of Ag nanoparticles

2.3 Characterisation Techniques

The UV-Vis spectrophotometer (JASCO V 750, PG Instruments) was used to measure the absorbance of the nanoparticles and dye samples. The size of the synthesized nanoparticles was determined by transmission electron microscopy (TEM)Jeol/ JEM 2100 using LaB6 source operated at 200 kV. The morphology of the nanoparticles and elemental compositionof the sample was investigated using Carl-Zeiss Gemini SEM 300 field emissionscanning electron microscope. The fluorescent measurements were conducted using PerkinElmer (LS55) in the visible range. The photocatalytic measurements were conducted using photocatalytic reactor (LZCX-XE) using 300W Xenon Lamp.

3. Results and Discussion

Fig. 2(a) shows the UV absorption spectrum of silver nanoparticles showing the characteristic peak around 425 nm [6]. Plasmonic metal nanostructures interact with incident light resulting in the local enhancement of electromagnetic fields in the neighbourhood of the nanostructures [7].

The TEM analysis of the Ag NPs indicates stable, well dispersed, near spherical nanoparticles in the size mostly around 25 nm as calculated using Image J software. Hot electron generation is generally seen in Ag nanoparticles around this range which are efficiently captured by forming Schottky barrier with semiconductors like TiO_2 who possess high density of states in its conduction band [8].

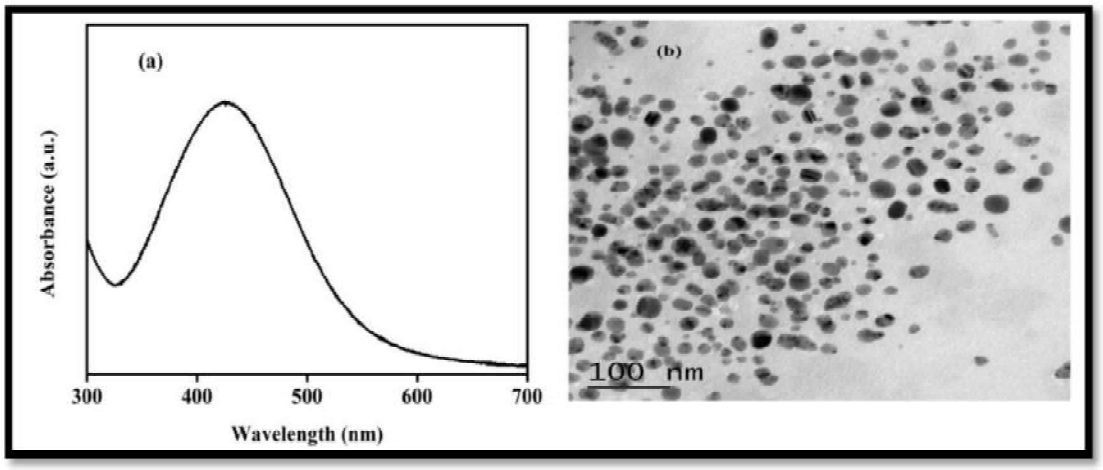

Figure.2 (a) Absorbance of silver nanoparticles (b) TEM image of silver nanoparticles

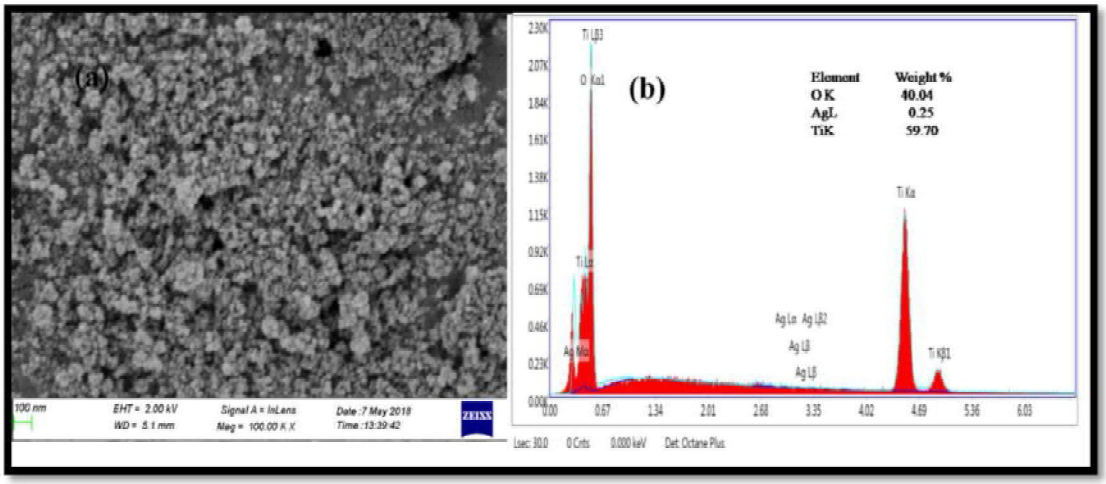

Figure. 3(a) SEM image of Ag- TiO_2 (b) EDAX spectrum of Ag- TiO_2

The SEM and EDAX spectrum of Ag- TiO_2nanocomposite is shown in Fig 3(a) and 3(b).The EDAX analysis shows a value of about 0.25 % Ag in TiO_2 which is much lower than the previous reports on Ag-TiO_2 photocatalysis [9] .

The Tauc plots (Fig.4) were drawn to calculate the bandgap of Ag-TiO_2 and bare TiO_2using UV-vis Spectrophotometer. Obtained E_g values are 3.3eV for bare TiO_2 and3.1 eV forAg-TiO_2 showing direct indication of bandgap narrowing due to the presence of metal nanoparticles in TiO_2. This bandgap narrowing is due to the downward shift of conduction band and upward shift of valence band due to the presence of large number of free electrons by virtue of Ag NPs[10]. Thus bandgap reduction shifts the optical absorbance towards the visible region acting favourably towards harnessing the solar spectrum for better photoactivity.

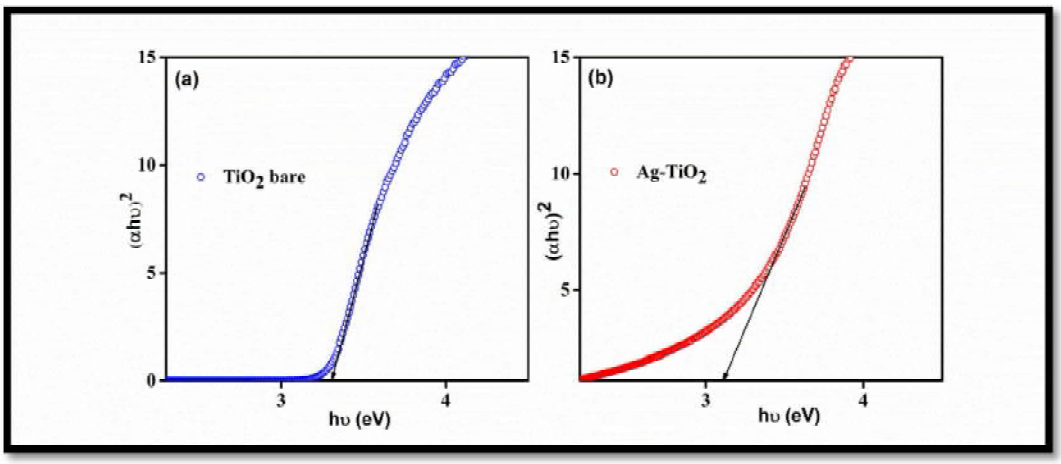

Figure.4 Tauc plot representing bandgap of (a) TiO_2 (b) Ag-TiO_2

The surface composition of Ag-TiO_2 XPS spectra are shown from Fig 5 (a) to5 (d). The survey spectrum of 5 (a) shows peak at 284.2 eV corresponding to carbon from the instrument, Ag peaks at 366.38 and 372.4 eV, Ti 2p peak at 457.4 eV and O 1s peak at 528.74 eV as seen in the figure. Fig .5 (b) shows O1s spectrum with two peaks due to Ti-O

at 528.74 eV being the dominant peak and O-H peak at 530.227 eV being the minor peak. The Ti 2p $_{3/2}$, Ti 2p $_{1/2}$ peaks at 457.4 and 463.03 eV are evidence of Ti^{4+} formation in TiO_2 (Fig. 5(c)).The Ag $3d_{5/2}$,$3d_{3/2}$ peaks appearing at binding energies 366.38eV and 372.4 eV (Fig.5 d) due to splitting of 3d doublet peak shows a difference of 6 eV which is indicative of the metallic nature of silver [11].

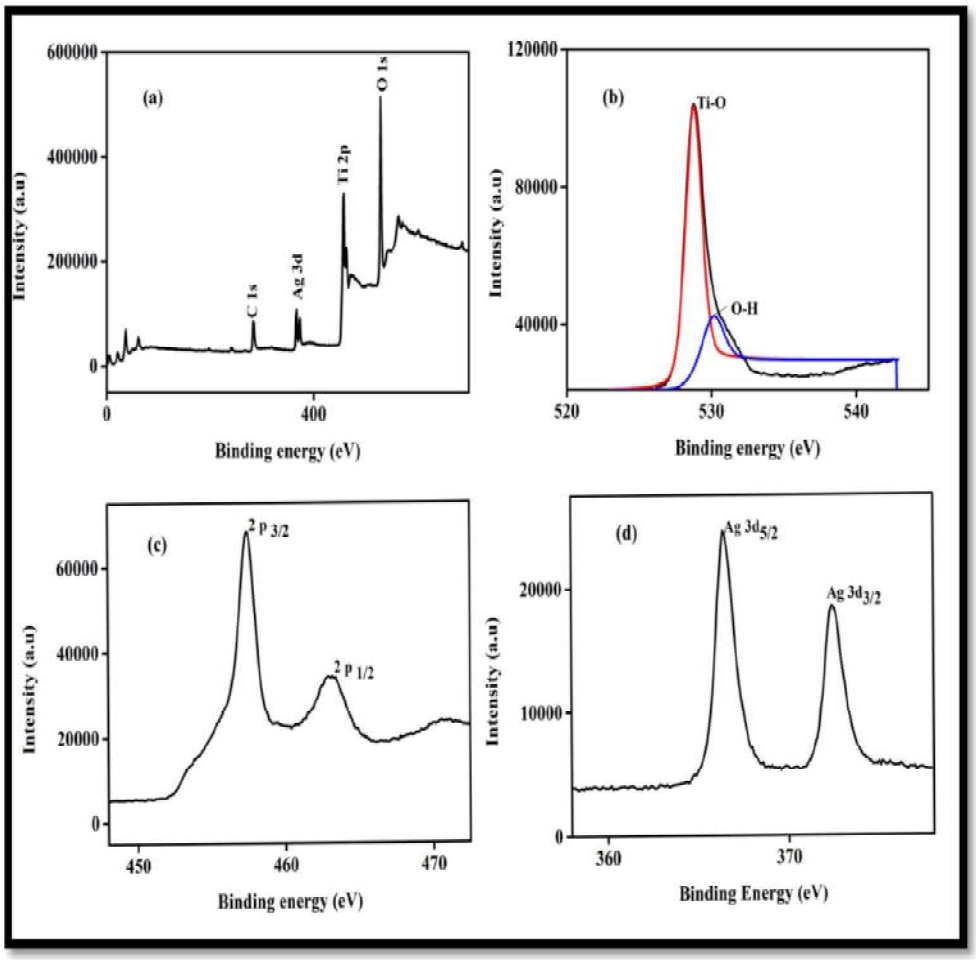

Figure.5 XPS (a) survey spectrum (b) O 1s (c) Ti 2p (d) Ag 3d

The PL spectra for Ag-TiO_2 nanocomposites samples after excitation (340 nm)are shown in Fig.6 (a).The spectra show three main emission peaks at 420nm (2.95 eV), 486 nm(2.55 eV) and 527 nm (2.35 eV). PL emission spectrum is an important tool to study the charge transfer/recombination dynamics for better performance of photocatalytic samples. It is seen that Ag- TiO_2 shows reduction in PL (Photoluminescence) intensity as compared to TiO_2 sample. The suppression of PL intensity in Ag-TiO_2can be attributed to the formation of Schottky barrier at Ag and TiO_2 interface retarding electron hole recombination processes and thereby promoting better transport of electrons[12].

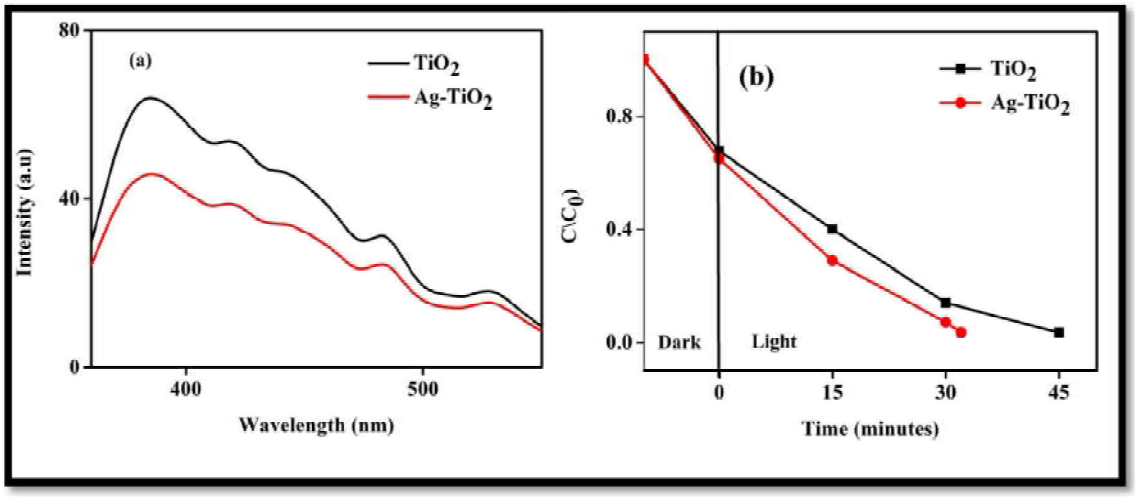

Figure.6 (a) Pl spectrum (b) photocatalytic degradation of MB dye of TiO_2 and Ag- TiO_2

The photocatalytic dye degradation of 20 ppm MB in presence of TiO_2, Ag- $TiO_2$is checked inside a photocatalytic reactor under 300 W Xe lamp. The plot of C/C_0 versus time was drawn as shown in Fig.6b where C_0 is the initial concentration and C is the concentration of MB dye at regular intervals. It is observed that Ag- TiO_2 nanocomposite shows almost complete degradation in 32 minutes compared to 45 minutes taken by commercial $TiO_2$to achieve the same. The improvement in the hybrid system of Ag- TiO_2 is due to to the various plasmonic enhancement mechanisms of silver nanoparticles like surface plasmon resonance, hot electron transfer and near field enhancement which ensures better charge separation and improved lifetime of the electron hole pairs. The photograph of the sample after 30 minutes has been presented in Fig.7.The Fig.7a corresponding to pure sample is normal blue colour, the TiO_2 sample (Fig.7b) is pale blue whereas Ag- TiO_2 is completely colourless (Fig.7c).

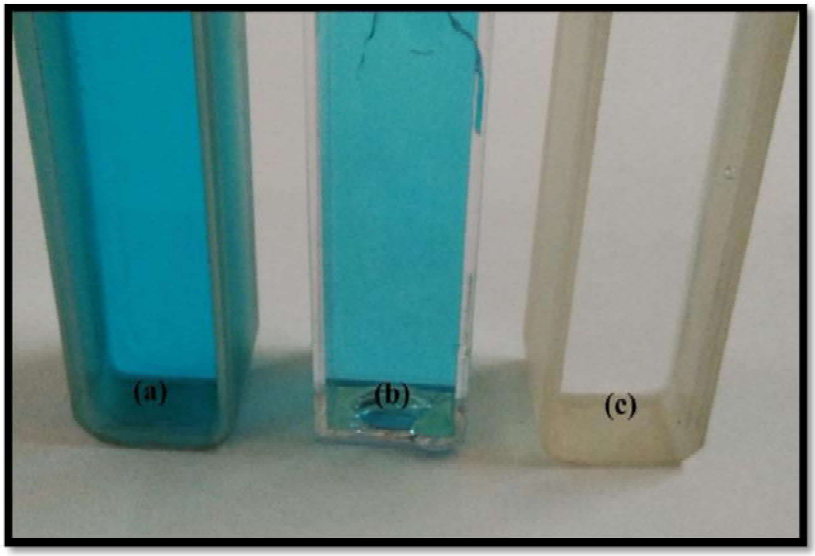

Figure.7 (a) MB dye, Dye degraded samples after 30 min (b) TiO_2 (c) Ag-TiO_2

The scheme depicting the photcatalytic degradation of pollutant dye Methylene Blue has been presented inFig.8. Ag nanoparticles absorb visible light due to LSPR characteristics and inject the excited electrons into the conduction band (CB) of TiO_2through various plasmonic mechanisms. These electrons (e–) combine with molecular oxygen to form superoxide (O_2^-) radicals which on protonation yield HO_2 radicals. The HO_2 become H_2O_2 before finally forming OH free radical which act on MB dye to form water, carbon dioxide and volatile organic compounds[13].

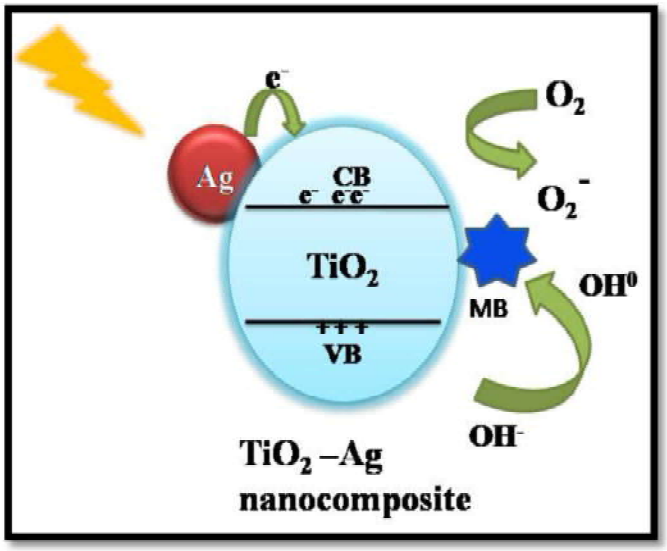

Figure.8 Schematic diagram illustrating, the photocatalytic degradation of MB dye

4. Conclusions

In this report the Ag-TiO_2 nanocomposite was prepared by direct mixing of TiO_2 and silver nanoparticles synthesized using a green method and characterized using various techniques. The Ag nanoparticles appear as prominent peaks on XPS spectra of Ag-TiO2 confirming the presence of silver on the surface of the photocatalyst. The Ag nanoparticle concentration was found to be about 0.25 wt % in the prepared nanocomposite as indicated by EDAX analysis. The incorporation of silver to TiO_2 had the advantage of narrowing of bandgap from 3.3 eV to 3.1 eV and reduction in PL intensity. The photocatalytic activities of the both samples Ag-TiO2 and bare TiO_2 examined by degradation of the MB dye under light irradiation showed increased photocatalytic activity of Ag-TiO_2 attributed to lower band gap energy as well as lower electron-hole recombination rate. The Ag-TiO2 nanocomposite shows complete degradation in 32 minutes as compared to 45 minutes taken by commercial TiO_2 powder. Overall it is proposed that synergetic effect of plasmonic effects like the surface plasmon resonance phenomenon, hot electron transfer and field enhancement contribute for enhanced photocatalytic behaviour of Ag-TiO_2.

Acknowledgements

The authors would like to acknowledge Central Sophisticated Instrumentation Facility (CSIF) of the University of Calicut for SEM analysis. The authors are grateful to Dr. Shaji and Mr. Sreed Sharma, Universidad Autonoma de Nuevo Leon, Mexico for the XPS analysis. The

authors thank Dr Libu Alexander (Assistant Professor) and Anju. K (Research Scholar) of Department of Physics, University of Calicut for UV measurements.

References

[1] A. Primo, A. Corma, H. García, Titania supported gold nanoparticles as photocatalyst, Phys. Chem. Chem. Phys. 13 (2011) 886–910.

[2] B. Ninnora, M. Rajita, R. Sindhu.S, Surface modification of oxygen-deficient ZnO nanotubes by interstitially incorporated carbon : a superior photocatalytic platform for sustainable water and surface treatments, Appl. Nanosci. (2018) 1–11.

[3] S.G. Ullattil, R.M. Ramakrishnan, Defect-Rich Brown TiO 2– x Porous Flower Aggregates: Selective Photocatalytic Reversibility for Organic Dye Degradation, ACS Appl. Nano Mater. (2018) 4045–4052.

[4] S. Linic, P. Christopher, D.B. Ingram, Plasmonic-metal nanostructures for efficient conversion of solar to chemical energy, Nat. Mater. 10 (2011) 911–921.

[5] C. Clavero, Plasmon-induced hot-electron generation at nanoparticle/metal-oxide interfaces for photovoltaic and photocatalytic devices, Nat. Photonics. 8 (2014) 95–103.

[6] S. Jain, M.S. Mehata, Medicinal Plant Leaf Extract and Pure Flavonoid Mediated Green Synthesis of Silver Nanoparticles and their Enhanced Antibacterial Property, Sci. Rep. 7 (2017) 1–13.

[7] J. Li, X. Chen, N. Ai, J. Hao, Q. Chen, S. Strauf, Y. Shi, Silver nanoparticle doped TiO 2 nanofiber dye sensitized solar cells, Chem. Phys. Lett. 514 (2011) 141–145.

[8] W.R. Erwin, H.F. Zarick, E.M. Talbert, R. Bardhan, Light trapping in mesoporous solar cells with plasmonic nanostructures, Energy Environ. Sci. 9 (2016) 1577–1601.

[9] C. Su, L. Liu, M. Zhang, Y. Zhang, C. Shao, Fabrication of Ag/TiO2nanoheterostructures with visible light photocatalytic function via a solvothermal approach, CrystEngComm. 14 (2012) 3989–3999.

[10] S.P. Lim, A. Pandikumar, H.N. Lim, R. Ramaraj, N.M. Huang, Boosting photovoltaic performance of dye-sensitized solar cells using silver nanoparticle-decorated N,S-Co-doped-TiO_2 photoanode, Sci. Rep. (2015) 1–14.

[11] J. Yu, J. Xiong, B. Cheng, S. Liu, Fabrication and characterization of Ag-TiO2multiphase nanocomposite thin films with enhanced photocatalytic activity, Appl. Catal. B Environ. 60 (2005) 211–221.

[12] R.S. Varma, N. Thorat, R. Fernandes, D.C. Kothari, N. Patel, A. Miotello, Dependence of photocatalysis on charge carrier separation in Ag-doped and decorated TiO2 nanocomposites, Catal. Sci. Technol. 6 (2016) 8428–8440.

[13] J. Tae Park, C. Soo Lee, C. Hun Park, J. Hak Kim, Preparation of TiO2/Ag binary nanocomposite as high-activity visible-light-driven photocatalyst via graft polymerization, Chem. Phys. Lett. 685 (2017) 119–126.

5.

Realistic Assessment of Radiation Protection aspects from Positron Emission Computed Tomography in Nuclear Medicine and from Medical Linear Accelerator in Radiation Therapy- An institution based analyses

Bhagyalakshmi AT[1,2], Arun Krishnan MP[2] , Sreejith PK[1],TS Sankaran Nair[1], Fasila NK[1], Simi TK[1], Nadiya K[1], Ummal Momeen[2], Velayudham Ramasubramanian[2*]

[1]Department of Medical Physics, Baby Memorial Hospital, Kozhikode

[2]School of Advanced Sciences, Vellore Institute of Technology,Vellore

*Corressponding Author: Velayudham Ramasubramanian

Email: vramasubramanian@vit.ac.in

Abstract *The purpose of this study is to quantify the amount of radiation exposure received by occupational workers as per the weekly workload in PETCT and Linac. To check for safety in extreme condition, exposure levels were calculated at the highest possible capacity in the PETCT department. Clinac iX (Varian) medical linear accelerator is capable of generating 6 and 15 Mega voltage X rays and these can be judiciously used for the treatment of several kinds of cancers. The penetration of 6 and 15MV beams are separately computed based on the tenth value layers of concrete for both the energies. The exposure levels measured were 15.76mSv/year with opened door and 8.18mSv/year with door closed, considering full occupancy at the console and corridor in interest. The radiation levels calculated behind the secondary barrier from the photons scattered through an angle of 90° is 0.0021mSv/day for 6MV and 0.0018mSv/day for 15MV. This accumulates to an annual radiation dose of 1mSv in a year from both 6 and 15 MV X-rays in Linear Accelerator. The calculated radiation doses outside the PET CT and Linear accelerator room account for the exposure at the prevailing conditions of use. The results show that, with adequate shielding, the exposure level calculated is well within the permissible dose limits. However, the cardinal principles of 'Time Distance and Shielding' should be strictly followed in both the departments to ensure maximum radiation safety.*

Keywords: Radiation safety, background radiation, PETCT, radiation therapy

1.Introduction

Radiation risks have always been a matter of concern among personnel involved in its use in health care services. Positron Emission Computed Tomography (PET CT) in Nuclear Medicine and Linear Accelerator (Linac) in radiation therapy are among the services that use high energy photons. Natural or man-made sources of radiation in small or large amounts can pose some kinds of biological effects.[1] Radiation causes ionizations of atoms which may affect molecules, which may then affect cells, then tissues, then organs and finally the whole body. In general there are two types of effects on cells- direct effect and indirect effect. In direct effect, DNA is damaged directly by the ionizing radiation and in indirect effect the hydroxyls (free radicals) formed by the ionization of water molecules affect DNA.

The effects associated with radiation are classified as stochastic and non-stochastic effects or deterministic effects. The risks involved with stochastic effects are based on Linear Non Threshold (LNT) model which states that such effects can occur either at very low or very high doses, however, the probability of occurrence of such effects increases with increased chronic radiation exposure. Cancer and genetic effects come under stochastic effects. Since no threshold doses are defined, even those from natural sources can contribute

to these effects and the exposure need not be occupational. Non-stochastic effects are deterministic effects which are certain to occur beyond a particular threshold doses and some of these may be lethal. For example, Nausea-Vomiting-Diarrhea (NVD) syndrome, Gastro-Intestinal (GI) syndrome, Central Nervous System (CNS) syndrome, etc. In addition to these, erythema, epilation, cataract etc can occur because of partial body exposure beyond certain tolerance doses. The doses expressed in Gray and the corresponding effects are summarized in table 1.

Sl no	Radiation effects	Threshold doses (Gy)	Type of exposure
1	NVD Syndrome	0.5-1	Whole Body
2	Bone Marrow Syndrome	3-10	Whole Body
3	GI Syndrome	10-30	Whole Body
4	CNS Syndrome	>30	Whole Body
5	Erythema	3-10	Partial body
6	Epilation	>3	Partial body
7	Cataract	2-5	Partial Body
8	Temporary Sterility(Testes)	0.3	Partial Body
9	Permanent Sterility(Testes)	3.5-6	Partial Body
10	Sterility (Ovaries)	2.5 - 6	Partial Body

Table 1: Threshold doses for various biological effects as per IAEA tech doc module IX[2]

Hence it becomes necessary for the radiation professionals to practice safe measures to keep their occupational exposures below stated dose limits. In spite of several harmful effects, use of radiation is a revolutionary development in the field of medicine, if used judiciously. It now finds its application in physiological and functional imaging and also in cancer therapy. Starting from the conventional X-rays that provide the planar imaging of high density components in the human body, Computed Tomography (CT) scanners provide more accurate information of all body tissues and pathological conditions. With the advent of Nuclear Medicine based imaging, radioisotopes can also be used to analyze the functional aspects of cells. This helps in the early detection of recurring tumors post therapy. Ionizing radiations also find its application in cancer therapy effectively. From the earlier effective modality using ortho-voltage therapy, the technology emerged through Mega voltage energy gamma and X rays and reached the proton and heavy ion therapy, improving the accuracy, better tumour control and improved quality of living post treatment.

The Atomic Energy Regulatory Board (AERB, Mumbai, India) is the national competent authority taking care of the installation and safe functioning of the radiation facilities throughout the country. For any institution to handle radioactive or radiation generating equipments, their installations and equipments should comply with the safety standards stipulated by AERB. License for the operations of the facility will be provided only if the design and equipment are in compliance with their given code of practice recognized separately for various types of installations. These codes take care of the principle of justification, optimization and dose limits for radiation safety. Any radiation exposure is justified only if the benefits override the risks associated with the exposure. Radiation safety is a multilevel process involving the competent authority, management of the institution and the occupational staff. The major role is played by the occupational staff to optimize the cardinal principles of time, distance and shielding while handling radiation and hence to keep

the exposure to staff and public to safe dose limits and confine to the concept of ALARA (As Low As Reasonably Achievable) . A dose greater than 20mSv should not be received by an occupational worker in a year, when averaged over five years is the dose limit, stated by national and international regulatory bodies. And as per AERB in any year the annual dose should not exceed a limit of 30 mSv. Similarly the facility design and equipment usage should ensure that annual dose to the public should not exceed 1 mSv in a year. The purpose of this study is to quantify the amount of radiation exposure received by the occupational workers as per the weekly workload of PET CT and Linear Accelerator.

2.Materials and Methods

The workload measurements were carried out on a Discovery IQ 3 ring PET facility with an integrated 16 slice CT scanner from GE and Clinac iX Medical Linear Accelerator with 6 and 15 MV photon energies and 5 electron energies (4, 6,9,12 and 15 MeV) from Varian.

Figure 1: Discovery IQ 3 ring PET CT scanner

Figure 2. Clinac iX Linear Accelerator

PET CT uses Fluorodeoxyglucose (FDG) as the radiopharmaceutical with F-18 as the radio-isotope. Radioactive F-18 emits a positron in order to achieve stability, which then interacts with another electron in the Coulombic field of the nucleus emitting a pair of 511 keV gamma photons in opposite directions to conserve both momentum and energy. The simultaneous detection of photons in oppositely placed detectors constitutes an event, which is then recorded and interpreted as signal.[3]

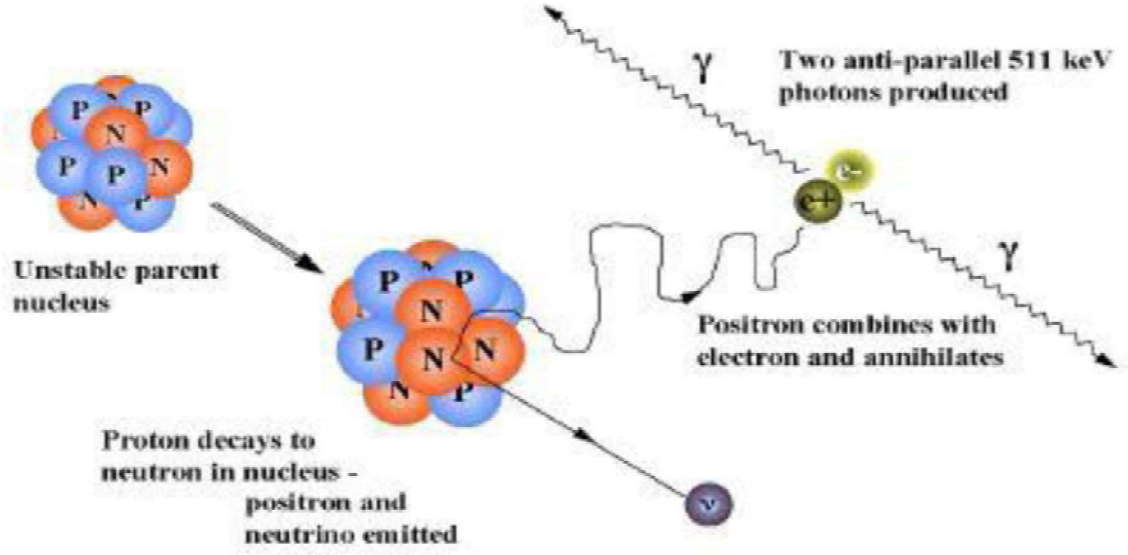

Figure 3: Annhilation of electron positron pairs to produce two anti-parallel 511keV gamma rays

Once FDG is injected into the patient body, maximum uptake occurs in brain, bladder, and heart and also in the site of tumour. Patient post administration is allowed to wait for one hour prior to scan so as to enhance its uptake in tumour (if present). The sources of radiation in PET CT facility are mainly:

a. Patient undergoing scanning
b. Dose administration room
c. Dose administered patient waiting area
d. Residual activity in vials

In this study a theoretical analysis has been carried out with the maximum capacity of the PET CT facility. It includes three patients in post administered patient waiting area and one patient on the couch undergoing scanning. Exposure to the occupational staff in the control console and the same person standing throughout entire working hours beside the patient waiting area were calculated. This helps in estimating the safety at maximum condition. Calculations were carried out by precisely evaluating the effect of time, distance and shielding. Two conditions were adopted while calculating the exposure level beside post dose administered patient waiting area- one with doors of waiting area opened and the other with doors closed.
For linac, the workload of 6MV and 15 MV photons were separately analysed. Different patients required different amount of radiation doses which were calibrated as

1monitor units (MU) = 1 centi-Gray,

for 10cm X 10cm field size, at a depth of maximum dose, keeping source to surface distance at 100 cm in a water phantom used for measurement; where Gray is the unit of absorbed dose and MU is the machines perceived format for dose. Control console of Linac is the region of full occupancy and the amount of exposure received by the staff occupying this region is

theoretically evaluated. The design of shielding barriers of Linac room is in such a manner that no primary radiation reaches the occupancy in control console, however it is the high energy scattered radiations that have the probability to penetrate the barrier. The radiations undergoing Compton scattering through 90 degree angle is highly energetic and for that reason, here we make an assumption that all the scattered radiations are emanated through 90 degree angle. This assumption characterizes safety in worst condition, as not all radiations are emitted at 90 degree scattering angles. Table 2 shows the leakage Tenth Value Layers (TVLs) of concrete for 90 degree scattered radiation for 6 and 15 MV beams

Energy	Leakage TVLs (cm)
6 MV	34 (29)
15 MV	36 (33)

Table2: First term is the first TVL and term in the bracket is for all other remaining TVLs. Data from NCRP #151[4]

The use factor of wall beside the control console was taken as 1, as the wall in interest was secondary barrier used to stop the scattered radiation, which prevails at all the exposure conditions. The factor of time, distance and shielding was again carefully considered during calculations.

3.Results

Table 3 shows the activity handled in a day in PET CT installation. The maximum possible exposures in the department of PET CT was calculated in two conditions; one with lead lined door in injected patient waiting area opened and second with the door closed. The exposure levels measured were 15.76mSv/year with opened door and 8.18mSv/year with door closed, considering full occupancy at the console and corridor in interest.

Patient No	Activity Injected(mCi)	Activity Remaining in syringe (mCi)	Time of injection (hrs)	Time of scanning (hrs)	Time when patient leaves dept(hrs)
P1	6.8	0.484	08:12	09:15	10:15
P2	6.1	0.052	09:31	11:15	12:15
P3	5.2	0.05	09:20	10:45	11:45
P4	7.8	0.062	08:21	09:50	10:50

Table 3: Activity handled in a day in PET CT installation.

A single day workload comprised a total of 5732 monitor units (MU) of 6MV photons which is divided as 1612 MUs towards the floor, 1522MUs towards the left wall, 1356 MUs towards the ceiling and 1242MUs towards the right wall. In addition to this a few patients were treated with 15 MV photons; 151MUs towards the floor, 457MUs towards the left wall, 174 MUs towards the ceiling and 298MUs towards the right wall making a total of 1080MUs in a day. The radiation levels calculated behind the secondary barrier from the photons scattered through an angle of 90° is 0.0021mSv/day for 6MV and 0.0018mSv/day for 15MV.

This accumulates to an annual radiation dose of 1mSv in a year from both 6 and 15 MV X-rays in Linear Accelerator.

4. Discussion and Conclusion

The study concluded that the occupational exposure for technologist in nuclear medicine facility and radiotherapy facility with existing workload were well within the tolerance stated by Atomic Energy Regulatory Board of India.[5] However additional advantages occur for the PET CT occupational workers, if the door of patient waiting area is kept closed throughout the procedure. The activity administered to patients undergoing PET CT is very less and hence following the concept of time, distance and shielding will effectively reduce the occupational exposure. Even more, the study has overestimated the time spent by the technologists near the post dose administered patient waiting area and thus in actual scenario the exposure received by the staff will be much less Sivert per year. Practice of rotation of occupational staffs in radiation areas enables sharing of doses and thus effectively reducing the average exposure per person.

In the case of Linac total exposure from 6 MV and 15 MV beams accumulates to 1 mSv in a year, which is very much below the maximum 30 mSv stipuated by AERB for a year. The exposure is highly controlled in linac as radiation exists only when the unit is energized, otherwise the room is free from any harmful radiations. The important factor to be taken care in a linac facility is the neutron production followed by the delivery of 15 MV photons. The threshold energy for photo nuclear reaction (production of neutrons) is 10 MV and beyond this energy its cross section increases. An example of such photonuclear reaction is the conversion ^{208}Pb to ^{207}Pb, by capturing photon and releasing neutron

$$^{208}\text{Pb}\ (\gamma,n)\ \text{Pb}^{207}$$

Neutron has the capability to induce artificial radioactivity in materials with which it interacts. These induced radio activities may last for few seconds to few hours. However, long lived isotopes will be lesser in number and may radiate equivalent to the background radiations. It is advisable to the radiotherapy technologists to wait for a minute or two before entering the treatment room after the delivery of 15 MV photons. This considerably reduces the exposure levels to radiotherapy technologists.

The design and construction of our installations has been meticulously planned, such that the dose levels for staff and public are within the stipulated tolerance values.[6] Routine quality assurance checks of equipments and radiation safety surveys of the installations are carried out to ensure adequate safety to staff and public. Thus adhering the dose limit of less than1mSv for general public and less than 20 mSv for occupational workers.

No area on the globe is free from radiation. Radioactive material is found throughout nature. Detectable amounts occur naturally in soil, rocks, water, air, and vegetation, from which it is inhaled and ingested into the body. In addition to this internal exposure, humans also receive external exposure from radioactive materials that remain outside the body. These include cosmic radiation and environmental radioactivity from naturally occurring radioactive materials such as radon, radium and potassium-40, and man-made fallout from nuclear weapons testing and nuclear accidents. The coastal belt of

Karunagappally, Kerala, India, is known for high background radiation (HBR) from thorium-containing monazite sand.[7,8]

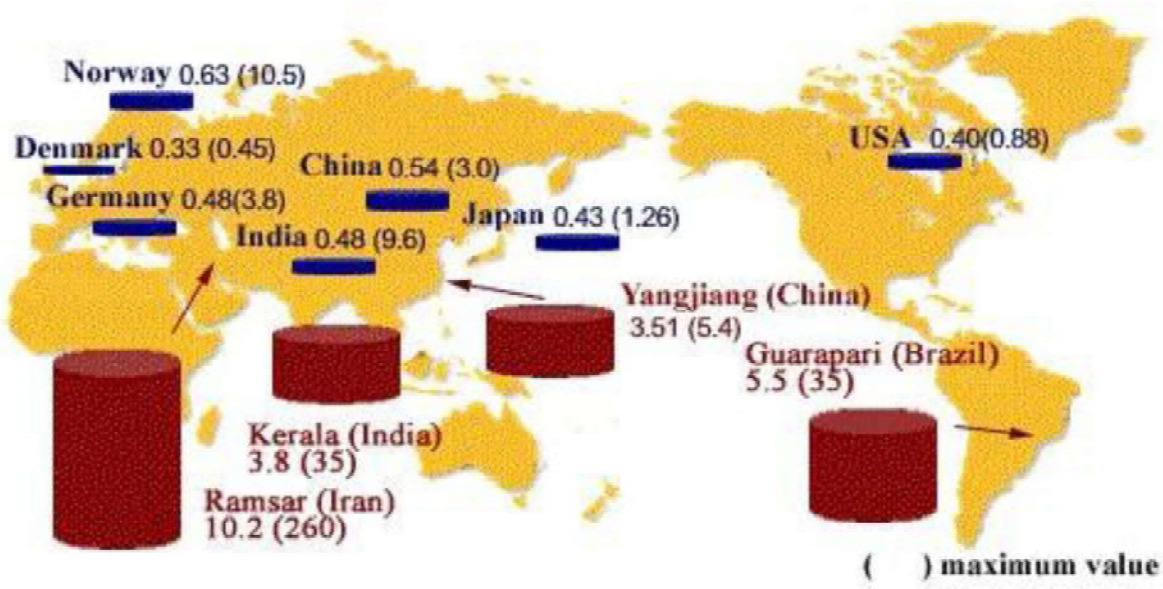

Figure 4: High Background Radiation Areas (HBRA) around the world, numbers are given in mSv/year. [9]

However, study conducted on the population has not shown any considerable increase in the incidence of cancer or any other genetic effects.[9] Figure 4 gives a picture of High Background Radiation Areas on the globe, where India secures 3rd place. There are regions where the background radiation is much greater than the dose limits stipulated. Over generations people are being affected by such radiation exposure. Studies have been carried out on short lived organisms like fruit flies - Drosophila melanogaster, which provided the first evidence of the influence of the radiation environment on life span, fertility and response to genotoxic stress at the organism level.[10] Since, humans are long lived organisms study over several decades are necessary to come to a conclusion. However, in the case of man-made exposures, any exposure unjustified or avoidable is considered as harmful, as the benefit with radiation exposure should very well override the risks associated with this.

References

1. Neil Fullera, Adélaïde Lereboursa, Jim T. Smithb, Alex T. Forda,* The biological effects of ionising radiation on Crustaceans: A review. 0166-445X/© 2015 the Authors. Published by Elsevier B.V
2. Threshold doses for various biological effects as per IAEA tech doc module IX
3. Burton E. Sobel, M.D. St. Louis, MO.Diagnostic promise of Positron tomography.AM HEART J 103:673, 1982.)
4. NCRP #151.
5. Radiation Protection Rule -2004, Department of Atomic Energy, India.
6. AERB SAFETY CODE. CODE NO. AERB/RF-MED/SC-1 (Rev. 1)
7. Nair RR[1], Rajan B, Akiba S, Jayalekshmi P et. al. Background radiation and cancer incidence in Kerala, India-Karanagappally cohort study.

8. M Krishnan Nair, KSV Nambi, N. Sreedevi Amma, et. Al. Population Study in the High Natural Radiation Areas in Kerala, India. Official Journal of the Radiation Research Society.
9. SM Javad Mortazavi(EFN). High Background Areas of Ramsar, Iran
10. Morciano P[1], Cipressa F[1,2], Porrazzo A et al. Fruit Flies Provide New Insights in Low-Radiation Background Biology at the INFN Underground Gran Sasso National Laboratory (LNGS).

6.

A Review on the study of electro-migration failure mechanism in metallic thin films and its effects on alloying the metals.

Hind. N
Department of Physics, DGM MES Mampad College, Malapuram-676542, Kerala, India
hindneelamkodan@gmail.com

Abstract *The electromigration failure mechanism becomes more dominant in microelectronics integrated circuit interconnects, since the size of interconnects becomes smaller and smaller as the technology develops. High current density needed is also a main key factor for electromigration failure in such circuits. Alloying the metallic thinfilm interconnects is predicted to be more resistant against EM failure. The purpose of this paper is to check the nature of electromigration phenomena in metallic thinfilms and alloying effect on EM damage in IC interconnects.*

Introduction

The miniaturization of device dimension offers high performace ICs operating at increased power loads and elevated temperatures. But as the dimensionof device is downscaled, the resistance and current densities increase subsiquenlty[1]. The increased current density causes joule heating film temperature to be increased which leads to the electromigration failure in IC interconnects. So reducing EM failure in microelectonic devices is a great challenge for thinfilm science and industry. Electromigration phenomena is a mass transport process under the influence of an external field[1].

In solid bodies Material migration can be occurred by various inducing forces[6]. 1. chemical diffusion due to concentration gradients, (2) material migration caused by temperature gradients, (3) material migration caused by mechanical stress, and (4) material migration caused by an electrical field. This last case is often referred to as electromigration. The electron wind force is the dominant force for migration of atoms in materials. This movement of atoms produces hillocks and voids which in turn results in the damage of device due to short circuit paths and open circuits[4].

Results and Discussions

In microelectronic industry electromigration mechanism is a serious problem[2]. This electromigration failure causes massive damages to very-large-scale-integration (VLSI) electronic devices[3].Aluminium and copper are the most common used materials for IC interconnects. But the recent observation point that both of them suffer electromigration failure at high current densities[2].It was reported that Cu is considered as a better candidate of interconnects due to its lower resistivity, minimal joule heating, larger resistance to electromigration. Hence the electromigration failure is less severe in Cu than that of in Al[4].

The table shows a comparison between Cu and Al properties [4]

Material	Resistivity Ohm cm	Melting Point (^{0}C)	Diffusivity at 100^{0}C(cm^2/s)		
			Lattice	GB	Surface
Cu	1.67	1083	$7x10^{-28}$	$3x10^{-15}$	10^{-12}
Al	2.67	660	$1.5x10^{-19}$	$6x10^{-11}$	

Al and Cu films prepared by e- beam evaporation were studied for electromigration effects [2]. Both of them were patterned in to different conducting channels by photolithography. The structural studies were done by STM. On comparing mechanical stress offered by electrical current with that of unstressed lines, a significant grain growth was observed in the areas of hillocks formation. But the structure was found to be remained unchanged in the area of unstressed lines. Hence the stressed areas were considered as damaged due to grain boundary migration. Also in stressed areas large boundary inclinations were observed which is an indication of grain boundary migration. The increased grain thickness and GB migration were the main processes involved in the hillock formation in stressed areas[2].

Since aluminium has the problem of fast oxidation, gold is a suitable metal for electromigration studies[3]. Electromigration induced effects in gold thinfilms prepared by free evaporation were studied by STM and Grazing X ray diffraction techniques. Topographic images obtained by STM showed that the surface of gold films is very rough with granular structures of various heights and width. But it was found that the electric current made a rearrangement of gold film surface to form perfect microcrystals. This is because application of large current produce joule heating effect which leads to EM mechanism. The electromigration in the surface produces the elimination of the surface strains formed during film growth. Grazing X ray diffraction peaks showed a shift in (111) peak on applying electric current, which is of gold standard. It was reported that this change in width and position of (111) reflection in diffractogram indication of surface electromigration in gold thinfilms[3].

Yan Zhang reported a noval EM failure mode, temporary extrusion in addition to permanent extrusion, in IC wafers fabricated by 0.13 μm Cu dual damascene technology. It is also reported that such temporary extrusion happened more frequently and recovery process also happened within a short period of time[4]

A.Bittner, F. Prewein, U. Schmid of Vienna University of Technology reported the electromigration behavior of Ag thin films patterned differently via wet chemically etching and a lift-off procedure.EM measurements in the temperature range from room temperature to 300^{0}C were studied[5]. Films patterned by lift of process had a homogeneous morphology. They showed less current crowding and joule heating effects. So they are assumed to be shown high resistance against EM failure and have longer life time. Hence it is reported that they better thinfilms for high power applications. The wet chemically etched thin film had a porous edge morphology and the highest electromigration occurs exactly at this area representing the highest local current density. The film might be damaged due to high current densities and joule heating.

A review by Stephen Kilgore[1] reported that electroplated Au based metallisation on GaAs substrate can handle high current densities and have longer life times.Since the EM failure is a common damage mechanism at higher current densities in IC interconnects, the EM lifetime enhancement is a challenging one in microelectronics industry.It was reported in many papers that alloying the metal improves the life to to some extent.

It is suggested that alloying Al and Cu films with magnesium and chromium reduces EM damage[1]. Among these two, magnesium shows better performance. Implementation of refractory materials to interconnect is an alternative method for improving IC lifetime[1].The layer of refractory material TiW can act as a diffusion layer and hence reduces EM effect. Another material is TiN, which by annealing life times can be increased.Although electromigration is a thoroughly researched topic, complete understanding of alloying effects on electromigration has not yet been achieved.

From this review study, it is proposed to grow Al-TiN and Cu-TiN thinfilms by laser deposition technique and study their EM migration behaviour , which are predicted to show better life times, for a future work[6]

References

1. Stephen Kilgore, Electromigration in Gold Interconnects, Graduate Supervisory Committee:
   James Adams, Co-chair Dieter Schroder, Co-chair Craig Gaw Stephen Krause, 2013
2. A. Gladkikh and Y. Lereah, E. Glickman , M. Karpovskia) and A. Palevski , J. Schubert Hillock
   formation during electromigration in Cu and Al thin films: Three-dimensional grain growth, Appl. Phys. Lett., Vol. 66, No. 10, 6,1994.
3. M. Aguilar , A.I. Oliva, P. Quintana, J.L. Pena, Electromigration in gold thin films, Thin Solid Films 317, 1998, 189–192
4. Yan Zhang, Electromigration phenomena in 0.13 micron Cu interconnects,Thesis, 2005
5. A.Bittner, F. Prewein, U. Schmid, Impact of Patterning Technique on the Long Term Stability of Ag Thin Film,Science direct, Procedia Engineering 87, 2014, 116 – 119
6. Leinig.J, Thiele. M, Fundamentals of electromigration,2018

ADVANCES IN CHEMICAL SCIENCES

7.

The Growing Applications of "Click Chemistry"

Thasnim. P[*1]
[1]*Department of Chemistry, MES Mampad College (Autonomous), Mampad, Malappuram 673635, Kerala, India*
**E-mail: thasnim6390@gmail.com*

Abstract *Mimicking natural biochemical processes, click chemistry is a modular approach to organic synthesis, joining together small chemical units quickly, efficiently and predictably. In contrast to complex traditional synthesis, click reactions offer high selectivity and yields, near-perfect reliability and exceptional tolerance towards a wide range of functional groups and reaction conditions. These 'spring loaded' reactions are achieved by using a high thermodynamic driving force, and are attracting tremendous attention throughout the chemical community. Originally introduced with the focus on drug discovery, the concept has been successfully applied to materials science, polymer chemistry and biotechnology.*

Introduction

The term "Click Chemistry" was introduced by Sharpless *et al.* in 2001 to describe chemistry tailored to generate substances quickly and reliably by selectively joining ("click") small units together similar to the modular strategies adopted by Nature.[1] These authors suggested a set of requirements to be fulfilled by a reaction to classify it as a 'Click' reaction.[1] The main goal was to encourage synthetic chemists to focus more on the production of arrays of simple molecules with the same properties available in complex natural molecules by making use of carbon-carbon and caron-hetero atom bond formations in a much simplar way similar to Nature's synthetic strategy.[1] Click reactions are modular reactions with wide scope, high product selectivity and high thermodynamic driving force, usually greater than 20 kcalmol^{-1}. Such "spring-loaded" reactions proceed rapidly to completion and also tend to be highly selective towards the formation of a single product. Generally, Click reactions are room temperature reactions based on readily available starting materials and benign solvents, yielding near quantitative amount of products via simple and non-chromatographic separation methods.

Among the various reactions that are fulfilling the Click criteria, the [3+2] azide-alkyne cycloaddition (Huisgen cycloaddition) is now emerged as an established tool in modern medicinal chemistry.[2] Azide and alkyne functionalities can be readily introduced and have a high tolerance for various other functional groups and have enough kinetic stability.[3] Since the work presented in the upcoming chapters are on the use of Copper (I) catalyzed the [3+2] azide-alkyne cycloaddition for the development of multipurpose small molecules for medicinal and materials applications, the focus of this review has been restricted to 1,3-dipolar click cycloadditions.

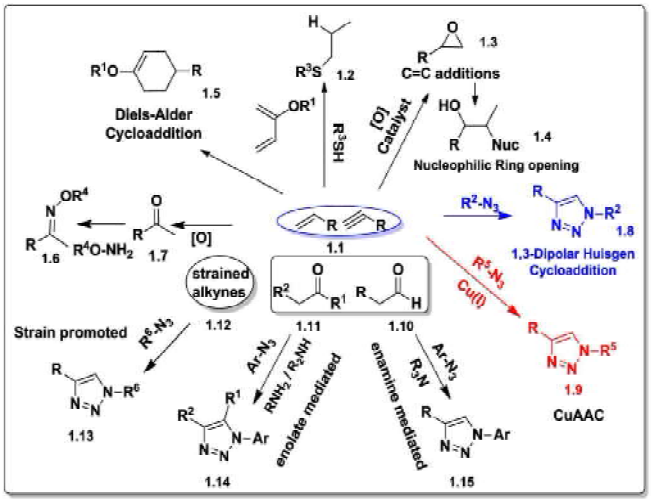

Figure 1: Classification of Click reactions

1,3 -Dipolar Cycloadditions and CuAAC

The 1,3-dipolar cycloaddition is a chemical reaction between a 1,3-dipole and a dipolarophile to form a five-membered ring. In 1960s, recognized this type of reaction for its generality, scope and mechanism by Huisgen, and he coined the term 1,3-dipolar cycloaddition.[4] Hence, the reaction is sometimes referred to as the Huisgen cycloaddition. Unfortunately, the thermal Huisgen 1,3-Dipolar cycloaddition of alkynes to azides requires high temperatures and often produces mixtures of the 1,4- and 1,5-disubstituted 1,2,3-triazoles when using asymmetric alkynes.[5] A copper-catalyzed variation of Huisgen's azide–alkyne cycloaddition (CuAAC reaction) was reported by the groups of Meldal and Sharpless independently in 2002.[6] This reaction fits the "click chemistry" concept well because a close examination of the azide-alkyne cycloaddition shows that it fulfills many of the prerequisites of click concept.

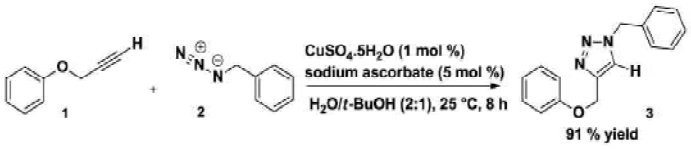

Scheme 1. Example for CuAAC reaction of benzyl azide with (prop-2-yn-1-yloxy)benzene

This reaction is applicable to a wide variety of substrates with various functional groups and the catalytic process is insensitive towards the presence of air and pH changes in a solvent mixture of water and *t*-BuOH. This strictly regioselective stepwise process selectively produce 1,4-disubstituted 1,2,3-triazole only and accelerates the reaction by a factor of up to 10^7 in comparison to Huisgen's thermal procedure.[7] In addition to this, since large number of monosubstituted alkynes and organic azides are commercially available and many others can easily be synthesized with a wide range of functional groups, it is easy to make large library of 1,2,3-triazoles derivatives for screening purpose.

Applications of Click Chemistry (CUAAC)

The popularity of the CuAAC is largely a result of the unique properties of both azides and the resulting triazoles.[8] The combination of the robustness of the triazole bond, the resemblance to an amide bond, and the potential biological properties it could endow make the triazole linkage not merely a benign, easily synthesized linker, but an integral part of the success of click chemistry. In addition to this, the simplicity, reliability and the bioorthogonality of the starting materials has made the CuAAC reaction an asset to a hugely varied range of scientific applications. The wide scope of CuAAC is firmly demonstrated by the use in different areas of life and material sciences such as drug discovery,[9] bioconjugation,[10] polymer and materialsscience,[11] including supramolecularchemistry.[12] DNA labeling[13] and oligonucleotide synthesis,[14] assembly of glycoclusters[15] and glycodendrimers,[16] preparation of stationary phases for HPLC column,[17] development of microcontact printing,[18] conjugation of molecular cargos to the headgroup of phospholipids,[19] and construction of bolaamphiphilicstructures[20] are a further examples of the use of CuAAC. It would be impossible to give a complete overview of the numerous applications of the CuAAC. For our purposes, the applications of 'click' chemistry have been summarized with illustrative examples in various categories; applications in materials science, for radiolabelling, for bioconjugation, and in drug discovery.

a) Material Science

The value of click chemistry for materials synthesis possibly becomes most apparent in the area of material chemistry. Several recent reviews have described the use of CuAAC for the synthesis of macromolecular structures like dendritic, branched, linear and cyclic co-polymers.[21] Triazole-based dendrons can be divergently synthesized via CuAAC reaction. These dendrons were then anchored to a variety of polyacetylene cores to generate dendrimers. Since then, the CuAAC reaction has been widely employed to synthesize or modify various dendrimers.[22] A click chemistry based dendrimer **4** is shown in Figure 2.

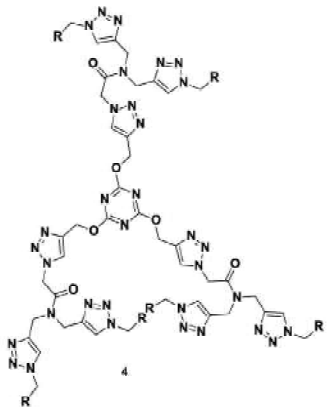

Figure 2.'Click' chemistry based dendrimers

b) Bioconjugation

Bioconjugation is the process by which synthetic molecules are attached to biological targets or by which biomolecules are linked together. It involves attachment of synthetic labels to biomolecular building blocks, such as fusing two or more proteins together or linking a carbohydrate with a peptide, and covers a wide range of science between molecular biology and chemistry. The possibility of applying click chemistry in bioconjugation was first demonstrated by Meldal *et al* for the preparation of peptidotriazoles *via* solid state synthesis.[6a] Their goal was to develop new and more efficient synthetic methods to prepare various [1,2,3]-triazole pharmacophores for potential biological targets. This initial report made possible the introduction of various novel functional and reporter groups into biomolecules such as peptides and proteins,[23] for DNA labeling and modification,[24] and for cell surface labeling.[25]

Finn and co-workers successfully labeled Cowpea mosaic virus particles (CPMV) with fluorescein with >95% yield.[26] Similarly, Tirrell and Link were able to modify *Eschericia coli* with an azide-bearing outer membrane protein C(OmpC). Schultz *et al* developed a method to genetically-encode proteins of *Saccharomyces cerevisiae* with azide- or acetylene-based synthetic amino acids.[27] The genetic modification was done by reacting an alkyne or an azide bearing protein with the counterpart unnatural amino acid. Click chemistry continues to attract attention for labeling of proteins and live organisms.

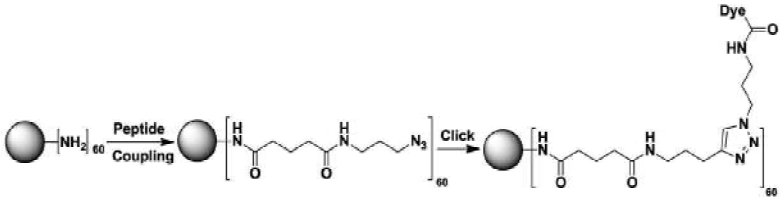

Scheme 2. Labelling of virus capsids by CuAAC

c) Radiochemistry

The CuAAC is an ideal ligation reaction for radiolabeling sensitive biomolecules. Alkyne or azide derivatives of radioisotope containing compounds could be used for labeling biomolecules such as folic acid, peptides, proteins, and glycopeptides. For example, an ^{11}C isotope label was introduced via converting [^{11}C]-CH_3I into [^{11}C]-CH_3N_3 by nucleophilic substitution and subsequently reacting the azide with an alkyne-modified peptide. ^{18}F labeling for PET imaging was achieved by clickingazidomethyl-4-[^{18}F]-fluorobenzene to a modified peptide.[28] CuAAC ligations have a significant impact on the synthesis and development of radiopharmaceuticals and it has vast application in the preparation of imaging agents for SPECT and PET, including small molecules, peptides, and proteins labeled with radionuclides such as ^{18}F, ^{64}Cu, and ^{111}In.[29] Various researchers have shown that CuAAC is a great approach for the construction of radiotracers also.

d) Drug Discovery

In history and even now a days, lead discovery and optimization had aided by combinatorial methods and high throughput screening to generate library of test compounds for screening. However, due to unreliability and new discoveries revealed click chemistry as a modular for the synthesis of drug-like molecules that can accelerate the drug discovery process by utilizing a few practical and reliable reactions. It is a new type of chemistry that able to synthesize complex molecule in an efficient manner.[1] It makes use of few chemical reactions for the synthesis and designing of new building blocks. Drug discovery based on Natures secondary metabolites is very slow and complex synthesis and thereby, click chemistry provides faster lead discovery and optimization.[1]

This commendably straightforward chemistry, which can be conducted in aqueous media, has been widely applied as a powerful tool for the selective modifications of enzymes[30] viruses[31]and cells.[32] Among the best-known examples of triazole-containing structures is, a β-lactamase inhibitor which is marketed in combination with the broad spectrum antibiotic piperacillin. Indeed, when first described, tazobactam and related triazole-containing compounds (**5**, Figure 3) turned out to be potent β-lactamase inhibitors with higher potency than clavulanic acid and sulbactam, and the triazole ring appears to play a pivotal role for its potency.[33] In the antibiotics field, triazoles have been also used to improve pharmacokinetic properties of the desired drug. For example, cephalosporins endowed with good oral availability were obtained linking the triazoles moiety to the cephalosporin core (**6**, Figure 3).[34] Indeed; it is not just antibiotics which benefit from the triazole ring.

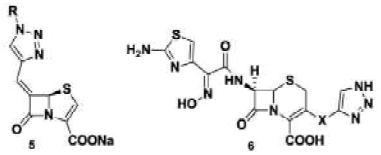

Figure 3. Example of β-lactamase inhibitors incorporating the 1,2,3-triazole moiety

Click chemistry, due to its highly modular and efficient reaction nature, has been identified as one of the most practical methods toward fragment-based enzyme inhibitor development. Using fragment pro-inhibitor library screening and click chemistry reaction, researchers developed a large class library of efficient enzyme inhibitors of various enzymes such as Protein Tyrosine Phosphatase Inhibitors, Protein Kinase Inhibitors, Transferase Inhibitors, Glycogen Phosphorylase Inhibitors, Serine Hydrolase Inhibitors, Metalloproteinase Inhibitors, Aspartic Protease Inhibitors, Oxidoreductase Inhibitors and Glycosidase Inhibitors etc.[35]

Click Derived Cancer Growth Inhibitors

Chemotherapy is considered as the most effective method among many other methods prevalent to treat cancer. Several nucleoside drugs have been developed as cancer treatment agents: cladribine, clofarabine, capecitabine, cytarabine,fludarabine, gemcitabine, decitabine, and floxuridine.[36] The development of new therapeutic approach to breast cancer remains one of the most challenging areas in cancer research. Inhibitors of cyclin-dependent kinases (CDKs) are an emerging class of drugs for the treatment of breast cancers. Experimental evidence suggests that CDK inhibitors inhibit the cyclin D–dependent kinase activity and thus prevent tumor growth and/or at least partially revert the transformed phenotype. Several compounds are currently in clinical trials including flavopiridol (**7**), R-roscovitine (CYC202) (**8**), BMS-387032 (**9**), and UCN-01 (7-hydroxystaurosporine) (**10**).[37] CDK inhibitors are currently under evaluation in clinical trials as single agents and as sensitizers in combination with radiation therapy and chemotherapies.

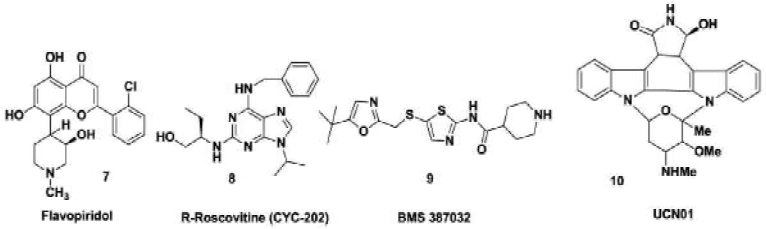

Figure 6. CDK inhibitors under clinical trials

Conclusions

In conclusion, this review summarizes the growing application of ''click'' chemistry in diverse areas such as bioconjugation, drug discovery, materials science, and radiochemistry. Click chemistry has found increasing applications in all aspects of drug discovery in medicinal chemistry, such as for generating lead compounds through combinatorial methods. Bioconjugation via click chemistry is rigorously employed in proteomics and nucleic research. In radiochemistry, selective radiolabeling of biomolecules in cells and living organisms for imaging and therapy has been realized by this technology. Click chemistry has proven itself to be superior in satisfying many criteria, thus, one can expect it will consequently become a more routine strategy in the near future for a wide range of applications since it links various types of chemistry with biology and can tailor various useful syntheses in future.

References

(1) Kolb, H. C.; Finn, M. G.; Sharpless. K. B. Angew. Chem. Int. Ed. 2001, 40, 2004-2021.

(2) (a) Huisgen. R. Pure Appl. Chem. 1989, 61, 613-628. (b) Huisgen, R.; Szeimies, G.; Moebius. L. Chem. Ber. 1967, 100, 2494-2507.

(3) Bock, V. D.; Hiemstra, H.; Van Maarseveen. J. H. Eur. J. Org. Chem. 2006, 51-68.

(4) (a)Huisgen R. Proc Chem Soc, London. 1961, 357–396. (b) Huisgen R. Angew Chem.1963, 75, 604–637. *Angew. Chem., Int. Ed. Engl.* **1963,** *2,* 565–598. (c) Huisgen R. *Angew. Chem., Int. Ed. Engl.* **1963,** *2,* 633–645.

(5) (a) Huisgen. R. 1,3-Dipolar Cyloaddition Chemistry (Ed.: A. Padwa), Wiley, New York, 1984, 1-176. (b) Bastide, J.; Henri-Rousseau. O. Bull. Chim. Soc. Fr. 1973, 2294-2296. (c) Clarke, D.; Mares, R. W.; McNab. H. J. Chem. Soc. Perkin. Trans. 1997, 1, 1799-1804.

(6) (a) Tornoe, C. W.; Christensen, C.; Meldal, M. J. Org. Chem. 2002, 67, 3057–3064. (b) Rostovtsev, V.V.; Green, L.G.; Fokin, V.V.; Sharpless, K. B. Angew. Chem. Int. Ed. 2002, 41, 2596–2599.

(7) (a) Himo, F.; Lovell, T.; Hilgraf, R.; Rostovtsev, V. V.; Noodleman, L.; Sharpless, K. B.; Fokin, V. V.J Am Chem Soc. 2005, 127, 210–216. (b) Hein, J. E.; Fokin, V.V. Chem Soc Rev. 2010, 39, 1302–1315.

(8) (a) Roper, S.; Kolb, H. C. Wiley-VCH: Weinheim, 2006, 34, 313-339. (b) Sharpless, K. B.; Manetsch, R. Expert Opin. Drug Discovery. 2006, 1, 525-538. (c) Tron, G. C.; Pirali, T.; Billington, R. A.; Canonico, P. L.; Sorba, G.; Genazzani, A. A. Med. Res. Rev. 2008, 28, 278-308.

(9) Alvarez, R.; Velazquez, S.; San-Felix, A.; Aquaro, S.; De Clercq, E.; Perno, C.-F.; Karlsson, A.; Balzarini, J.; Camarasa, M. J. J. Med. Chem. 1994, 37,4185–4194.

(10) (a) Pieters, R. J.; Rijkers, D. T. S.; Liskamp, R. M. J. QSAR Comb. Sci 2007, 26, 1181-1190. (b) Dirks, A. J.; Cornelissen, J.; van Delft, F. L.; van Hest, J. C. M.; Nolte, R. J. M.; Rowan, A. E.; Rutjes, F. QSAR Comb. Sci. 2007, 26, 1200-1210. (c) Salisbury, C. M.; Cravatt, B. F. QSAR Comb. Sci. 2007, 26, 1229-1238.

(11) (a) Binder, W. H.; Kluger, C. Curr. Org. Chem. 2006, 10, 1791-1815. (b) Nandivada, H.; Jiang, X. W.; Lahann, J. Adv. Mater. 2007, 19, 2197-2208. (c) Fournier, D.; Hoogenboom, R.; Schubert, U. S. Chem. Soc. Rev. 2007, 36, 1369-1380. (d) Golas, P. L.; Matyjaszewski, K. QSAR Comb. Sci. 2007, 26, 1116-1134. (e) Devaraj, N. K.; Collman, J. P. QSAR Comb. Sci. 2007, 26, 1253.

(12) (a) Zhou, Z.; Fahrni, C. J. J. Am. Chem. Soc. 2004, 126, 8862-8863. (b) Link, A. J.; Vink, M. K. S.; Tirrell, D. A. J. Am. Chem. Soc. 2004, 126, 10598- 10602. (c) Lewis, W. G.; Magallon, F. G.; Fokin, V. V.; Finn, M. G. J. Am. Chem. Soc. 2004, 126, 9152-9153. (d) Sivakumar, K.; Xie, F.; Cash, B. M.; Long, S.; Barnhill, H. N.; Wang, Q. Org. Lett. 2004, 6, 4603-4606.

(13) For selected reviews, see: (a) Miljanic, O. S.; Dichtel, W. R.; Aprahamian, I.; Rohde, R. D.; Agnew, H. D.; Heath, J. R.; Stoddart, J. F. QSAR Comb. Science. 2007, 26, 1165-1174. (b) Aprahamian, I.; Miljanic, O. S.; Dichtel, W. R.; Isoda, K.; Yasuda, T.; Kato, T.; Stoddart, J. F. Bull. Chem. Soc. Jpn. 2007, 80, 1856-1869. (c) Braunschweig, A. B.; Dichtel, W. R.; Miljanic, O. S.; Olson, M. A.; Spruell, J. M.; Khan, S. I.; Heath, J. R.; Stoddart, J. F. Chem. Asian J. 2007, 2, 634-647. For selected papers see: (d) Aucagne, V.; Haenni, K. D.; Leigh, D. A.; Lusby, P. J.; Walker, D. B. J. Am. Chem. Soc. 2006, 128, 2186-2187. (e) O'Reilly, R. K.; Joralemon, M. J.; Hawker, C. J.; Wooley, K. L. Polym. Sci. Polym. Chem. 2006, 44, 5203-5217.

(14) Gierlich, J.; Burley, G. A.; Gramlich, P. M. E.; Hammond, D. M.; Carell, T. Org. Lett. 2006, 8, 3639-3642.

(15) Nuzzi, A.; Massi, A.; Dondoni, A. QSAR Comb. Sci. 2007, 26, 1191-1199.

(16) Dondoni, A.; Marra, A. J. Org. Chem. 2006, 71, 7546-7557 and references therein.

(17) (a) Joosten, J. A. F.; Tholen, N. T. H.; Ait El Maate, F.; Brouwer, A. J.; van Esse, G. W.; Rijkers, D. T. S.; Liskamp, R. M. J.; Pieters, R. J.; Eur. J. Org. Chem. 2005, 3182-3185. (b) Fernandez-Megia, E.; Correa, J.; Rodrı´guez-Meizoso, I.; Riguera, R. Macromol. 2006, 39, 2113-2120.

(18) Guo, Z.; Lei, A.; Liang, X.; Xu, Q. Chem. Commun. 2006, 4512-4514.

(19) Rozkiewicz, D. I.; Janczewski, D.; Verboom, W.; Ravoo, B. J.; Reinhoudt, D. N. Angew. Chem., Int. Ed. 2006, 45, 5292-5296.

(20) (a) Musiol, H. –J.; Dong, S.; Kaiser, M.; Bausinger, R.; Zumbusch, A.; Bertsch, U.; Moroder, L. ChemBioChem. 2005, 6, 625-628. (b) Cavalli, S.; Tipton, A. R.; Overhand, M.; Kros, A.; Chem. Commun. 2006, 3193-3195. (c) Hassane, F. S.; Frisch, B.; Schuber, F. Bioconjugate Chem. 2006, 17, 849-854.

(21) (a) Franc, G.; Kakkar, A. K. Chem. Soc. Rev. 2010, 39, 1536–1544. (b) Gao, C.; Yan, D. Prog. Polym. Sci. 2004, 29, 183–275. (c) Tang, B.Z. Chem. Soc. Rev. 2010, 39, 2522–2544. (d) Hadjichristidis, N.; Pitsikalis, M.; Pispas, S.; Iatrou, H. Chem. Rev. 2001, 101, 3747–3792.

(22) (a) Wu, P. et al. Chem. Commun. 2005, 5775–5777. (b) Joralemon, M.J. et al. Macromolecules, 2005, 38, 5436–5443.

(23) Baskin, J. M.; Bertozzi, C. R. QSAR. Comb. Sci. 2007, 26, 1211.

(24) (a) Chevolot, Y.; Bouillon. C.; Vidal, S.; Morvan, F.; Meyer, A.; Cloarec, J. P.; Jochum, A.; Praly, J. P.; Vasseur, J. J.; Souteyrand, E. Angew. Chem. Int. Ed. 2007, 46, 2398. (b) Weisbrod, S. H.; Marx, A. Chem. Commun. 2008, 5675. (c) Gramlich, P. M. E.; Warncke, S.; Gierlich, J.; Carell, T. Angew. Chem. Int. Ed. 2008, 47, 3442.

(25) Link, A. J.; Tirrell, D. A. J. Am. Chem. Soc. 2003, 125, 11164.

(26) Wang, Q.; Chan, T. R.; Hilgraf, R.; Fokin, V. V.; Sharpless, K. B.; Finn. M. G. J. Am.Chem. Soc. 2003, 125, 3192-3193.

(27) Deiters, A.; Cropp, T. A.; Mukherji, M.; Chin, J. W.; Anderson, J. C.; Schultz. P. G. J Am Chem Soc. 2003, 125, 11782.

(28) Carroll, L.; Boldon, S.; Bejot, R.; Moore, J. E.; Declerck, J.; Gouverneur V. Org. Biomol. Chem. 2011, 9, 136- 140.

(29) Dexing, Z.; Brian, M.Z.; Jason, S. L.; and Carolyn, J. A. J. Nucl. Med. 2013, 54, 829–832.

(30) Schultz, P. G. J. Am. Chem. Soc. 2003, 125, 11782-11783.

(31) (a) Wang, Q.; Chan, T. R.; Hilgraf, R.; Fokin, V. V.; Sharpless, K. B.; Finn, M. G. J. Am. Chem. Soc. 2003, 125, 3192–3193. (b) Gupta, S. S.; Kuzelka, J.; Singh, P.; Lewis, W. G.; Manchester, M.; Finn, M. G. Bioconjugate. Chem. 2005, 16, 1572-1579. (c) Gupta, S. S.; Raja, K. S.; Kaltgrad, E.; Strable, E.; Finn, M. G. Chem. Commun. 2005, 4315-4317

(32) Link, A. J.; Vink, M. K. S.; Tirrell, D. A. J. Am. Chem. Soc. 2004, 126, 10598-10602.

(33) (a) Bennett, I. S.; Brooks, G.; Broom, N. P.; Calvert, S. H.; Coleman, K.; Francois, I. J. Antibiot. 1991, 44, 969–977. (b) Bennett, I. S.; Broom, N. P.; Bruton, G.; Calvert, S.; Clarke, B. P.; Coleman, K.; Edmondson, R.; Edwards, P.; Jones, D.; Osborne, N. F.; Walker, G. J. Antibiot. 1991, 44, 331–337.

(34) Kume, M.; Kubota, T.; Kimura, Y.; Nakashimizu, H.; Motokawa, K.; Nakano, M. J. Antibiot. 1993, 46, 177–192.

(35) Prakasam, T.; Dariusz, M.; Krzysztof, J. Chem. Rev. 2013, 113, 4905–4979 and references therein.

(36) (a) Lauria, F.; Benfenati, D.; Raspadori, D.; Rondelli, D.; Zinzani, P. L.; Tura, S. Leuk. Lymphoma. 1993, 11, 399. (b) Pui, C. H.; Jeha, S.; Kirkpatrick, P. Nat. Rev. Drug Disc. 2005, 4, 369. (c) Bonate, P. L.; Arthaud, L.; Cantrell, W. R.; Stephenson, K.; Secrist, J. A.; Weitman, S. Nat. Rev. Drug Disc. 2006, 5, 855; (d) Issa, J.-P.; Kantarjian, H.; Kirkpatrick, P. Nat. Rev. Drug Disc. 2005, 4, 275. (e) Gore, S. D.; Jones, C.; Kirkpatrick, P. Nat. Rev. Drug Disc. 2006, 5, 891.

(37) Benson, C.; Kaye, S.; Workman, P.; Garrett, M.; Walton, M.; De Bono, J. British Journal of Cancer. 2005, 92, 7 – 12.

8.

SYNTHESIS OF SOPHOROLIPID FROM THE FUNGAL CULTURE MEDIUM CANDIDA BOMBICOLA AND THEIR SEPARATION

K Shabana[a], K M Suhada[b] and B LV Prasad[c]

[a,b]PG Department of chemistry, KAHM Unity Women's College, Manjeri, Narukara P.O, Kerala
[c]Physical and Material Chemistry Division, National chemical Laboratory, Pune
Email: shabshabana@gmail.com

Abstract *Sophorolipids (SL) formely named sophorosides is found and excreted in to the culture medium by Candida or related Yeast species and is good surfactants. Sophorolipids exhibit surfactant activity because of their amphiphilic structure. Among the sophorolipid producers, Candida bombicola is the most studied species because it produces sophorolipid molecule in large quantities. Products yields up to 300 g of sophoroses per liter of culture medium have been reached. Sophorolipids act as a body care products, therapeutic agents for cancer and immune disorders, Oil recovery agents etc. In this study C14-COOH –SL prepared. It is a yellowish brown, honey like viscous liquid. The yield for a flask of 250ml of sophorolipid was approximately 1.045g. We found that this new sophorolipid is indeed capable of reducing Ag ions in to Ag nanoparticles. Preparing them and capping them with active molecules like SLs can enhance their utility and open new avenues for research and applications.*

Keywords: Sophorolipid preparation, Sophorolipid Extraction, Candida bombicola

An Introduction to Sophorolipid Molecule

Sophorolipids (SL) formerly named sophorosides is found and excreted into the culture medium by Candida or related yeast species and is good surfactants. They were first described by Tulloch AP and found to be composed of a disaccharide moiety linked to one hydroxyl group of one ω or (ω -1)-hydroxy fatty acid (saturated or monounsaturated). The sugar (sophorose or 2-O-glucopyranosyl--D-glucopyranose) may further show mono- or diacetylation at the 6' and 6" positions. The nature of the hydroxy fatty acid is characteristic, with the hydroxyl group being located on the n or n-1 carbon atom. In general, fatty acids of carbon chain length of 16, 17 or 18 are used and subjected to modification to lead to different SLs by the composition of the growth medium. Sophorosides with unsaturated C18 fatty acids have been recognized in Candida bogoriensis. Sophorolipids exhibit surfactant activity because of their amphiphilic structure. Among the sophorolipid producers, Candida bombicola is the most studied species because it produces sophorolipid molecule in large quantities. Products yields up to 300 g of sophoroses per liter of culture medium have been reached. The composition of the hydroxylated fatty acid varies depending on the culture conditions. Furthermore, lactonization frequently occurs between the carboxyl group and the 4" OH group of the sophorose. Sophorolipids are used as bacteriocides in the formulation of skin and body-care products (deodorant, anti-acne ingredient, from Soliance) but these emerging biosurfactants may have many other application potentials such as use as a capping agent for providing stability to nanoparticles. Hydroxy fatty acids may

be released from sophorolipids and lactonized into macrocyclic esters; they are used in the perfume and fragrance industry.

Materials and Method

Chemicals used: Synthesis of sophorolipids

Malt extracts (Hi-media chemicals), Glucose extracts (Hi-media chemicals) , Yeast extracts (Hi-media chemicals) ,Peptone (Hi-media chemicals) , Ethyl acetate , Sodium sulphate , Precursors: Oleic acid (Aldrich chemicals), C-12-COOH (CH3- (CH2)11 –O-CH2 –COOH), C-14-COOH (CH3-(CH2)13-O-CH2 – COOH) (Synthesized) ,Pure culture of yeast.
Synthesis of SL-Ag: [Silver nitrate, Sophorolipids, Sodium borohydride, Potassium hydroxide]
Methods: MGYP broth (Composition of 100ml MGYP broth):- Maltose extract: 0.3g, Glucose extract: 2g, Yeast extract: 0.3g, Peptone: 0.5g, Millipore water: 100ml

Organism: - The fungal culture, Candida bombicola was used for the sophorolipid synthesis.
Synthesis of sophorolipids: Two to three weeks old culture of Candida bombicola grown on MGYP slant was used for the pre-inoculum preparation. Colonies were transferred to 20ml MGYP broth in a test tube and kept at room temp for 18 hrs. 2ml of this culture were added to each of 100ml and 200ml MGYP broth in 500ml and 1000ml conical flask respectively and kept it on rotary shaker for 2 days. The biomass of culture grown for 2 days were separated by centrifugation at 5000rpm for 10 minute at 20^0C and these cells were redispersed in 100ml of 10% glucose solution and 10^{-3}M precursor (oleic acid, C14-1-OH, C12-1-OH) were added in each flask and kept on rotary shaker for 24hrs (All precursors are dissolved in 1ml ethanol). After 1day, 10^{-2}M of precursors in ethanol was again added to the respective flask and kept on rotary shaker for 3-4 days followed by addition of 50ml of 10% glucose in each flask and kept on shaker for 8-10 days till complete conversion of precursor to sophorolipid occurred.

Separation of sophorolipid: Sophorolipid formed was taken out and was collected in a test tube. Remaining sophorolipid along with biomass was collected as a pellet by centrifugation at 5000rpm for 10 minute and supernatant was discarded. The pellet was redispersed in 100ml of 10% glucose and with 10^{-2}M respective precursor and kept on rotary shaker for 10-15 days until the formation of sophorolipid. The sophorolipid formed was then extracted by mixing with equal volume of ethyl acetate in a separating funnel, organic layer was dried over anhydrous sodium sulphate and the excess solvent was removed using rotary evaporation.

A yellowish brown, honey like viscous liquid was obtained. This is the sophorolipid. The yield for a flask of 250ml of sophorolipid was approximately 1.045g. A minimum of three batches were required to make sufficient amount of sophorolipid enough for further analysis.This Sophorolipid act as capping agent and reducing agent on the formation of silver nano particles.

Conclusions

In this study, we have described the synthesis of C14-COOH-SL. It is a yellowish brown, honey like viscous liquid. The yield for a flask of 250ml of sophorolipid was approximately 1.045g. This sophorolipid act as capping agent and reducing agent on the formation of silver nano particles.

References

1. http://www.Nanoscience.com/education/overview.html
2. www.nanotec.org.uk/
3. www.en.wikipedia.org/wiki/Nanotechnology
4. New methods for the synthesis of magnetic nanoparticles- Thesis by Tanushree Bala University of Pune.
5. www.crnano.org/whatis.htm
6.Sophorolipid production by candida bombicola: Medium composition and culture methods-Journal of Bioscience and Bioengineering 88,No.5,488-494.1999.
7. Phadtare Sumant, Parekh Parag, Shah sachin, Tambe Amruta, Joshi Rohini, Sainkar S.R, Prabhune Asmita, and Sastry Murali Biotechnol. Prog. (2003) 19, 1659-1663.
8. Http: // en. Wikipedia. Org /wiki /UV/VIS _spectroscopy.
9. Http: //en.wikipedia. Org/wiki/Top-down- and-Bottom-up-design.
10. Http: // nobelprize. Org/ educational –games/physics/microscopes/ tem/ind ex.html.
11. Cavelaro David A.,Cooper David G;Biotechnology; (2003); 103; 31-41.

PROCESSED FOOD:
HEALTHY OR CONVENIENCE?

9.

DEVELOPMENT OF GABA ENRICHED RTE FLAKES FROM RAKTASALI, KAKASALI AND KUMKUMASALI PADDY VARIETIES

Anjali P. N., *Sudheer K. P. and *Sankalpa K. B.
Guest Lecture, Department of Food Technology, DGMMES College, Mampad P. O. Malappuram
**Department of Agricultural Engineering, College of Horticulture, Kerala Agricultural University, Vellanikkara, Thrissur – 680 656*
pnanjali005@gmail.com

Abstract *The rapid replacement of healthy traditional snacks with modern westernized junk foods has accelerated the rate of occurrence of several health problems in our country. The production and consumption of expanded RTE products has escalated recently throughout the world. Eating patterns are changing, snack foods play very important role in the diet of modern consumer. Hence efforts were taken to develop RTE rice flakes from specialty rice with enriched GABA (gamma amino butyric acid). GABA is the chief inhibitory neurotransmitter in the mammalian central nervous system. Its principal role is reducing neuronal excitability throughout the nervous system. In humans, GABA is also directly responsible for the regulation of muscle tone. Since Kerala is home to a number of specialty rice varieties such as Raktasali, Kumkumasali, Kakasali etc., enrichment of GABA content along with their medicinal properties will enhance health benefit of RTE flakes.*

Introduction

Indian traditional foods have been recognized as functional foods due to the presence of body healing chemicals, dietary fibres, high vitamins and mineral constituents. The rapid replacement of healthy traditional snacks with modern westernized junk foods has accelerated the rate of occurrence of several health problems in our country. The production and consumption of expanded RTE products has escalated recently throughout the world. Eating patterns are changing, snack foods play very important role in the diet of modern consumer. Kerala is home to a number of specialty rice varieties such as Raktasali, Kumkumasali, Kakasali, Jeerakasala, Gandhakasala, Njavara, etc. Many of these varieties have medicinal properties, special taste and some are scented rice varieties. So these specialty rice varieties are processed to develop RTE snacks for greater acceptance.

Grain germination has also an important role on chemical composition, nutritional value and acceptability characteristics of products for human consumption (Ruiz and Bressani, 1990). Germination process activates many enzymes in raw seeds, especially glutamate decarboxylase (GAD) enzyme which catalyzes L-glutamic acid to gamma amino-butyric acid (GABA) (Komatzuzaki *et al*., 2007). According to the report of Ohtsubo, 2004, GABA content increases during the germination period. Hence efforts were taken to develop RTE rice flakes from specialty rice varieties with enriched GABA.

Materials and methods

Germination rate test

Three varieties of paddy namely, Raktasali, Kakasali and Kumkumasali were soaked individually and all the samples were allowed for germination in moist cloth for different time period, 12, 18, 24 and 36 hour. The germination time was standardized based on the germination rate, calculated using the equation (1).

$$\text{Germination rate} = \frac{\text{Number of germinated seeds}}{\text{Total number of seeds}} \times 100 \quad \ldots\ldots\ldots (1)$$

Quantification of GABA content

GABA content of samples was evaluated by spectrophotometric method described by Karladee and Suriyong (2012). Ground rice samples (3 mg) was extracted with 80% ethanol and then filtered with filter paper. The filtered solution was boiled in a water bath (80°C) to evaporate the ethanol. This was followed by addition of 0.5 ml distilled water and then centrifugation at 10,000 rpm for 10 minutes. The floating portion on top was aspirated and aliquot of samples was taken for analysis. For the aliquot of sample 0.2 ml of 0.2 M borate buffer and 1.0 ml of 6% phenol were added. For the standard GABA solution 0.1-0.3 ml was added to test tubes. The solutions were mixed thoroughly and cooled in a cooling bath for 5 minutes. Further, 0.4 ml of 10-15% NaClO was added and the solution was shaken vigorously for 1 minute and again cooled in a cooling bath for 5 minutes. Finally, the solution was boiled in a water bath (100°C) for 10 minutes and allowed to cool. Optical density was determined by spectrophotometer at a wavelength of 630 nm.

Production of flakes

Based on the results obtained from germination test, best condition was selected for germination of paddy. The germinated paddy was roasted at three different temperature viz. 100°C, 120°C and 140°C and flaking was carried out with heavy rollers. The procedure used for flaking of germinated paddy is described in Fig. 1

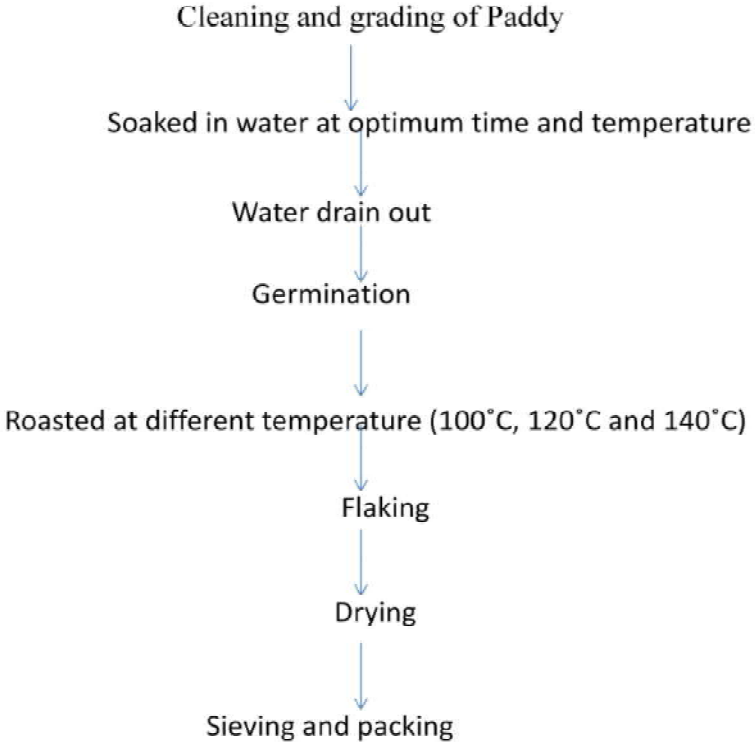

Figure. 1 Process flow chart for production of GABA enriched RTE flakes.

Evaluation of quality parameters

Thousand-flakes weight (g)

The thousand-flake weight was determined on the raw flakes by weighing 100 flakes and multiplying their weight by 10 (Cruzy *et.al*., 1996).

Bulk density (g/ml)

The bulk density of GABA enriched rice flakes was determined by placing the rice flakes into a 500 ml graduated cylinder. The volume and weight of the flakes were recorded to determine the bulk density of flakes (Rahman, 1995).

Size and Thickness (mm)

The size and thickness of GABA enriched rice flakes were determined on 30 flakes per treatment using vernier calipers.

Sogginess (min)

Sogginess is determined subjectively by placing 20 g flaked rice in cold milk (10ºC) and chewing a soaked flakes at 1 minute intervals until crispiness disappeared. The time (minutes) for crispiness to disappear was recorded as sogginess (Cruzy *et al.,* 1996).

Sensory evaluation of flakes

The GABA enriched flaked rice samples were evaluated for sensory characteristics. The judges scored the product for appearance, aroma, texture, taste and overall acceptability on a 9-point hedonic scale. The commercially available rice flakes was used as the control

.

Results and discussion

In this study, four different germination periods were taken for the test. The results obtained for germination rate test of all the three paddy varieties are given below as Table 1.

Table 1. Germination rate of Raktasali, Kakasali and Kumkumasali paddy varieties during various germination periods.

Sl. No.	Treatments	Raktasali	Kakasali	Kumkumasali
1	T1	20	9	8
2	T2	71	71	64
3	T3	76	87	71
4	T4	99	100	80

T1- Germination for 12 hours, T2- Germination for 18 hours, T3- Germination for 24 hours, T4- Germination for 36 hours

It was found that rate of germination increases with increase in germination period in all the three paddy varieties. The highest germination rate was observed at 36 h germination period (T4) and the lowest germination rate was observed at 12 h germination period (T1). Maisont and Narkrugsa (2010) mentioned that the GABA content increased continuously with germination time. The increase in GABA content during germination might have been due to the seed growth and development of the plant.

Quantification of GABA content

The three varieties of paddy germinated at various period of germination time were analyzed for GABA concentration. Effect of germination period on GABA concentration is given in Table 2.

Table 2. GABA content (mg/g) in paddy varieties germinated for various time periods.

Sl. No.	Treatments	Raktasali (mg/g)	Kakasali (mg/g)	Kumkumasali (mg/g)
1	T0	0.080	0.113	0.026
2	T1	0.150	0.316	0.100
3	T2	0.163	0.533	0.200
4	T3	0.200	0.700	0.230
5	T4	0.266	1.060	0.650

T0= Soaked paddy without germination.

Amino acid such as GABA is synthesized during germination and its accelerated increase can be detected at 12 h germination. The acceleration is still rapid from 12-24 h and 24-36 h, when GABA content reaches its highest levels and show a peak at 36 h germination (Komatzuzaki *et al.*, 2007). The results obtained showed a presence of lower amount of GABA content in soaked paddy varieties without germination. It may be due to the gamma amino acid which consists mainly of globulin and a minor portion of albumin (Bewley and Black., 1985). The GABA content increases with increase in germination period and among the three varieties of paddy, Kakasali was found to have highest GABA content.

Effect of roasting temperature on GABA content of rice flakes

GABA content of rice flakes varied significantly with different roasting temperature and it was analyzed with the results obtained for three varieties of flakes processed without germination (FWG) and also with commercially available flakes

Table 3. GABA content (mg/g) in flaked samples roasted at different temperature, flakes without germination and commercially available flakes.

Sl. No.	Treatments	Roasting Temperature (°C)	Raktasali (mg/g)	Kakasali (mg/g)	Kumkumasali (mg/g)
1	T1	100	0.050	0.100	0.083
2	T2	120	0.046	0.054	0.050
3	T3	140	0.033	0.033	0.042
4	T4	FWG	0.030	0.026	0.023
5	T5	MF	0.013		

FWG= Flakes without germination.
MF= commercially available flakes (Market flakes)

It was found that GABA content retained in all the flaked samples in different concentration (Table 3). The highest concentration of GABA was observed in Kakasali flakes roasted at 100℃ (0.100 mg/g). The GABA content was found to be decreasing with increase in roasting temperature in all three paddy varieties. The concentration of GABA in flakes without germination is comparatively lower than all flakes germinated for 36 hours. Market flakes has the least concentration of GABA content (0.013 mg/g).

Thousands flakes weight (g)

Thousand flakes weight of roasted flaked rice was found to be decreased on roasting, which may be due to loss of moisture and breakage of endosperm on the flattened sides. The highest value of thousand flakes weight was observed for flakes commercially available (MF) and the lowest value was observed for Kumkumasali roasted at 120 ℃ (KU-120, 7.54 g).

Bulk density (g/ml)

It was found that Kumkumasali roasted at a temperature of 140℃ (KU-140) has the highest bulk density (0.509 g/ml) and Kumkumasali roasted at a temperature of 120℃ (KU-120) has the lowest bulk density (0.203 g/ml). Flaking process decreases the voids existing within the sample particles resulting in an ordered arrangement of particles and consequently lowering down the density (Ghasemi *et al*., 2008).

Size and thickness (mm)

It was found that Kumkumasali flakes roasted at 120℃ (KU-120) have the minimum value of size and thickness (0.062 mm) and the maximum value been obtained for Kakasali flakes roasted at 100℃ (0.122 mm). Size and thickness of commercially available flakes (MF) was found to be 0.113 mm. Flake thickness varies depends on the intended use. Thicker flakes require longer cooking time and maintain flake integrity during extended holding time (Samuel, 1991).

Sogginess (min)

Sogginess is the measure of disappearance of crispiness. Kumkumasali variety roasted at a temperature of 120℃ (KU-120) showed the highest value of sogginess (6.3 min). The lowest value was observed in Raktasali roasted at 100℃ (3 min). Commercially available flakes (MF) have comparatively lower sogginess value (3.3 min).

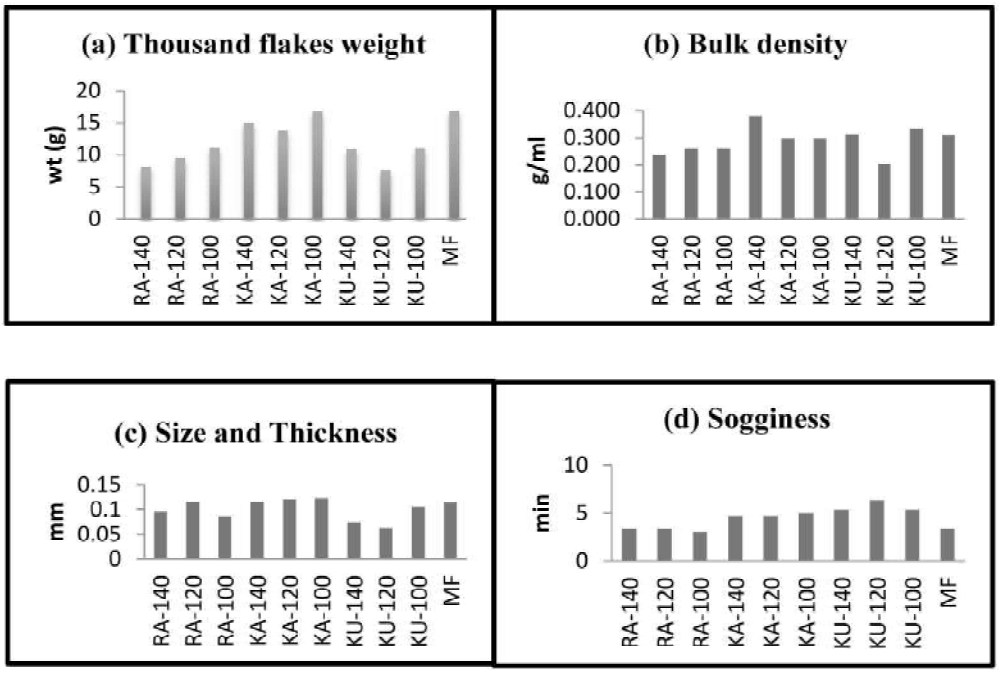

Figure. 2. Effect of different temperature on physical properties of GABA enriched rice flakes.

Sensory evaluation of GABA enriched flakes

Sensory evaluation was conducted by a consumer panel of twelve trained members. It was found that overall acceptability of flakes samples varied from 6 to 8.125. The best sample selected by the sensory panel was KU-120 with overall acceptability of 8.125, along with the control sample MF.

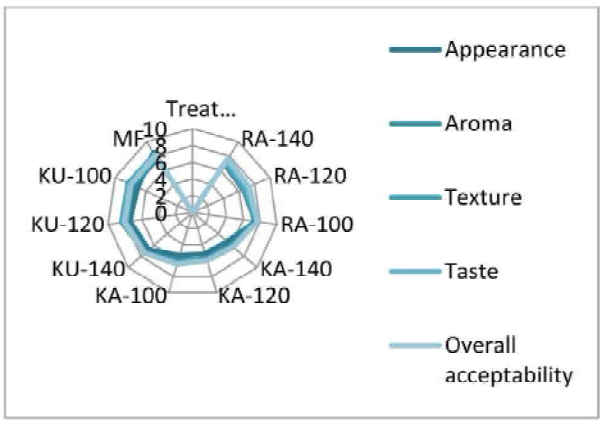

Summary and conclusion

GABA enrichment in specialty rice flakes requires optimization of germination conditions of paddy. So by analyzing the results obtained from germination tests, 36 hour germination was selected for further processing. Different roasting temperature for flakes also effect GABA content. Three temperatures viz. 100°C, 120°C and 140°C were provided for rice

flake varieties and Kumkumasali flakes roasted at 120℃ was selected as the best sample based on its sensorial attributes and other physical properties.

References

1. Bewley, J. D. and Black, M. 1985. Seeds physiology of Development and Germination. Second edition, Plenum press, New York, pp 18-26.
2. Ghasemi, M., Varnamkhastia., Mobila, H., Jafaria, A., Keyhania, A. R., Soltanabadib, M. H., Rafieea, S. and Kheiralipour, K. 2008. Some physical properties of rough rice grain. *J. Cereal Sci.* 47, pp. 496-501.
3. Karladee, D. and Suriyong, S. 2012. γ- Aminobutyric acid (GABA) content in different varieties of brown rice during germination, Research article.
4. Komatsuzaki, N., Tsukahara, K., Toyoshima, H., Suzuki, T., Shimizu, N. and Kimura, T. 2007. Effect of soaking and gaseous treatment on GABA content in germinated brown rice. *J. Food. Eng.* 78: 556-560.
5. Maisont, S. and Narkrugsa, W. 2010. The effect of germination on GABA content, Chemical composition, Total phenolics content and Antioxidant capacity of Thai waxy paddy rice. *Kasetsart J. (Nat. Sci.)* 44: 912-923
6. Ohtsubo, T., 2004. Studies on textural and chemical changes in aged rice grains. Fd sci. Technol. Res. 11: 385-389.
7. Ruiz, A. and Bressani, R. 1990. Effect of germination on the chemical composition and nutritive value of amaranth grain. Cereal chem. 67: 519-522.
8. Samuel, A. M. 1991. Chemistry and Technology of Cereals as Food and Feed. Spriger Science and Business media.

10.

Compromise of Sensory Attributes Towards the Healthy Nutritious Food: A Case Study of Aonla juice

Vishal Sharma[1], Tanishq Das Gupta[1]
[1]National Institute of Food Technology Entrepreneurship and Management (NIFTEM), Sonipat, Haryana 131 028, India

Abstract *Nowadays, Sensory attributes of Foods are being given less importance over health. Sensory attributes are classified under intrinsic quality attributes, involving factors like taste, color, flavor, texture, and appearance etc. Most food production branches by responding well to their segmented product's higher demand in the market, sometimes neglect issues regarding quality of Foods. Their main focus aims at healthy foods for more sales and profit, thinking as people are more health conscious nowadays, will compromise even on sensory attributes over health. Surprisingly, companies do not spend many resources on good storage and packaging, rather spend more on value addition to launch their new product to target new health-conscious segments. With accretion in healthy foods for customers, various different flavored compounds are being singled out by neglecting issues on smell and taste. Addition of ingredients for sensory improvements like for texture and flavor, without affecting the perception of sensory parameters is a technically tough challenge for the food sectors. Evaluation of customer responses for the lessening of different sensory ingredients over health can help in analyzing the responsibility of food manufacturers and nutritionists. This review considers a case study on the improvement in the acceptance of aonla juice by reducing the bitter taste as perceived due to the presence of the polyphenol, Emblicanin. Influence and acceptance level of consumers over such compromised foods is also being focused.*

Keywords: Aonla juice, bitterness, food quality, health, sensory, polyphenols

Introduction

Aonla (*Emblica officinalis*) or Indian gooseberry is indigenous to Indian sub-continent, belongs to the *Euphorbiaceae* family. India is on the top of the world in terms of area and yield of aonla. This fruit has a greenish yellow color with an astringent taste. Aonla fruit or juice being sour in nature, cannot be consumed in raw form. However, they have unique medicinal and therapeutic values. Despite the high nutrition content of the Aonla juice (Table 1), its astringent nature and bitterness tend to hinder the overall consumer acceptability and choice. The anti-oxidative property of aonla is high due to the high vitamin C content. Clinical assays have demonstrated that the extract of fruit juice has anti-inflammatory and antioxidant properties, which can create convincing effects on, insulin, foam cell formation, dyslipidemia, glycemia and blood pressure (Lo KM et al., 2005).[1] Aonla carries a tremendous potential in the world market, yet it is presently an underutilized fruit. There is also vast scope to dig into the possibilities for utilization of aonla in the beverage industries. Also, there are many reported efforts on the aonla fruit utilization in the various products utilization.

Utilization of Aonla with certain additional blends including CMC (carboxymethylcellulose), milk, sucrose, aloe vera, ginger juice, apple, lime, pomegranate etc. can improve the overall sensory attributes and nutritional content (Jain et al.,2004).[2] Aloe Vera (*Aloe barbadensis miller*) is a part of *Liliaceae family*. Around 250 species of aloe vera are grown around the world (Valverde JM et al.,2005).[3] Nonetheless, just two main species viz., *A. aborescens and A. barbadensis miller* are crucial from the utilization viewpoint. Aloe

vera gel may be unpleasant in the raw state due to its bitter taste, however, its palatableness can be improved with the accession of other fruit juices.

Carboxymethyl cellulose

One of the derivatives of a polysaccharide, cellulose with adhered carboxymethyl groups to some of the hydroxyl (OH) groups of the monomers of glucopyranose that make up the polysaccharide (cellulose) backbone. Formulation of foods with the carboxymethylcellulose (CMC), a common hydrocolloid, may conceal the bitterness of polyphenols, which help in health-boosting. For instance, the sensing of the astringent flavors of the polyphenolic extracts of green tea, chokeberry and walnut was significantly reduced by CMC (A. Troszynska et al.,2010).[4]

Ginger

Ginger is advised in people having bile stones, to take as an herb and it encourages the gallbladder to release bile. The usefulness of ginger in decreasing arthritis-originated joint pain and the cholesterol level, which may help in treating heart diseases (Fahlberg et al.,1969).[5] The mix of Aonla, aloe vera and ginger juice extracts extend to experience a considerable amount of attention regarding an increasing cognizance about the capability of these products in the market. The high nutritional properties and the energy content of these beverages tend to enhance the remedial properties of the beverages (Table 2). These could be specifically useful in places having food storage and not proper nutrition.

Milk

Milk can also act as a carrier source for the polyphenol-rich antioxidant extracts, which could in turn help masking the astringent flavor of the polyphenols. Milk contains the disaccharide lactose in the major proportion of 3.7-5.1%. The acerbity of the polyphenolic compounds can be reduced by both sucrose and milk, as they can act as a carrier source for the polyphenol-rich antioxidant extracts (G Ares et al., 2009).[6] Milk is an excellent source of high-quality protein, in addition to minerals and vitamins. Milk and dairy products are well known for providing the correct amount of nutrients, particularly protein, calcium, phosphorus, vitamin D, magnesium, vitamin B_{12}, potassium and zinc (Table 4).

Chitosan

To reduce the bitterness of the polyphenolic compounds, β- cyclodextrin- chitosan, a polysaccharide is used. Cyclodextrins come under the class of macrocyclic compounds incorporating several glucose subunits. They are cyclic oligosaccharides and these cyclodextrins are produced from starch by the action of enzymatic conversion. The cyclodextrins (oligosaccharides), which have a cyclic nature, are deduced enzymatically from starch hydrolysates and they are a widely accepted food ingredient having better solubility in water and only a modest sweet taste (Fenyvesi et al.,2004).[7] The modified binding properties can be obtained from the chemically modified cyclodextrins, however, they are not all the allowed as food additives (Binello et al.2008).[8] The derivation of cyclodextrins to form the amphiphilic molecules which can spontaneously auto-assemble to turn into nanoparticles and link better with the biological membranes (Bilensoy E, 2008).[9] The formation of a tapered cone structure by the cyclodextrin molecules having an internal diameter of 4.9–10 A with a hydrophilic external face and a hydrophobic inner face. The hydrated cone in the solution

having hydrophobic groups or hydrophobic small molecules on bigger molecules can readily replace the interior water, which leads to the formation of a thermodynamically stable complex. The amphiphilic molecules can be bound by cyclodextrins with the hydrophilic group excluded, and the hydrophobic group inside the ring. For liquid preparations, the hydrophobic compounds can be made soluble with the help of cyclodextrins (Brewster ME, 2007).[10] Whenever the bitter part of the molecule interacts with the bitter receptor and is admitted inside the ring, thus, it may not conduce the sensed bitter flavor.

Table 1. Nutritive value of the fresh fruits of different aonla varieties

Variety of Aonla fruit	TSS (°Brix)	Polyphenols (%)	Total Sugar (%)
Banarasi	14.43 ± 0.05^{c}	25.77 ± 0.81^{a}	29.33 ± 0.01^{a}
Chakiya	12.10 ± 0.10^{a}	28.81 ± 0.08^{b}	36.91 ± 0.04^{c}
Desi	15.06 ± 0.11^{d}	31.80 ± 0.18^{c}	28.01 ± 0.06^{a}
Kanchan	14.20 ± 0.11^{b}	25.33 ± 0.47^{a}	28.84 ± 0.02^{a}
NA-7	12.13 ± 0.00^{a}	26.94 ± 0.02^{a}	32.85 ± 0.02^{b}

Source: Khatkar and Praveen, year

Table 2. Major Nutritional Components in Ginger affecting sensory attributes

Major Nutritional Components of Ginger affecting Sensory Attribute	Value per 100 g
Water	79g
Protein	2.6g
Carbohydrate	17.23
Sodium	40mg
Vitamin C	44mg

Source: USDA, National Nutrient Database, 2011

Table 3. Major Nutritional Components in Aloe- Vera affecting sensory attributes

Nutrition Declaration	Per 100ml	Per 45ml serving
Energy	10.4 kj per 2.4 kcal	4.6kj/ 1.1 kcal
Fat	0.2g	0.09g
Of which saturates	< 0.1g	<0.04g
Carbohydrates	0.4g	0.2g
under which sugars	< 0.1g	<0.04g
Salt	<0.01g	<0.004g
Protein	<0.1g	<0.04g

Source: Pukka herbs,2018

Table 4. Major Nutritional Components in Milk affecting sensory attributes

Constituent	Normal Milk (%)
Milk nonfat solid	8.9
Fat	3.5
Whey protein	0.8
Sodium	0.058
Chloride	0.092
Potassium	0.174
Protein	3.6
Casein	2.79
Lactose	4.9
Calcium	0.12

Source: Harmon, 1994

Materials and methods

Juice extraction- Aloe vera

The method of juice extraction will lead to the variable chemical composition of the juice (Table 5). The separation of aloe vera gel was performed by the method of cold extraction and the processing of the extract into juice was done as per the method reported by Satwadhar PN et al. (2011).[11] Throughout the method of pasteurization, the pectolytic enzyme was made inactive. The results obtained suggest that the aloe vera leaves, which are fully developed and long, are the best choice for the high yield extraction of the gel. The nutritional components in Aloe vera have an impact on the sensory quality of the aonla juice (Table 3).

The sensory quality of combined Ready to serve beverage were ascertained on a 9-point Hedonic Scale. The evaluation of the juice samples as described by (Larmond,1985)[12] for the identification of their sensory attributes mainly taste, appearance, flavor and color by a panel of 20 panelists drawn from faculty members, undergraduate and postgraduate students of their specified department. The taste, color, appearance, overall acceptability and flavor of the blended juice made was approximately same for few of the proportions like 70:15:15 and 80:10:10, where the proportions were in the ratio of aloe vera, ginger and aonla.

Table 5. Chemical properties of Aloe vera, ginger juice and aonla

S.No.	Constituents	Aloe vera juice	Aonla juice	Ginger juice
1	Moisture (%)	97.6	82.5	81.9
2.	TSS (°Brix)	2.1	2.8	2.4
3.	Acidity (%)	1.2	2.6	0.6
4.	pH	4.4	3.1	3.9
5.	Vitamin C (mg)	7	900	2

Source- AOAC (1995) Official Methods of Analysis

The chemical properties of the ginger, aloe vera have a cumulative and direct effect on the quality of the sensory attributes of the aonla fruits, including taste improvement, flavor and

keeping the quality of Aonla fruit (Singh et al.,1995).[13] The better physical properties, keeping quality and flavor of the blended juice extract resulted due to the freshness including various factors such as variety, growth stage, and maturity of the fresh fruits.

Fruit blend with aonla juice

The improvement in the flavor of aonla juice was accompanied by fruits viz. apple, lime, pomegranate, grapes. The preparation of the RTS beverage by blending goose-berry juice in a ratio of 20:80 was found to be excellent on the ground of vitamin C content and overall sensory quality. The pasteurization of all the mix/ blends was done at 90°C for one minute prior to the pre-sterilized bottled packaging in 0.2 L capacity. (Jain et al., 2004).[2]
All the blends were acceptable, even though, they differed importantly in terms of flavor and color. The Ready to serve beverages as prepared from the grape juice of Pusa Navrang variety blended with aonla juice, were superior in terms of flavor, taste and color (Table 6). However, it was found that the increment of aonla juice affected the gradual declination in color of the juice of the accompanying pomegranate and grapes variety. On the other hand, increasing of aonla juice content up to 15% in few of the non-colored juice like apples, lime and grapes increased the color score up to some extent yet later on decrement in the score observed (Jain et al. 1995).[2] The flavor of the aonla-lime blended RTS beverages was in higher order as of (7.31 out of 9.00), disregarding of the ratio of blending of the aonla juice. This increment was due to the superior flavor of the lime (Singh, 1995).[13] Preparation of ready to serve beverages by blending of lime juice and 15% aonla juice was the best having a score of (8.39 out of 9.00).

Table 6. Overall sensory quality (score out of 9) of the RTS beverages as affected by fruit and proportion of aonla juice

Proportion of Aonla juice (%)	Apple	Lime	Grape (Perlette)	Grape (Pusa Navrang)	Pomegranate	Mean
0	6.35	6.95	6.96	8.16	7.25	7.13
5	6.67	7.67	7.07	7.89	7.22	7.30
10	7.17	7.74	7.28	7.90	7.31	7.48
15	7.51	8.38	7.19	7.79	6.97	7.57
20	7.21	7.65	7.03	7.64	6.56	7.22
25	6.84	7.22	6.64	7.43	6.33	6.89
30	5.95	6.53	6.18	6.43	5.56	6.13
50	5.95	6.53	6.18	6.43	5.56	6.13
Mean	6.75	7.39	6.85	7.51	6.63	7.03
Critical difference at 5%						

Source- Akinwale PO (2000)

Milk contains 4.9% Lactose as a carbohydrate, which in turn decreases the bitterness caused due to Polyphenols present in Aonla. Lactose, which is disaccharide composed of simple sugars- Glucose and Galactose, is sweet in nature thus masks the acerbity of Aonla juice. Milk fat, which is another component of Milk is an emulsion and has a substantial consequence on the suppression of bitterness of only a few polyphenolic extracts of plants as considered. (John N. Coupland, John E. Hayes., 2014)[14]

β- cyclodextrin- chitosan is also capable to conceal the bitterness of bitter compounds, as one such present i.e. Emblicanin. If the design of the physical structures is intelligent according to these principles, the requirement of suitable sensory and physicochemical characterization by these physical structures is necessary. The physicochemical characterization mainly pronounces the location of the bitterant, its method of binding and the time taken to release. The sensory characterization focusses on the specific taste comparison with real-time consumption conditions. (Coupland et al. 2016).[14]

CMC masks the bitterness by interacting polyphenol (*Emblicanin*) present in Aonla fruit in combination with the taste receptors. Since taste acts through the specific receptors, it can block certain specific receptors. CMC can act as a taste-blockers thus can act as inhibitors. Thus, they block the receptors by attaching itself to the receptor but does not trigger the taste sensation. So, no firing of neurons takes place, thus no sensing of that particular bitter taste arises, in turn removing the unpleasant bitter taste from the Aonla fruit.

New ways to improve the flavor and astringency of the Aonla fruit juice by utilizing novel compounds such as CMC (carboxymethylcellulose), milk and Sucrose needs attention. The formulation of foods with the common hydrocolloid, carboxymethylcellulose (CMC) can mask the bitter flavor of health-promoting polyphenols.

Acknowledgments

We are grateful to the respected authors for their precious work that helped us to support our review on this topic. We are also thankful to MES Mampad College, Kerala for providing us the opportunity to present our work.

References

1. Lo KM, Cheung PCK (2005) Antioxidant activity of extracts from the fruiting bodies of Agrocybe aegerita var. alba. Food Chem 89: 533-539.
2. Jain, S.K. and Khurdiya, D.S. 2004. Vitamin C enrichment of fruit juice based Ready-to-Serve beverage through blending of Indian Gooseberry (Emblica officinalis Gaertn.) juice. Plant Foods for Human Nutrition 59: 63-64.
3. Valverde JM, Valero D, Martinez-Romero D, Guilln F, Castillo S, et al. (2005) Novel Edible Coating Based on Aloe vera Gel to Maintain Table Grape Quality and Safety. J Agric Food Chem 53: 7807-7813
4. Troszynska A., O. Narolewska, S. Robredo b, I. Estrella b, T. Hernández b, G. Lamparski a, *, R. Amarowicz the effect of polysaccharides on the astringency induced by phenolic compounds
5. Fahlberg (1969) The Pungent principles of ginger and their importance in certain ginger products. Food Tech Aust 21: 570-571.
6. Ares, G.; Barreiro, C.; Deliza, R.; Gambaro, A. 2009. Alternatives to reduce the bitterness, astringency and characteristic flavor of antioxidant extracts
7. Fenyvesi É, Vikmon M, Szente L 2004. Cyclodextrins in Food Technology and Human Nutrition: Benefits and Limitations
8. Binello A, Robaldo B, Barge A, Cavalli R, Cravotto G. Synthesis of cyclodextrin-based polymers and their use as debittering agents. J Appl Polym Sci. 2008; 107:2549–57.
9. Bilensoy E. Nanoparticulate delivery systems based on amphiphilic cyclodextrins. J Biomed Nanotechnol. 2008; 4:293–303.

10. Brewster ME, Loftsson T. Cyclodextrins as pharmaceutical solubilizers. Adv Drug Deliv Rev. 2007; 59:645–66
11. Satwadhar PN, Deshpande HW, Syed IH, Syed KA (2011) Nutritional Composition and Identification of Some of the Bioactive Components in Morinda citrifolia Juice. Int J Pharm Pharm Sci 3: 58-59.
12. Larmond E 1985 Laboratory Methods for Sensory Evaluation of Foods. Department of Agriculture. Ottawa, Canada.
13. Singh IS, Kumar S (1995) Studies on processing of aonla fruits II. Aonla products. Prog Horticulture 27(1/2): 39–47.
14. Coupland John N., John E. Hayes 2014 Physical Approaches to Masking Bitter Taste: Lessons from Food and Pharmaceuticals
15. Prasad PSRK, Surya Prakash Rao PV, Nageswara Rao G, Giridhar N (1968) Some preliminary studies on utilization of aonla (Phyllanthusemblica Linn.). Indian Food Packer 22(6): 8–11.

11.

Formulation and shelf life studies of jaggery based sweet (base sweet) and its utilization for various food preparations"

Najwa khader KT, Hasker.E
Dept .of Food Technology
MES Mampad College , Malappuram Dt. , Kerala

Abstract *Sugar and jaggery are prepared from cane sugar, both are used for various preparations as sweeteners. Jaggery is having more health benefits than sugar. So this study is to make awareness about the health benefits of jaggery and to make base sweet and also for making some novel products from it. Jaggery production in our country is a traditionally labour intensive cottage industry, mostly confined to rural areas ,jaggery is an eco friendly sweetener but meets about only 35 percent of the demand of the sweeteners in the country. Since jaggery contains lots of moisture, often melts on heating and contracts fungal infection and also undergo deterioration due to wind and rain. Hence developing shelf life based jaggery additives seems to be essential. Usually jaggery is not pure as sugar. So we need to clean even it is using as a syrup. So tried to make some novel products and their quality parameters were analyzed. Similarly sensory evaluations of the products are recorded. The reason why most people use sugar is due to lack of knowledge about health benefits of jaggery. Hence this research would be beneficial to encourage and educate society about use of jaggery as a substitute for sugar*

Introduction

Sugarcane, *Saccharum officinarum*,is a perennial grass in the family poaceae grown for its stem(cane)which is primarily used to produce sucrose. The major producers of sugarcane in the world are Brazil, India, China, ,Thailand, Pakisthan and Mexico. Sugarcane reach a height of upto 6m(3.3 ft)and once harvested ,the stalk will regrow allowing the plant to live for between 8-12 years.The stems grow into cane stalks ,which when mature constitutes around 75%of the entire plant. A mature stalk is typically composed of 11-16% fiber, 12-16% soluble sugars, 2-3% non-sugars and 63-73% water. Sugarcane has thick tillering stem which is clearly divided into nodes and internodes. The leaves of the plant grow from nodes of the stem.

Sugarcane is primarily used to produce Sugar and Jaggery. Both Jaggery and sugar are predominantly made of sucrose,but sugar has only sucrose unit while jaggery has traces of minerals,salt,iron,vitamins and some fibre along with sucrose. The first stage of manufacture of jaggery and sugar is same,the first step is the boiling of sugarcane juice. After the intial boiling, in case of sugar, this syrup is treated with charcoal(preferably bone charcoal) to absorb unwanted particles and then crystallized. In case of jaggery, there is no treatment with charcoal or crystallization. The another liquid is boiled continuously to form thick paste. Jaggery is produced in different forms Viz Solid, Liqiud and powder or granular forms. Solid and liquid Jaggery are obtained by concentrating sugarcane juice. In case of granular jaggery concentrating slurry is rubbed in the wooden scrapper for formation of grains.

Industrial aspescts and marketing

The industries of sugar is very well organised and highly merchandised, as almost all sugar coming to the market is manufactured in sugar mills run by big companies. Hence

sugar is branded and has big influence on the CPI and thus on ecocnomy .Despite the fact that jaggery manufacturing has been practiced for centuries, much before sugar cane came into being and there is a big market for it ,this industry is still not organised and would not come out of the realms of the rural areas. Due to lack of infrastructurural facilities in jaggery production and insufficient price dissemination in jaggery marketing. Jaggery manufacturies faced many constraints. It is therefore imperative to expand the sector ,as it provides higher food value jaggery at lower cost and boost up the rural economic system. Due to its nutritional and medicinal value ,the jaggery has great export potential in the world.

.



Health benefits of Jaggery.

Digestive Agent, ,Prevent,Constipation,,Source of Minerals,Sweetening agent, Detoxification of the liver,Treats flu-like symptoms,Blood purifier,Boosts immunity, Cleanses the body,Eases menstrual pain, Prevents anaemia
Boosts intestinal health,Cools the stomach,Controls blood pressure,Prevents respiratory problems,Relieves joint pain,Weight loss,Good source of energy.

Objectives of the study

1. To develop sweet base with jaggery
2. To educate society about use of jaggery as a substitute for sugar
3. To find out some techniques for developing novel products from jiggery
4. To conduct sensory analysis of the developed products
5. To reduce the spoilage and wastage of food like amla ,dates, guava, jackfruit ,pineapple, cherry through value addition by jaggery
6. To study the chances of improving the nutritional status of the society through jiggery
7. Study the chances of incorporation of some ingredients to jaggery to develop new products.

Social relevance of the work

Study provides some new information regarding the fromulation of jaggery based sweet. The significance of this study was that all formulation and preparation methods developed were very easily adaptable for common peoples. Due to lack of knowledge about health benefits of jaggery people use sugar to meet their sweetening needs which is more proximous than jaggery. . Among the methods and products developed Cherry In Jaggery, Jaggery Date Cake, Jaggery Mango Candy, Osmotic Dried Guava ,Jaggery Amla Mixture And Jaggery Pineapple Jam requires very simple machines and equipments and lab setup. Jaggery jack biscuit was found to be very good when the incorporation of the soya flour was 10% compared with 20% and 30%. Testing of moisture, testing of brix etc can be determined now a day the simple digital machines. Operations of oven and driers are also very simple. The

developed methods help farmers and entrepreneur to start new units which can process jaggery as base sweet. There is no R&D assistance and marketing institution so far to support commercialisation of jaggery in the country. Also lack of scientific literature as well as process technologies form barrier to commercial exploitation of jaggery. Work and research on this topic is very relevant because of its amazing health benefits that common people are not aware .The reason why most people use sugar as sweetener is its proximity and lack of knowledge about health benefits of jaggery. Hence this research will help to encourage and educate society about use of jaggery as a substitute for sugar. Another important aspect of this project is cheap processing and production cost. Raw materials are easy to store and is cheaply available. Amazing health benefits jaggery will help this project study to develop various types of jaggery without any artificial colour flavour which will promote conventional packaging jaggery in hygienic packs and producing jaggery free from impurities. All the developed products have specific nutritional and socialsignificance .Jaggery can be treated for supplementation of minerals and nutrients which have wide range of target groups from kids to elderly groups. Formulation with amla is more suited even for diabetic patients. Date cake can be highly recommended for pregnant women

Jaggery processing

Jaggery (Gur):
Manufacturing of Jaggery is from sugar cane followed by clarification and concentration process . It is Uncentrifuged sugar (i.e Without separation of molasses) with minimum sucrose 70 to 80% by mass. It is also called as Gur.
Main steps in jaggery making process:

- Extraction of Juice
- Clarification of juice
- Concentration of juice

Extraction of Juice:

Generally three roller mills used for juice extraction. It is driven by electrical motor or diesel engine. This extraction of juice is in the range of 60 to 70%. After extraction of juice, suspended matters are removed by cotton cloth or finr mesh screen.

Clarification of juice:

- The sugar juice contains colloidal matter, inorganic salts, fiber, various nitrogenous substances, lipids, gums, wax organic acid, inorganic acid, pectin etc. All these impurities removed totally or partially in this clarification process.
- In the clarification process generally used two types of clarificants are used .They are Organic Clarificants and Inorganic Clarificants. In organic clarificants are form vegetable origin like Bendi, Sulkali and Doela. Inorganic clarificants used like Lime, Super phosphate etc
- The screen juice taken in open pan and firing starts slowly so that dissolved air escaped and gummy, colloidal substances get coagulated by the adding of clarificants as per requirement. It comes at top surface of the juice know as scum and it is removing continuously . In this process temperature requirement is 70degree C to 80 degree.

- First added vegetable origin simultaneously small quantity of lime water is added to reduce the acidity of juice but not to the extent to make juice neutrals because taste and colour of gur produced will be inferior. In this lime process pH maintained 6.2 to 6.5 . In some cases super phosphate. P O and 0.25% concentrated hydrous power are also added to obtain good colour of Gur (jaggey). While juice temperature rising scum is removed by perforated strainers.

Concentration of juice:

After clarification completed by vigorous boiling, temperature of boiling mass is around 110 to 115 Boiling take place about 2 to 3 hours. The stage at which semi fluid material is formed then it is transferred rectangular boxes or Bucket shape boxes as per requirement. This mass is allowed to cool for solid form.

Specifications Of Jaggery

S.No.	Characteristic	Grade 1	Grade 2
1	Sucrose % by mass (Min)	80	70
2	Reducing Sugars% by mass (max)	10	20
3	Moisture % by mass (max)	5	7
4	Water Solubility % by mass (max)	1.5	2
5	Sulphited Ash % (max)	3.5	5
6	Ash Insoluble in dilute HCL % by mass (max)	0.3	0.3
7	Sulphur Dioxide In PPM	5	5

Materials and Methods

The study was centralised in the Food Technology Department of M E S Mampad College, which includes the Processing, analytical Lab and Pilot Plant. The materials are collected from Three different Districts of Kerala which include Mannuthy from Thrissure, station of Kerala Agricultural university, Kondotty and Pandikkad In Malappuram District and Cherode of Calicut District of Kerala. For the data collection, Interaction, materialising the process and product formulations, faculty and researchers of the Agricultural station at Anakkayam, KAU Thrissure both in Kerala and TNAU Tamilnadu are significant.

a)Study areas, Collection and primary processing

Preparation

The sugarcane stem is cut at the nodes into pieces of uniform size. Cane juice is extracted from this using crusher. Usually 2-5 roller crusher is used for extraction of juice which may be power operated (engine/electrical). Then a small portion of lime is added to the sugarcane juice and set to boil in a open pan. As the liquid begins to boil the molasses is separated out. As the temperature of the liquid raises it begins to foam and gradually the foam vanishes. At a certain stage the juice begins to boil, which is identified by formation of bubbles. Upon further boiling the juice condenses into a thick viscous liquid.

Once the right temperature is reached the boiling is stopped and the liquid is then transferred into a flat pan, to facilitate faster cooling. The liquid is stirred in the flat pan and when it cools down sufficiently, it is transferred into various moulds of different shapes and sizes.

The jaggery is then left aside to solidify and after a day it is extracted out of the mould and is ready for use. This jaggery is used for research works

b) Preservation Methods and techniques

Products developed

Jaggery Mango Candy.

Fully ripened mango after primary processing, cut in to small pieces and grind with jaggery powder and kept in open cooker ,mild heating . Mild heating for 20-25 minutes .Addition of 10 % fruit weight of washed, seed- removed dates and and mix well. After forming a thick consistency scrapped coconut is added and powdered sugar and corn flour. Three types of corn flour inclusions are practiced. Candy with10, 20, and 30% inclusions of corn flour were prepared.

Osmotic Dried Guava

Candied fruits are also known as crystallized fruit. They are made by submerging fruit pieces in sugar syrup solutions of gradually increasing strength, then drying. During the soaking, sugar is absorbed by fruit and moisture is lost from the fruit. They can be kept for several months when stored in a cool dry place. Here an innovation is done by submerging guava in jaggery syrup solution

Guava is washed and sliced length wise (1 Cm breadth), It is then put in jaggery at three levels of concentrations.40, 50, 60 Brix were prepared .Kept one hour for soaking then first stage heating at a temperature of 55 for 12 hours and in second stage 65 degree for 12 hours .the product is the packed air tight in polythene bags.

The guava is washed and sliced length wise. There were four treatments comprising of four concentration of jaggery syrup as follows:

T1 = 35 Brix jaggery syrup
T2 = 40 Brix jaggery syrup
T3 = 45 Brix jaggery syrup
T4 = 50 Brix jaggery syrup

Jaggery Jack biscuit
High protein incorporating soya flour)

Biscuit is a popular snack item with a wide range of target groups. In this study an attempt has been made to increase the protein and mineral content of biscuits made of jaggery and jack fruit. Biscuits can be used especially to feed malnourished children and can also be used in mid-day meal programme to improve the protein and mineral intake of children. So this study is an attempt made to in corporate jaggery soya flour in jack fruit biscuit .

Cherry in Jaggery

Matured cherry after washing is cooked on low flame with water in a pan till cherry turns soft. Grated jaggery and pepper powder is added.. stirred well and cooked for another 110-15 minutes on low flame till cherry coats well with jaggery syrup. Lemon juice is added before removing from the flame. Stored the cherry in jaggery in three different types of containers

Glass container
Mud pots
PET bottles

After 1 months performed sensory analysis .There is no much change in the taste and falvour of the product stored in all containers, but the sensory evaluation data shows that quality of the product stored in mud pot was comparatively with superior quality

Jaggery Date Cake

Washed dates is crushed .To this shredded jaggery is added along with peanut

Steps

- Wash dates and remove seeds.
- Smash the core of the fruit.
- Powder the jiggery cubes
- Mix powdered jaggery with dates .
- Roast peanut
- Take some gram flour and roast it
- Shred a piece of coconut and roast in ghee
- Blend all the ingredients into a compact mass
- Mould into different shapes

Shelf life study and sensory analysis was conducted in the following proportion.

No.	Dates(in%)	Jaggery(in %)	peanut(in%)	gram flour(in%)	coconut(in%)
1	30	25	20	15	10
2	40	25	25	15	5
3	50	20	20	8	2
4	55	20	20	3	2

Shelf life study was conducted and performed sensory analysis. Maximum shelf life was found to be 3 weeks for the dates jiggery proportion 50:20. But sensory evaluation data shows peanut 25% is mostly preffered by people.

Jaggery Amla Mixture

Matured variety of amla after washing is ooked on low flame with water in apan till amla turns soft. Seed is removed. Powdered jaggery is added.stirr gently the amla jagggery mixture on low flame. Cardamom is added. Cooked it for 5minutes till the consistency is reached. A pinch of salt is added for neutralizing the taste. Percentage of jiggery were 30,40,50,60 and 70.

Quality was found to be safe till 2 week in 55%jaggery. These can be taken as desserts after every meal.

Jaggery Pieapple jam

Good quality riope pineapple is selected .After washing well in cold water peel and core is removed. Peeled fruit is cut into small pieces.Jaggery and acid is added. Cooked the mixture slowly by occasional stirring. Cooking is continued till the temperature of mass is reached 105.5 degree C.

Jaggery Oatmeal Cookie

Preheated the oven to 180 degree C . Greesed a baking tray with oil. Put oatmeal ,wheat flour, olive oil, powdered jiggery,black pepper powder,cinnamon powder and ginger powder in a bowl mix well. Added soda and mixed well. Then added ,milk and mixed well. Droped dollops of oatmeal mixture on the greesed tray keeping some distance between each. Place the tray in the preheated oven and baked for 20 minutes . removed the tray from the oven and cooled down to room temperature.

Results and Discussion

The work was mainly focussed to develop new preservation methods for jack fruit. The main products developed are Jaggery mango candy,Osmotic dried guava,Jaggery jak biscuit , Cherry in jaggery, Jaggery date cake, Jaggery amala mixture, jiggery pineapple jam ,Jaggery oatmeal cookies.The raw materials for developing the above mentioned Products by varied methods and techniques mainly include sugarcane, jackfruit ,cherry, dates, mango, guava, amla, pineapple, oatmeal, peanut, coconut. Considering the sensory analysis report and shelf life of the products, cherry in jaggery, jaggery mango candy, jaggery jack biscuit, jaggery oatmeal biscuit were superior in overall quality to other products. Even though jaggery amla mixture, jaggery date cake have very short shelf life they are highly accepted when consumed freshly.

All the products have specific nutritional and social significance.. .Jaggery can be treated for supplementation of minerals and nutrients which have wide range of target groups from kids to elderly groups. Formulation with amla is more suited even for diabetic patients. Date cake can be highly recommended for pregnant women.Cherry in jaggery showed slight textural changes after 2 month time. Jaggery Jack biscuit was found to be good in texture and taste. More over as biscuit is a popular snack food; it was easy to attract more peoples and to widen the consumer community and target group. Product made from dates and amla was highly accepted. The thin slices of osmotic dried guava made the product highly novel to the consumers. The variety jiggery pineapple added more appreciation from the panel members of sensory evaluation.

Jaggery mango Candy with10, 20, and 30% inclusions of corn flour were prepared. 10% was superior in quality.

Among the products developed, jaggery jack biscuit was with high quality and overall acceptance. Jack biscuit was found to be very good when the incorporation of the soya flour was 10% compared with 20% and 30%.

Summary and conclusion

Study provides some new information regarding formulation and shelf life of jaggery based sweet and its utilization for various food preparations. The main significance of the study is that the raw material l(sugarcane and jaggery) is cheaply available . It can be used as substitute of sugar which has much negative effect on body. The methods developed are very easily followed even by farmers and at home. Among the methods and products developed Cherry In Jaggery, Jaggery Date Cake, Jaggery Mango Candy, Osmotic Dried Guava ,Jaggery Amla Mixture And Jaggery Pineapple Jam requires very simple machines and equipments and lab setup. Jaggery jack biscuit was found to be very good when the incorporation of the soya flour was 10% compared with 20% and 30%. Testing of moisture,testing of brix etc can be determined now a day the simple digital machines. Operations of oven and driers are also very simple. The developed methods help farmers and entrepreneur to start new units which can process jaggery as base sweet.The general idea and methods developed are to be translated to regional languages and published in local journals in order to equip more farmers and layman to have knowledge in those matters and to make use of. The research outcome of the work is of very interesting to the academic community also. Many projects are going on these lines even the students can put forward and make modifications of the works and develop many other products from . Output of this work is also having some national and international relevance. Out of total world production more than 70% sugarcane is produced in India. Added sugar is the single worst ingredient on the modern diet. It can have harmful effects on the metabolism and contribute to all sorts of disease. Hence use of jaggey as a substitute for sugar is much importance so as to meet the dietary nutritional needs and to support for the food security of the nation.

Reference

1. FAO(2007) The panela Agro industry in Columbia,An altenative for diversifying Income for small scale rural producers. Food and Agricultural Organization of United Nations. Rural infrastructure and Agro- industries Division ,agricultural and consumer protections department(AG)database,Rome.
2. Jaganadha Rao PVK,Das, M,Das SK(2007)Jaggery-A traditional Indian Sweetener Indian Journal of Traditional Knowledge 6:95-102.
3. Singh J,Singh RD, Anwar SI, Solomon S(2011) Alternative sweetness production from sugarcaneinIndiaLumpsugar(jaggery).SugarTech13:366-371
4. Roma Rao IYP,Babu GSK (2011)Value addition in sugar cane : A critical amylase of various consummative produced in Andhra Pradesh .Indian Journal Of sugar cane technology 26:51-54.
5.AshtangaHrudayanSutrasthana5/47-48.
6.Organic facts-www.organicfacts.net.
7.Ayurtimes-Scientific Analysis and critical Reviews-Jaggery-nutritional value-nutrition-facts-analysis
8.HealthandLifestyleBlog-DrJV
9.Maanasi(May3,2016) styleraze-32 marvellous benefits of jaggery (gur) for skin and health .
10.http://herbpathy.com/benefits of jaggery-cid 4195

BIO-EPISTEME

12.

High intensity light induced photoinhibitory stress effects on photosynthetic efficiency and antioxidant defence mechanism in rice (*Oryza sativa* L.) seedlings

P. Faseela and Jos T. Puthur*

Plant Physiology and Biochemistry Division, Department of Botany, University of Calicut, C.U. Campus P.O., Kerala, 673635, India. Telephone: +91-9447507845, Fax: +91-494-2400269, E mail: jtputhur@yahoo.com
*Author for correspondence

Abstract *In order to investigate the high intensity light stress effects on rice (Oryza sativa var. Karuna) at seedling stage, the seedlings were grown in Hoagland solution and nine day old seedlings were exposed to high intensity light stress of 2000 µmol$m^{-2}s^{-1}$ (0, 2, 4, 6 and 8 h). To assess the effects of high light stress on lipid peroxidation, various parameters related to antioxidant defence mechanism (carotenoids, proline and ascrbate) were monitored in rice seedlings. The effects on photochemistry were also studied in intact leaves by the application of qualitative and quantitative analysis of various chlorophyll (Chl) a fluorescence parameters like Fm, Fv/Fo, performance index, area over the florescence curve, Vj, $SFI_{(abs)}$ and phenomenological energy fluxes per cross section (ABS/CSo, TRo/CSo, ETo/CSo, DIo/CSo and RC/CSo). When seedlings were exposed to high light for different time periods in controlled condition, the results related to PSII performance showed that some Chl a fluorescence parameters (performance index, Vj, $SFI_{(abs)}$, ETo/CSo and DIo/CSo) were highly affected. It was noticed that malondialdeyde content was increased after exposing the plants to high light stress. Also, there was an increase in carotenoids, proline and ascorbate content with increasing light exposure period which in general is meant for scavenging the reactive oxygen species.*

Keywords: High light stress; Chl *a* fluorescence; photochemistry; photosystem II.

Abbreviations: ABS/CSo - absorption flux per cross section at t =0; Chl – chlorophyll; DIo/CSo - dissipated energy flux per cross section at t =0; ETo/CSo - electron transport flux per cross section at t =0; Fm - maximal chlorophyll fluorescence; Fv/Fo - efficiency of the water-splitting complex on the donor side of PSII; MDA – malondialdehyde; $PI_{(abs)}$ - performance index; PS – photosystem; $SFI_{(abs)}$ - PSII structure-function-index; TRo/CSo - trapped energy flux per cross section at t =0; Vj - the relative variable fluorescence at J step.

Introduction

Plants produce their own energy via photosynthesis. Although photosynthesis requires sunlight, it also has a negative effect on photosynthesis. When the absorbed light energy exceeds the rate of the photochemical process, photoinhibition occurs. High intensity light above saturation point of photosynthesis initiates high light stress, reduction of oxygen molecules and reactive oxygen species may be generated by electrons leaking from the photosynthetic electron transport system which induces various responses in plants including membrane destruction, structural damage to chloroplasts and other organelles and increase in heat or fluorescence emission (Roach and Krieger-Liszkay, 2014; Faseela and Puthur, 2017).

Plants have various protective and response mechanisms to mitigate the negative effects of high light stress. The protective system of higher plants, through which they survive the oxidative stress, is composed of enzymatic and non-enzymatic antioxidant systems. Enzymatic antioxidant system includes SOD, ascorbate peroxidase, catalase, MDHAR, DHAR, and GSH reductase, etc. Several non-enzymatic antioxidants such as ascorbate, glutathione, α-tocopherol, carotenoids, flavonoids, amino acids, etc. contribute to the protective system in plants against oxidative stress (Gill and Tuteja, 2010; Faseela et al., 2018).

Plant chloroplasts harmlessly dissipate light energy that exceeds photosynthesis requirements through chlorophyll (Chl) *a* fluorescence production, thereby protecting the chloroplasts from light-induced oxidative damage. It is well established that the emission of Chl *a* fluorescence provides an indicator of the primary photochemistry of photosynthesis and measuring of fluorescence might be a more accurate indicator of plant state and be able to detect stress impacts at earlier growth stages and also it enables for the *in vivo* investigation of the PSII performance through the calculation of several phenomenological and biophysical expressions (Strasser et al., 2010).

Rice is one of the leading food crops in the world. As such, it is a staple food of over a half of the world's population mostly in Asia. With increase in population, rice production also has to be increased (Dogara and Jumare, 2014). There are various abiotic stress factors that affect rice production and in the present study we have determined the effects of high intensity light on photochemistry, lipid peroxidation and antioxidant defence mechanism in rice seedlings.

Materials and methods

Rice seeds of 'Karuna' variety were obtained from regional agricultural research station (RARS), Pattambi, Kerala, India and surface sterilized with 0.1% $HgCl_2$ solution for 4 minutes. The seedlings were grown in half strength Hoagland solution at 14/10 h light-dark cycles at 300 $\mu molm^{-2}s^{-1}$, 24±2ºC and R.H. 55±5%. Rice seedlings grown for 9 d in the plant growth chamber were exposed to high intensity light stress of 2000 $\mu molm^{-2}s^{-1}$, provided by 1000 W (Philips) metal halide lamps. A trough of transparent glass (20 cm depth) with circulating water was placed under the lamp to protect the seedlings from the heat generated by the lamp. Air was circulated around the seedlings and thus the temperature was maintained at 24±2ºC. Light intensity at the surface of the leaves was measured by a solar radiation monitor (EMCON, India). Seedlings were photo inhibited for different time periods such as 0, 2, 4, 6 and 8 h and Chl *a*

fluorescence parameters, the extent of lipid peroxidation and antioxidant defence mechanism during photoinhibition was investigated.

Malondialdehyde (MDA) content was determined by the thiobarbituric acid (TBA) reaction as described by Heath and Packer (1968). Two hundred milligrams of plant tissue was weighed and homogenized in 5 ml of 5% trichloroacetic acid solution. The homogenate was centrifuged at 12,000 rpm for 15 min and two millilitre of the supernatant was mixed with an equal aliquot of 0.5% of thiobarbituric acid in 20% TCA and the solution was heated at 95°C for 24 min, cooled and then centrifuged at 3000 rpm for 2 min. The absorbance of the supernatant was measured at 532 and 600 nm against reagent blank using UV-VIS spectrophotometer (Systronics 2201, India). MDA concentration was calculated using its molar extinction coefficient of 155 mmol L^{-1} cm^{-1}.

Total carotenoids were extracted in 80% acetone and calculated according to Arnon (1949). Free proline content was extracted from leaf using 3% sulphosalicylic acid and estimated following the method of Bates et al. (1973) using L-proline as standard. Two hundred milligrams of fresh leaf tissues were homogenized in 10 ml of 3% (w/v) aqueous sulfosalicylic acid, the homogenate was centrifuged for 10 min at 10,000 rpm and the supernatant was collected. Two ml of supernatant was taken in test tubes in triplicate and equal volume of glacial acetic acid and 2.5% acid ninhydrin (1.25 g of ninhydrin dissolved in a mixture of 30 ml of glacial acetic acid and 20 ml of 6 M ortho phosphoric acid) were added to it. The tubes were then heated in a boiling water bath for 1 h and then the reaction was terminated by placing the tubes in ice bath. Four ml of toluene was added to the reaction mixture and stirred well using a vortex mixer. The chromophore-toluene layer was separated carefully and the optical density of the separated solution was measured at a wavelength of 520 nm using spectrophotometer (Genesis 20).

Ascorbate content was measured after the method of Gillespie and Ainsworth (2007). A standard curve was prepared using commercial L-ascorbic acid. Two hundred mg of plant tissue was homogenized with 5 ml 5% (w/v) TCA and the homogenate was centrifuged at 12,000 rpm for 15 min at 4°C. An aliquot of 0.1 ml of the supernatant was mixed well with 0.3 ml of 200 mM NaH_2PO_4. To this mixture, 0.5 ml of 10% (v/v) TCA, 0.4 ml of 42% (v/v) H_3PO_4, 0.4 ml of 4% (w/v) bipyridyl (dissolved in 70% alcohol) and 0.2 ml of 3% $FeCl_3$ (w/v) was added. The mixture was incubated at 42°C for 15 min and the absorbance was measured immediately after incubation at 524 nm.

Chl *a* fluorescence transients were measured with the Plant Efficiency Analyzer (Handy PEA, Hansatech Ltd., Norfolk, UK). All measurements were performed following a dark adaptation period of 20 min using the leaf clips and the maximal fluorescence was induced by a 1s pulse of white light (3,000 $\mu molm^{-2}s^{-1}$). Thereafter, Chl *a* fluorescence signals were analyzed with the Biolyzer HP3 software. The average values from 30 measurements done on second leaves of the plant for each treatment. Various parameters like Fm, Fv/Fo, performance index, area over the fluorescence curve, Vj, $SFI_{(abs)}$ were measured and the phenomenological leaf model was figured out in response to high light stress in rice seedlings.

Results and discussion

Various Chl *a* fluorescence parameters were derived to evaluate the effects of high light stress on the photochemical efficiency of PSII and have been presented in the form of spider plot (Fig. 1). The performance index provides quantitative information about the vitality of plants and it was decreased upon severity of stress upto 94% in respect to the control seedlings. Kalaji et al. (2012) reported that it is a sensitive indicator to explore the effect of high light on PSII in barley cultivars. It was showed that Fm and Fv/Fo also declined in rice seedlings when exposed to high light and the percentage decrease in Fm was about <20% and that of Fv/Fo was <53% as compared to the control plants and it indicated that an inhibition of electron flow occurred at oxidizing site of PSII and also decrease in efficiency of the water-splitting complex on the donor side of PSII in high light treated plants. The results also showed that high light stress in rice seedlings reduced PSII structure-function-index ($SFI_{(abs)}$) and the percentage of decrease was 86% as compared to control under 8 h high light exposure. Area above the fluorescence curve was decreased upon severity of high light exposure (55% in respect to control) and this decrease in area above the fluorescence curve suggests that high light stress inhibits the electron transfer rates at the donor side of PSII. It also causes increase in the relative variable fluorescence at J step of the fluorescence induction curve (Vj) and it is interpreted as a decreased efficiency of Q_A^- reoxidation and it was more prominent at 8 h high light exposure (70% compared to control).

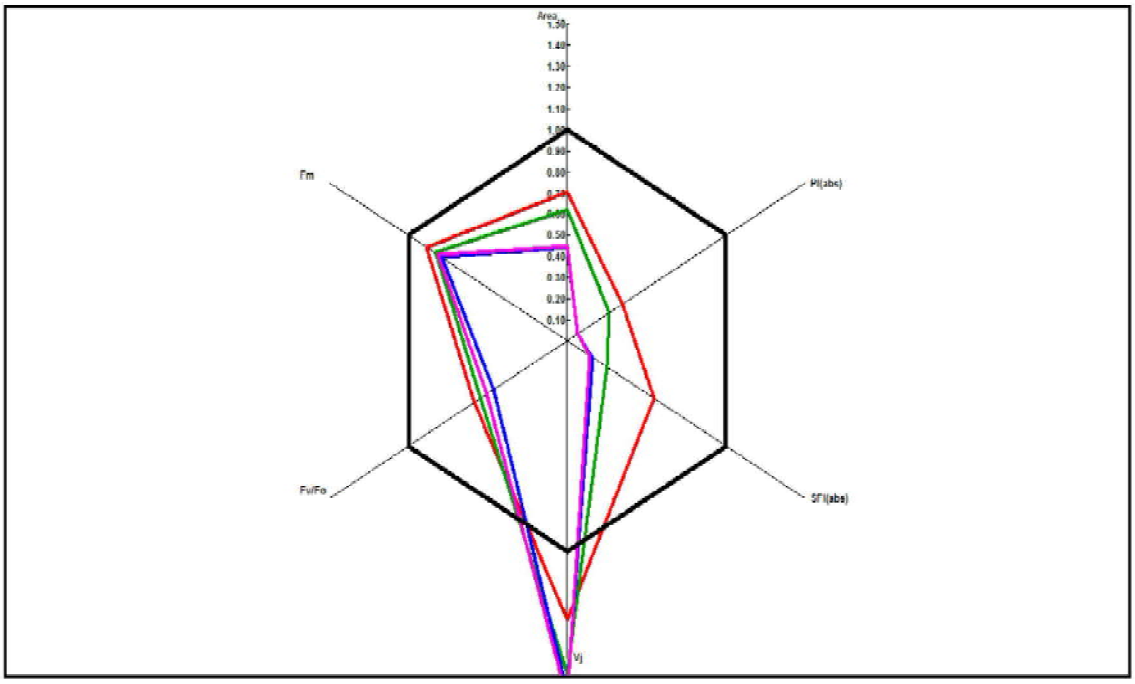

Figure. 1. Spider plot of selected parameters characterizing PSII when subjected to high light stress of 2000 µmol $m^{-2}s^{-1}$ (0, 2, 4, 6, 8 h). Control, 2 h, 4 h, 6 h, 8 h.

The derived parameters can be visualized from energy pipeline leaf model and it deals with the phenomenological energy fluxes per cross section (Fig. 2). A decrease in electron transport in a PSII cross section (ETo/CSo) and the density of the active reaction centers

(RC/CSo) was observed after the high light treatment and this decrease was to the extent of 70% and 22% as compared to that of control. DIo/CSo, the ratio of total dissipation to the cross section increased and the increase was more prominent (273% in respect to the control). At 8 h light stress, there was no significant change in trapping flux by the cross section (TRo/CSo) with increase in high light exposure. An increase in the energy absorbed per excited cross section (ABS/CSo) upto 32% under severity of high light stress depicts an increase in initial fluorescence absorbed during high light exposure and it should be leading to the phenomenon of photoinhibition; this result was corresponding to some earlier reports wherein the related changes were noticed in *Camellia* plants when treated with high light (120 Wm^{-2} or 420 W m^{-2}) (Krüger et al., 1997).

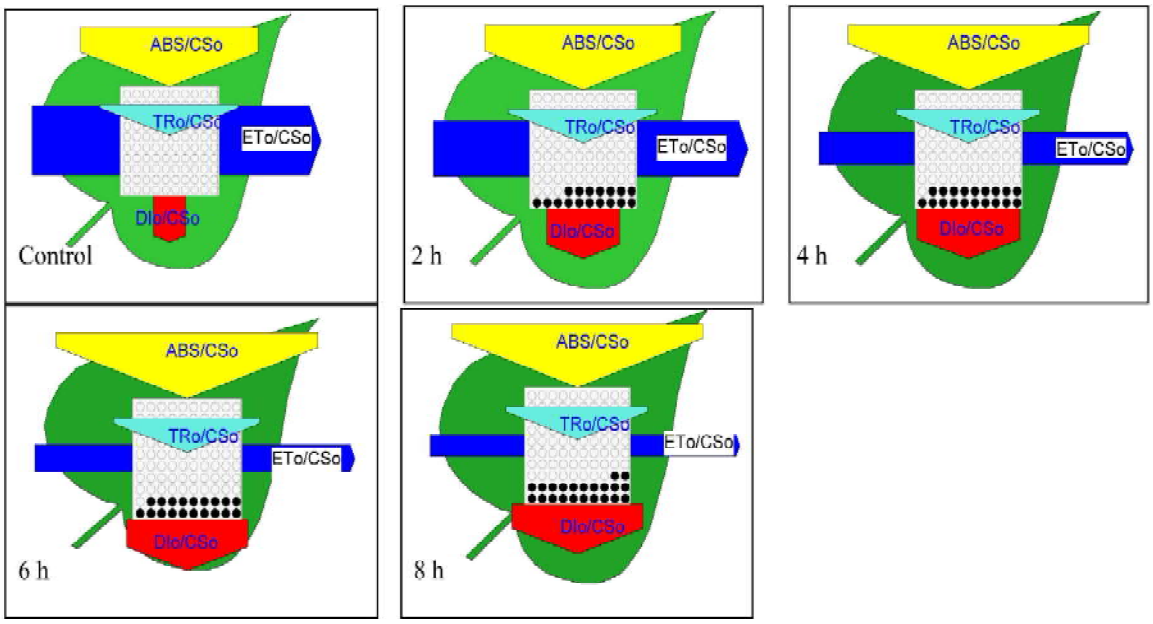

Figure. 2. Energy pipeline leaf model of phenomenological fluxes (per CS) in rice seedlings exposed to high light stress of 2000 µmol $m^{-2}s^{-1}$ (0, 2, 4, 6, 8 h). The value of each parameter can be seen in relative changes in width of each arrow. Active RCs are shown as open circles and inactive RCs are closed circles.

High light stress caused a significant increase in the MDA content of rice seedlings. On imparting 2 h high light stress, MDA content was 79% higher and with increase in duration of high light exposure, it was significantly increased and reached upto 186% in respective to the control. Ali et al. (2005) reported the significant increase in the level of MDA in micropropagated *Phalaenopsis* orchids when treated with high light stress (300 µmol$m^{-2}s^{-1}$). The levels of different non enzymatic antioxidants were also found to be enhanced upon imposition of high light stress in rice seedlings. The carotenoid was showing an increased pattern of accumulation under high light treatment and reached upto 61% with 8 h high light exposure. According to Jahns and Holzwarth (2012) also, carotenoids are able to protect the photosynthetic electron transport chain against damage by light stress. The proline content was only slightly increased with 6 and 8 h light stress (15%) as compared to control. In the case of total ascorbate, an enhanced pattern of increase was noticed and 590% was recorded with severity of high light treatment (Fig. 3). This result was corresponding to some earlier reports wherein the similar

changes were noticed to confer oxidative stress tolerance in maize (Chugh et al., 2011) and wheat (Chakraborty and Pradhan, 2012).

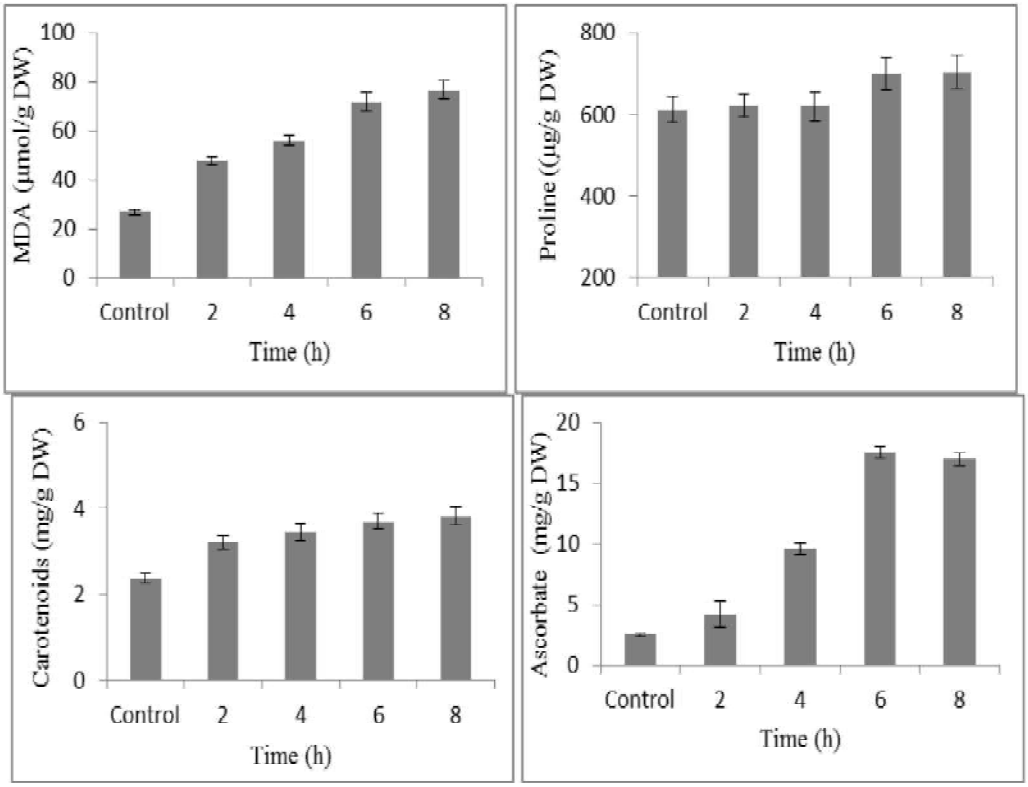

Figure. 3. Effect of high light stress of 2000 µmol $m^{-2}s^{-1}$ (0, 2, 4, 6, 8 h) on MDA, proline, carotenoids and ascorbate content in rice seedlings.

Acknowledgements

This work was financially supported by University Grants Commission (India) (39-367/2010(SR) and KSCSTE, Govt. of Kerala (India) (011/SRSLS/2010/CSTE) and Department of Science and Technology, New Delhi, India through INSPIRE fellowship (IF130020).

References

1. Ali M.B, Hahn E, Paek K, Effects of light intensities on antioxidant enzymes and malondialdehyde content during short-term acclimatization on micropropagated *Phalaenopsis* plantlet, *Environmental and Experimental Botany*, 2005; 54:109-120.
2. Arnon, D.I, Copper enzymes in isolated chloroplasts. Polyphenoloxidase in *Beta vulgaris*, *Plant Physiology*, 1949; 24:1-15.
3. Bates L.S, Waldren R.P, Teare I.K, Rapid determination of free proline for water studies, *Plant and Soil*, 1973; 39:205.
4. Chakraborty U, Pradhan B, Oxidative stress in five wheat varieties (*Triticum aestivum* L.) exposed to water stress and study of their antioxidant enzyme defense system, water stress responsive metabolites and H_2O_2 accumulation, *Brazilian Journal of Plant Physiology*, 2012; 24:117-130.

5. Chugh V, Kaur N, Gupta A.K, Evaluation of oxidative stress tolerance in maize *(Zea mays* L.) seedlings in response to drought, *Indian Journal of Biochemistry and Biophysics*, 2011; 48:47-53.
6. Dogara A.M, Jumare A.I, Origin, Distribution and Heading date in Cultivated Rice. *International Journal of Plant Biology & Research*, 2014; 2:1008.
7. Faseela P, Puthur J.T, Chlorophyll *a* fluorescence changes in response to short and long term high light stress in rice seedlings, *Indian Journal of Plant Physiology*, 2017; 22:30-33.
8. Faseela P, Thomas D.T.T, Sinisha A.K, Puthur J.T, Oxidative stress and its management in plants subjected to different abiotic stresses. In: Ramakrishna A, Gill SS (ed) Metabolic adaptations in plants during abiotic stress. Taylor & Francis, CRC Press, USA, 2018, 111-126.
9. Gill S.S, Tuteja N, Reactive oxygen species and antioxidant machinery in abiotic stress tolerance in crop plants, *Plant Physiology and Biochemistry*, 2010; 48:909-930.
10. Gillespie K.M, Ainsworth E.A, Measurement of reduced, oxidized and total ascorbate content in plants, *Nature Protocols*, 2007; 2:871-874.
11. Heath R.L, Packer L, Phytoperoxidation in isolated chloroplasts. I- Kinetics and stoichiometryof fatty acid peroxidation, *Archives of Biochemistry and Biophysics*, 1968; 125:189-198.
12. Jahns P, Holzwarth A.R, The role of the xanthophyll cycle and of lutein in photoprotection of photosystem II, *Biochimica et Biophysica Acta*, 2012; 1817:182-193.
13. Kalaji H.M, Carpentier R, Allakhverdiev S.I, Bosa K, Fluorescence parameters as early indicators of light stress in barley, *Journal of Photochemistry and Photobiology B: Biology*, 2012; 112:1-6.
14. Krüger G.H.J, Tsimilli-Michael M, Strasser R.J, Light stress provokes plastic and elastic modifications in structure and function of photosystem II in camellia leaves, *Physiologia Plantarum*, 1997; 101:265-277.
15. Roach T, Krieger-Liszkay A, Regulation of photosynthetic electron transport and photoinhibition, *Current Protein and Peptide Science*, 2014; 15:351-362.
16. Strasser R.J, Tsimilli-Michael M, Qiang S, Goltsev V, Simultaneous in vivo recording of prompt and delayed fluorescence and 820-nm reflection changes during drying and after rehydration of the resurrection plant *Haberlea rhodopensis*, *Biochimica et Biophysica Acta*, 2010; 1797:1313-1326.

13.

PHYTOREMEDIATION POTENTIAL EVALUATION OF FOUR SELECTED AQUATIC MACROPHYTES

Shahanas N.S. and Jisha K.C.*
Assistant Professor
Department of Botany
MES Asmabi College, P. Vemballur, Thrissur
jishakc123@gmail.com

Abstract *Heavy metal pollution in the water bodies is a serious threat to the world. Phytoremediation is the better solution of this serious threat, since most of the conventional methods are less effective, time consuming and expensive when compare to phytoremediation technology. In the present research work the phytoremediation potential of four aquatic macrophytes (Azolla pinnata R.Br., Lemna minor L., Pistia stratiotes L., and Salvinia molesta D. Mitch.) were compared by studying their stress related metabolism, photosynthetic pigment content and by estimating heavy metals using atomic absorption spectrophotometry. The various physiological and biochemical parameters as well as anatomical attributes were analyzed in the selected four aquatic macrophytes growing in less polluted and highly polluted aquatic habitats. From the results it was found that, all the selected four aquatic macrophytes growing in less polluted aquatic habitat showed more dry weight percentage and less moisture percentage. The photosynthetic pigments like chlorophyll-a, chlorophyll-b and carotenoids decreased under stressed conditions. The most common stress indicating compounds like proline and MDA was also higher in the samples collected from highly polluted aquatic habitats, except in few cases. Quantification of heavy metal showed high Fe content in all samples than Mg, Mn, Zn and Cu. Fe and Mg was the heavy metals which present in all the four aquatic macrophytes under investigation. While analyzing the anatomical attributes, the major difference was seen in the measurements of air cavities and body hairs which provide them buoyancy. Even though the stress related metabolism showed certain differences among the four aquatic macrophytes, they all showed their potentiality to be used as a phytoremediators.*

Keywords: Heavy metal pollution, phytoremediation, abiotic stress, metabolism, macrophytes

Introduction

The industrial revolution has gifted with a number of environmental problems, such as extensive devastation of forests and grasslands, large-scale desertification of arable and habitable regions severe environmental pollution and unfavourable climatic changes. Of all the current environmental issues heavy metal contamination of aquatic habitats is of major concern, because of their persistent and bio accumulative nature (Chang et al., 2009; Yadav et al., 2009). They are added to the aquatic systems either naturally by slow leaching from soil rocks to water or through anthropogenic sources. In recent times, anthropogenic inputs, such as discharge of untreated effluents (waste water), have contributed to the predominant causation. The chemical methods to effectively decrease heavy metals to acceptable levels require a large excess of chemicals, which increase the costs because of generating the voluminous sludge. The conventional methods applied to clean heavy meal pollution have benefits and limitations but in general none of them is cost effective (Volesky, 2001; Rai, 2009).

Nowadays most of the water bodies are invariably polluted with heavy metals. Most of the pollution is due to human activities. Thus it is our responsibility to make our water bodies free from these pollutants. If we could identify the aquatic plants which can effectively remove these heavy metals from the water, it could be a great achievement in mitigating the adverse effects of heavy metal pollution in water bodies. Several research works were conducted to analyze the phytoremediation potential of different aquatic plants, but a comparative study of the different aquatic macrophytes in terms of heavy metal stress is lacking. By taking account these factors, our work is intended to identify the most suitable aquatic plant which can effectively carry out phytoremediation.

In the present research work, the phytoremediation potentials of four selected aquatic macrophytes were compared. The plants selected for the study include *Azolla pinnata* R.Br., *Lemna minor* L., *Pistia stratiotes* L., *and Salvinia molesta* D. Mitch. These macrophytes were shown high biomass production. These were commonly used as fodder and organic fertilizer. The phytoremediation potentials of these plants were assessed through heavy metal quantification (Cu, Zn, Mn, Fe, Mg) and by analyzing anatomical and major biochemical parameters like proline content, Malone dialdehyde (MDA) content, photosynthetic pigment content etc.

Materials and Methods

The research was carried out with four aquatic macrophytes. They were *Azolla pinnata* R.Br (Salviniaceae), *Lemna minor* L. (Lemnaceae), *Pistia stratiotes* L. (Araceae), and *Salvinia molesta* D. Mitch (Salviniaceae). All the plants were collected from two aquatic habitats ie, from a highly polluted and less polluted aquatic habitats. The area which taken as the polluted habitat was a canal at P. Vemballur, and a paddy field at Chalakudy was considered as the less polluted aquatic habitat. In both habitats luxurious growth of aquatic macrophytes were seen. For further reference, the plants growing in the highly polluted aquatic habitat are referred as "plants (HP)", plants growing in less polluted aquatic habitats are referred as "plants (LP)".

Physiological studies

For dry weight percentage and moisture content percentage measurements, the samples were weighed using electronic balance. For fresh weight and dry weight measurements, the samples were blotted and wrapped separately in paper boats. Fresh weight of the samples was determined by weighing them immediately after wrapping. For dry weight measurements, the samples were kept in hot air oven at 100°C. After 48 hours the samples were allowed to cooled and then weighed. Then dry weight percentage was calculated by using the following formula:

$$Dry\ weight\ prcentage = \frac{Dry\ weight}{Fresh\ weight} * 100$$

Moisture content percentage was calculated by using the following formula

$$\text{Moisture content percentage} = \frac{\text{Fresh weight - Dry weight}}{\text{Fresh weight}} \text{ x } 100$$

Anatomical studies

The anatomical characters were studied to find out the differences in the anatomical characters between the plants growing in less and highly polluted aquatic habitats by taking hand sections of the fronds of the four macrophytes. Fresh specimens directly from their natural habitats were used for the study. Thin sections were made and were temporarily mounted on a clean slide using glycerine and a cover-glass. Digital photographs of the plant sections were taken by using digital camera attached to microscope.

Biochemical parameters

Estimation of chlorophyll and carotenoids were done according to the method of Arnon (1949). Proline content was estimated according to the method of Bates *et al* (1973) and the MDA content estimation was done according to Health and Packer (1968).

Quantitative estimation of heavy metals

For quantitative estimation of heavy metals, all the selected plant samples were dried at 60^{0}C in a hot air oven. Known weight of the dried sample were digested by refluxing in 10:4 ratio of Nitric acid and perchloric acid until the solution become colourless using Kjeldahl's flask heated in a sand bath. Then the digest was transferred to a standard flask and volume was made up to 50 ml and kept in screw capped containers. Same method was adopted for the water samples also. Atomic absorption spectrophotometer (ICPOES Optima 8000) available at Agriculture university, Kasargode was used for the estimation of heavy metals present in the digested samples.

Statistical analysis

Data from observations were recorded and analyzed in the Microsoft office excel sheet. Standard deviation and standard error were determined in the MS Excel programme.

Results

Dry weight percentage and moisture content percentage

In the present study, dry weight percentage and moisture content percentage were varied in high polluted and less polluted samples. Dry weight percentage was found to decreases with increase in the rate of pollution. Moisture percentage was increased with increase in the pollution level. Result showed in table 1.

Table 1: Dry weight percentage and moisture percentage of four aquatic macrophytes collected from high polluted and less polluted aquatic habitats.

PLANTS	DW % (HP)	DW % (LP)	MC % (HP)	MC % (LP)
Azolla pinnata	11.02	3.5	88.97	96.5
Lemna minor	51.23	47.62	48.77	52.38
Pistia stratiotes	9.213	5.54	90.79	94.46
Salvinia molesta	11.07	6.06	88.92	93.93

Anatomical studies

The anatomical studies of samples collected from less and highly polluted aquatic habitats showed some clear cut differences, including the length and width of air cavities, the number of chloroplasts presents, width and size of rhizoids etc.

In *Azolla pinnata,* difference in the air cavity measurements was noticed between the samples collected from less and highly polluted aquatic habitats. The sample collected from the less polluted habitat had a cavity measurement (Length-364.09 µm, Width-199.05 µm) (Fig. 1A) higher than that collected from highly polluted habitats (Length-241.03 µm, Width-103.91 µm) (Fig. 1B). The samples collected from the highly polluted habitats has a hair larger (Length-419.21 µm) (Fig. 1B) than that collected from less polluted habitats (Length-241.03 µm, Width-103.91 µm) (Fig. 1A). The samples collected from the highly polluted habitat have been found to have a symbiotic association with *Anabaena* (Fig. 1C & 1D). *Lemna minor* shows large sized air cavities in the samples that collected from highly polluted aquatic habitats (Length-164.50 µm, Width-199.10) (Fig. 2A) than those collected from less polluted aquatic habitats (Length-101.38 µm, Width-41.41 µm) (Fig. 2B). No characteristic hairs are seen on both sections. *Pistia stratiotes* have larger cavities in the samples from highly polluted aquatic habitats (Length-527.99 µm, Width-297.36 µm) (Fig. 3A) than those collected from less polluted aquatic habitats (Length- 96.01 µm, Width-67.03 µm) (Fig. 3B). The hair length of *Pistia stratiotes* varies among the less polluted and highly polluted aquatic habitats. The samples from highly polluted aquatic habitat have larger hairs (Length-358.32 µm, Width-60.65 µm) (Fig. 3C) than those collected from less polluted aquatic habitat (Length-138.26 µm, Width-17.42 µm) (Fig. 3D).

Large sized cavities are present in *Salvinia molesta* collected from highly polluted aquatic habitats (Length-397.96 µm, Width-122.21 µm) (Fig. 4A) than those collected from less polluted aquatic habitats (Length-24.74 µm, Width-14.75 µm) (Fig. 4B). The amount of chloroplast is also decreases as the degree of pollution increases (Fig. 4C) & (Fig. 4D).

Photosynthetic pigment content

Samples collected from highly polluted aquatic habitat (HP) showed a decreased amount of total chlorophyll content those collected from comparatively less polluted aquatic habitats (LP). The amount of total chlorophyll varies as *Salvinia molesta* > *Azolla pinnata* > *Pistia stratiotes* > *Lemna minor* (Fig. 5A). The aquatic macrophytes collected from highly polluted aquatic habitats (HP) have a decreased amount of carotenoid content than those collected from less polluted aquatic habitats (LP). The amount of carotenoid varies as *Salvinia molesta* > *Lemna minor* > *Pistia stratiotes* > *Azolla pinnata* (Fig. 5B).

Proline and MDA content

Under polluted condition the amount of proline is significantly increased. The amount of proline is higher in the samples collected from highly polluted habitats than those collected from less polluted habitats, except in *Azolla pinnata.* The proline amount varies as *Pistia stratiotes* > *Salvinia molesta* > *Azolla pinnata* > *Lemna minor* (Fig. 6A). The plants under the two habitats showed variation in the MDA content. The samples from less polluted habitat showed comparatively lower amount of MDA compared to samples from highly polluted habitat, except in *Pistia stratiotes.* The MDA amount varies as *Salvinia molesta* > *Pistia stratiotes* > *Azolla pinnata* > *Lemna minor* (Fig. 6B).

Heavy metal quantification

Quantification of heavy metal revealed that among the four metals quantified, amount of Fe was higher in all the samples when compared to other metals. It was found to be highest in the *Lemna minor* sample collected from highly polluted aquatic habitats. Among the tested metals, Mg is the metal which showed presence in all samples other than Fe. Its amount was found to be higher in the *Pistia stratiotes* sample collected from highly polluted aquatic habitats. Mn was found to absent in *Pistia stratiotes* collected from less polluted aquatic habitats, whereas, Zn was absent in *Salvinia molesta* and *Pistia stratiotes* collected from less polluted aquatic habitats. Cu is the metal which was absent in three samples namely *Salvinia molesta* and *Pistia stratiotes* collected from less polluted and *Lemna minor* collected from highly polluted aquatic habitats. Among the selected and tested macrophytic samples *Azolla pinnata* is the only one aquatic macrophyte which showed the presence of all the five heavy metals tested. Fe is the heavy metal which present abundantly in it (Table 2).

Table 2: Heavy metal quantification in four aquatic macrophytes under less polluted and highly polluted habitats.

PLANT	LP/HP	Cu (µg/g fw)	Zn (µg/g fw)	Mn (µg/g fw)	Fe (µg/g fw)	Mg (µg/g fw)
Azolla pinnata	LP	0.08	0.33	1.61	4.71	4.59
	HP	0.24	0.4	6.78	21.5	5.07
Lemna minor	LP	4.43	0.17	5.82	9.14	4.89
	HP	_	0.37	14.8	36.6	4.61
Pistia stratiotes	LP	_	_	_	20.8	4.64
	HP	0.03	1.53	3.93	6.17	6.38
Salvinia molesta	LP	_	_	2.04	16.2	5.03
	HP	0.29	0.18	8.78	27.1	4.69

Discussion

Phytoremediation include green and environment-friendly methods which employ plants to remove pollutants from the surrounding environment. It has attracted increasing attention in ecological studies because of its safety, high efficiency, low cost, and recyclability of plant harvests. But this method is often limited by its time consuming features because the life cycle of most plants used for phytoremediation is excessively long (Agunbiade *et al*., 2009). However, this disadvantage is not significant to aquatic macrophytes because of their enormous biomass production.

In the present study various physiological and biochemical parameters as well as anatomical attributes were analyzed in the selected four aquatic macrophytes namely, *Azolla pinnata* R.Br, *Lemna minor* L., *Pistia stratiotes* L., *and Salvinia molesta* D.Mitch growing in less polluted and highly polluted aquatic habitats. In the case of dry weight and fresh weight, there is

a considerable difference seen between the macrophytes selected from the less polluted and highly polluted aquatic habitats. Under polluted conditions, it was already reported that growth attributes like fresh weight and dry weight decreases in aquatic macrophytes when compared with the plants which are growing under unpolluted or less polluted aquatic habitats. It may be due to increased utilization of metabolites for competing with stress rather than for growth and reproduction of plants. Treatment of *Azolla pinnata* with As, Pb, Cu, Cd and Cr (2 and 5 mg l^{-1} each), decreased dry weight percentage in with respect to control (Sarkar and Jana, 1986). The chlorophyll content under stressed condition is highly reduced when compared with that of macrophytes under unstressed conditions, because the chlorophyll is most sensitive to environmental stress. Chlorophylls are important to maintain photosynthesis activity in plants (Nageswara et al., 2001). Thus changes in environmental conditions certainly caused decline in the quantity of chlorophylls.

The macrophytes collected from the highly polluted aquatic habitats showed high accumulation of proline when compared to the samples collected from less polluted aquatic habitas, with the exception of *Azolla pinnata*. *Azolla pinnata* showed a higher amount of proline in the samples collected from less polluted aquatic habitats than in the samples collected from highly polluted aquatic habitats. Proline, an imino acid, is well known to get accumulated in wide variety of organisms ranging from bacteria to higher plants on exposure to abiotic stress (Saradhi *et al*., 1993; Ahmad *et al*., 2006). Quantification of MDA content in the samples revealed slight increase in highly polluted aquatic habitats than in the less polluted aquatic habitats, except in *Pistia stratiotes.* In *Pistia stratiotes* the amount of MDA is higher in the less polluted aquatic habitats in comparison with the highly polluted aquatic habitats. MDA is the decomposition product of fatty acids of membranes and its increase shows plants are under high-level oxidative stredd. MDA is already known as a stress indicator. So in the present study also, increase in MDA denotes the increased stress for plants. Under stress condition plant cell undergoes membrane damage and leakage due to the action of free radicals. According to Anjum et al. (2012), water stress increases the MDA content in *Zea mays*.

Fe and Mg accumulation was found to present in all samples. From the data it was clear that accumulation of heavy metals was higher in those samples which were collected from highly polluted aquatic habitats than those collected from less polluted aquatic habitats. The accumulation of Cu, Zn and Fe was higher in *Lemna minor*, and that of Mn was higher in *Salvinia molesta*, and more Mg content was present in *Pistia stratiotes*. *Azolla pinnata* was the only one aquatic macrophyte which showed the presence all the studied heavy metals inboth less and highly polluted aquatic habitats. The order of heavy metal accumulation was Fe > Mn > Mg > Zn > Cu in *Azolla pinnata*, and Fe > Mn > Mg > Cu > Zn *in Lemna minor*, and Fe > Mg > Mn > Zn > Cu in *Pistia stratiotes*, and Fe > Mn > Mg > Cu > Zn in *Salvinia molesta.* There were several noticeable differences in the anatomical features also. The samples collected from highly polluted aquatic habitats have larger air chambers and trichomes than when compared to the samples collected from less polluted aquatic habitats. The number of layers in the palisade parenchyma is higher in the samples collected from highly polluted habitats than that collected from less polluted habitats.

Reference

1. Agunbiade F.O, Owolabi B.I.O, Adebowale K.O, Phytoremediation potential of *Eichornia crassipes* in metal-contaminated coastal water, *Bioresource Technology*, 2009; 100(19):4521-4526.
2. Ahmad P, Sharma S, Srivastava P.S, Differential physio-biochemical responses of high yielding varieties of Mulberry (*Morus alba*) under alkalinity (Na_2CO_3) stress in vitro, *Physiology and Molecular Bioolgy of Plants*, 2006; 12:59-66.
3. Anjum S.A, Xie X, Wan L, Morphological, physiological and biochemical responses of plant to draught stress, *African Journal of Agricultural Research,* 2012; 6:2026-2032.
4. Arnon D.I, Copper enzymes in isolated chloroplast polyphenoloxidase in *Beta vulgaris, Plant Physiolology*, 1949; 24:1-5.
5. Bates L.S, Waldren R.P, Teare I.D, Rapid determination of free proline for water stress studies, *Plant and Soil*, 1973; 205-208.
6. Chang J.S, Yoon J.H, Kim K.W, Heavy metal and arsenic accumulating fern species as potential ecological indicators in As-contaminated abandoned mines, *Ecological Indicators*. 2009; 9: 1275-1279.
7. Heath R, Packer L, Photoperoxidation in isolated chloroplasts. I Kinetics and stochiometry of fatty acids peroxidation, *Pakistan Journal of Botany,* 1968; 125: 189-198.
8. Nageswara R.R.C, Talwar H.S, Wright G.C, Rapid assessment of specific leaf area and leaf nitrogen in peanut using chlorophyll meter, *Journal of Agronomy and Crop Science,* 2001; 189: 175-182.
9. Rai P.K, Heavy metal phytoremediation from aquatic ecosystems with special reference macrophytes, *Critical Reviews in Environmental Science and Technology,* 2009; 39: 697-753.
10. Saradhi P, Alia, Vani B, Inhibition of mitochondrial electron transport is the prime cause behind proline accumulation during mineral deficiency in *Oryza sativa*, 1993; 155/156: 465-468.
11. Sarkar A, Jana S, Heavy metal pollutant tolerance of *Azolla pinnata*, *Water, Air, and Soil pollution*, 1986; 27: 15-18.
12. Volesky B, Detoxification of metal-bearing effluents: Biosorption for the next century. *Hydrometallurgy,* 2001; 59: 203-216.
13. Yadav S.K, Juwarkar A.A, Kumar G.P, Thawale P.R, Singh S.K, Chakrabarti T, Bioaccumulation and phyto-translocation of arsenic; chromium and zinc by *Jatropha curcas* L.: Impact dairy sludge and biofertilizer, *Bioresource Technology*, 2009; 100: 4616-4622.

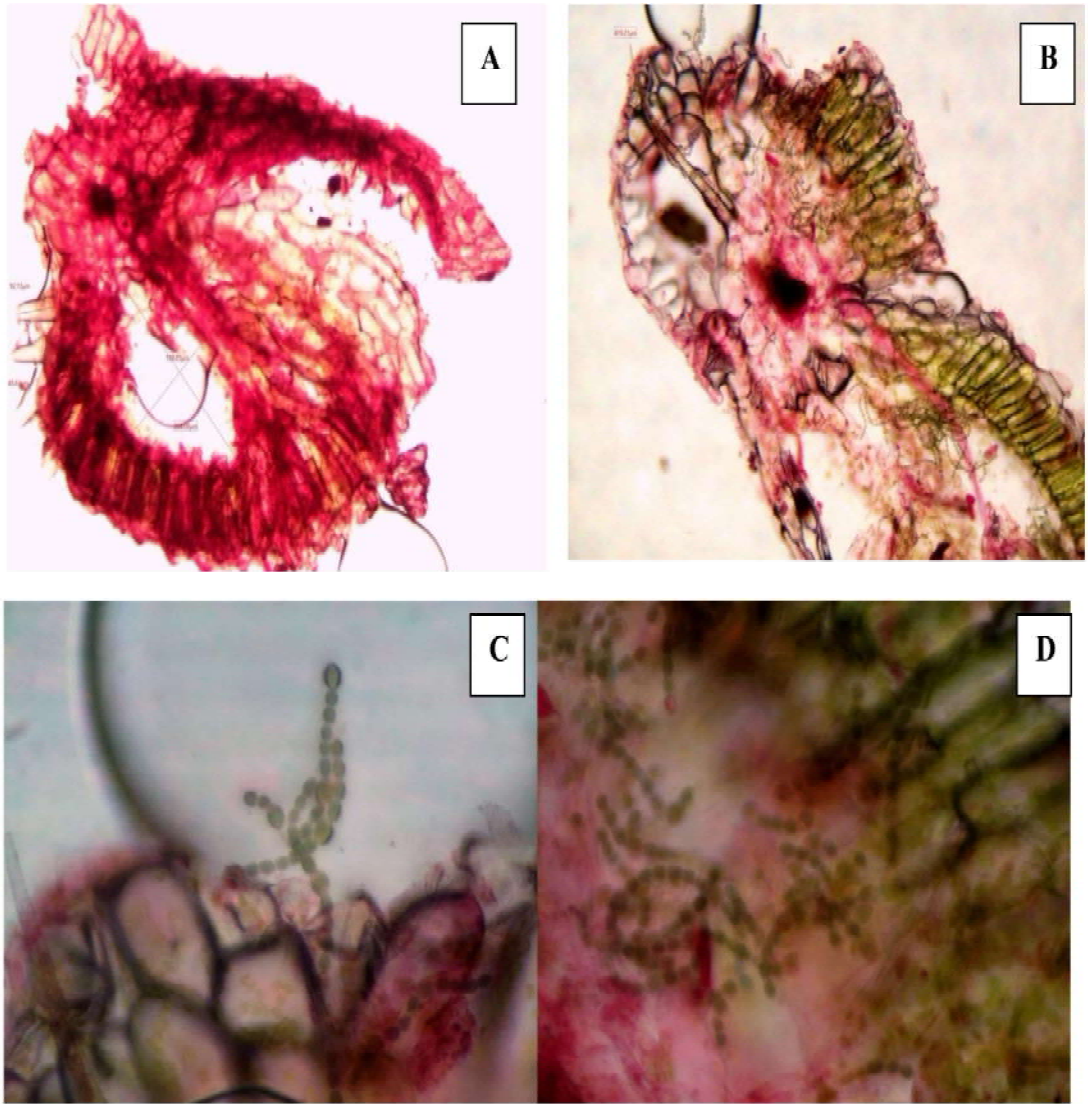

Figure 1: T.S. of *Azolla pinnata* frond. **1A**: Plant LP (Air cavity and hair measurements); **1B**: Plant HP (Air cavity and hair measurements); **1C and 1D**: Symbiotic association with *Anabaena*.

Figure 2: T.S. of *Lemna minor* frond. **2A**: Plant LP (Air cavity and hair measurements); **2B**: Plant HP (Air cavity and hair measurements).

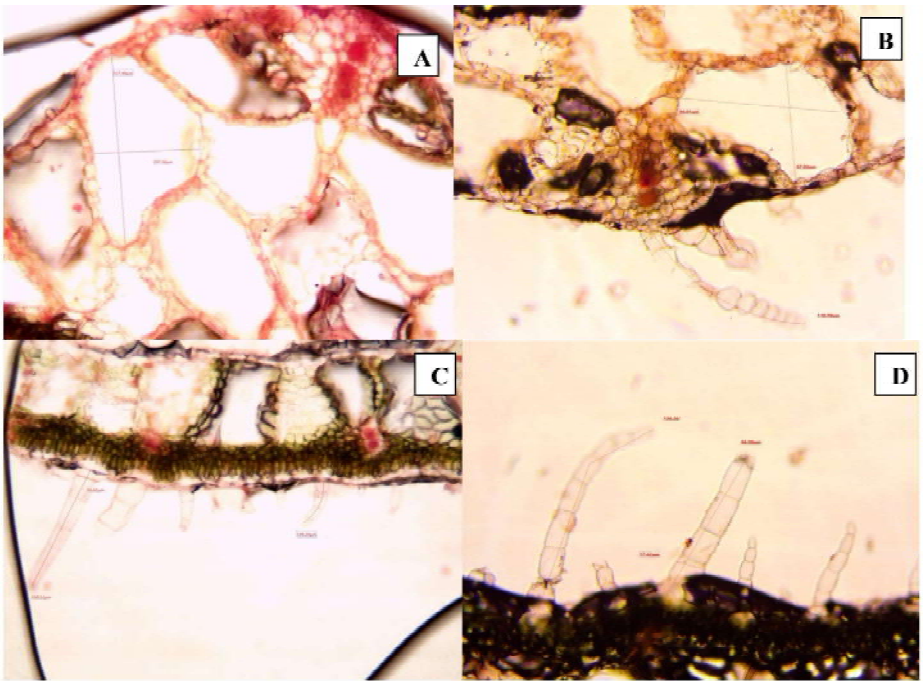

Figure 3: T.S. of *Pistia stratiotes* frond. **3A**: Plant HP (Air cavity); **3B** Plant LP (Air cavity); **3C**: Plant HP (hair measurements); **3D**: Plant LP (hair measurements).

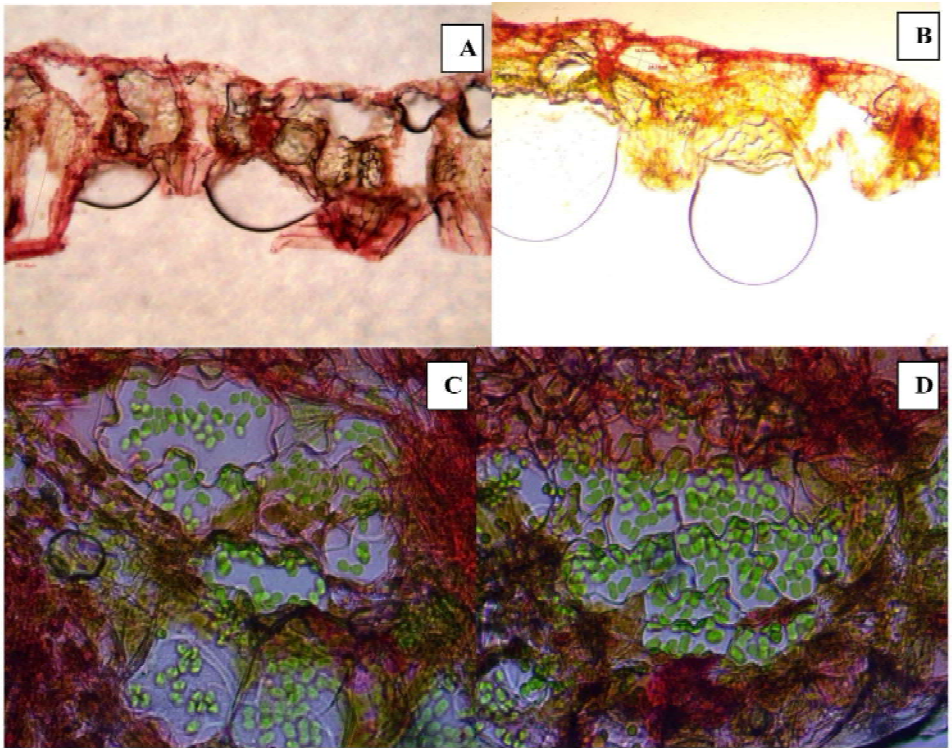

Figure 4: T.S. of *Salvinia molesta* frond. **3A**: Plant HP (Air cavity); **3B** Plant LP (Air cavity); **3C**: Plant HP (chloroplast); **3D**: Plant LP (chloroplast).

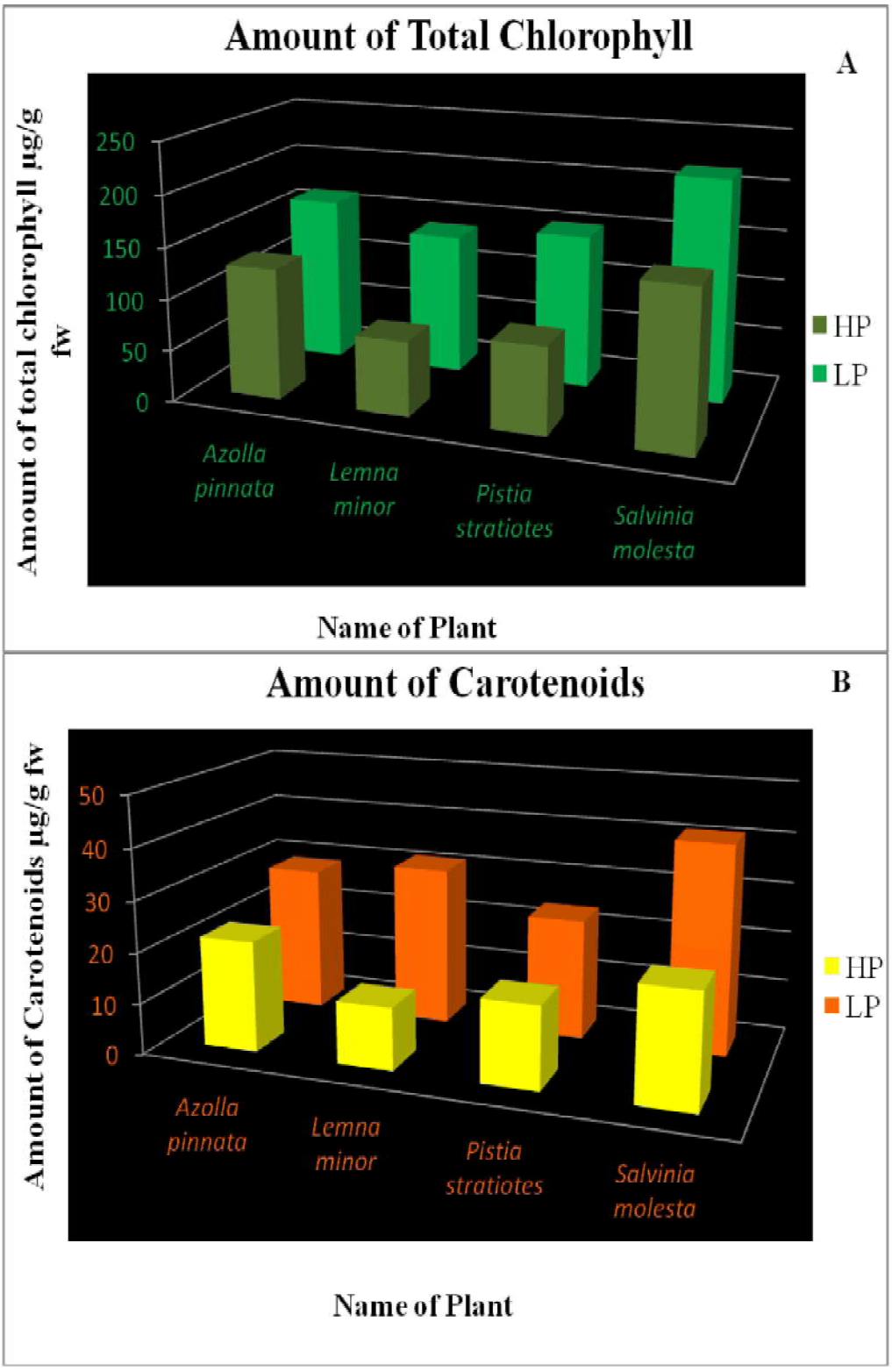

Fig. 5: Total chlorophyll content (Fig. 5A) and carotenoid content (Fig. 5B) of four selected aquatic macrophytes under high polluted and low polluted habitats.

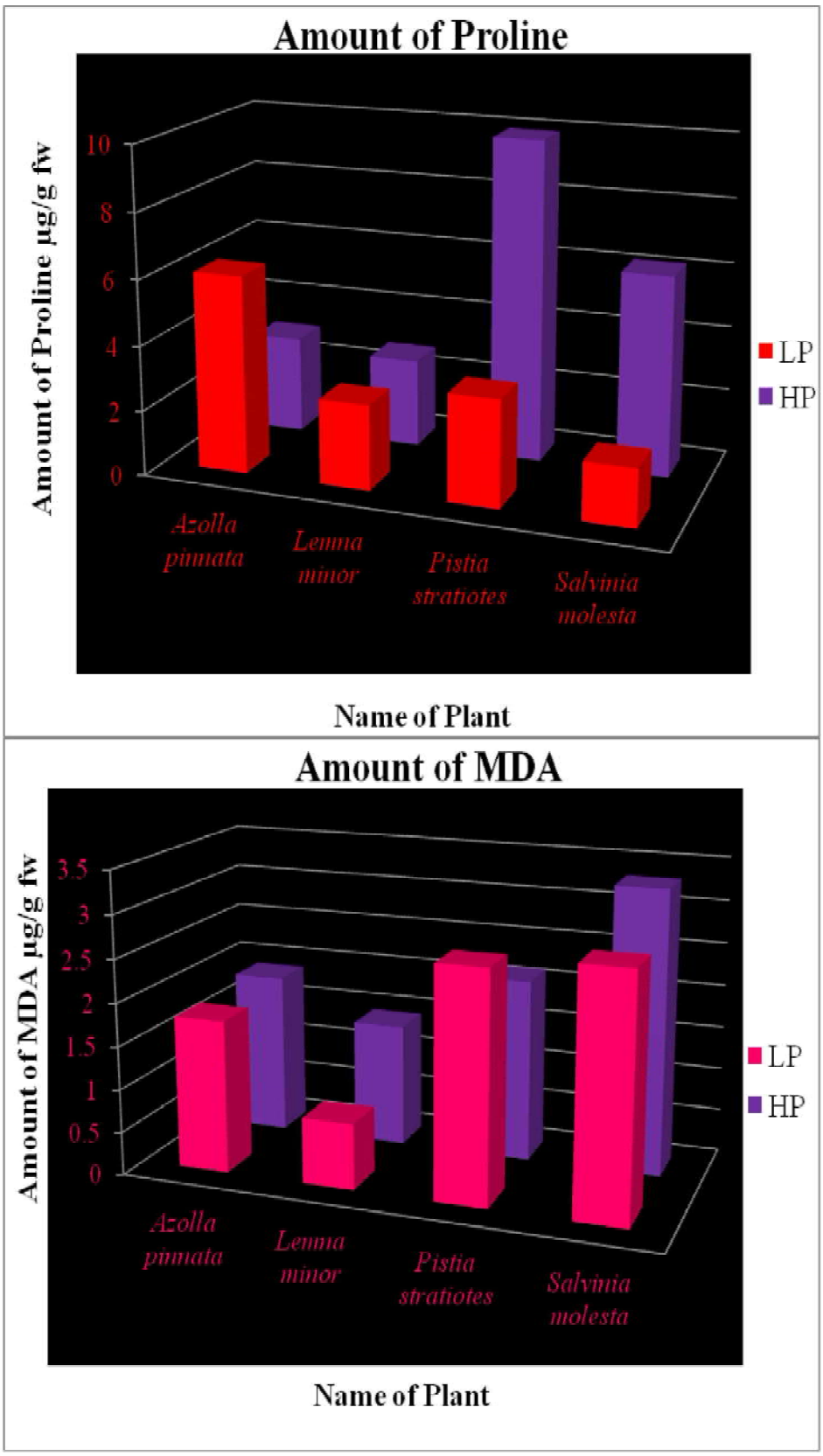

Fig. 6: Proline (**A**) and MDA (**B**) content of four selected aquatic macrophytes under high polluted and low polluted habitats.

14.

PHYTOCHEMICAL STUDIES AND BIOACTIVITY POTENTIAL OF *CAESALPINIA SAPPAN* HOT WATER EXTRACTS.

Manju Madhavan[1] and Sheeja T Tharakan[2]
[1,2]Department of Botany, Vimala College, Thrissur

Herbal medicines for therapeutic purposes have been explicitly used since the dawn of human civilization. WHO estimates that about three-quarters of the World's population currently uses herbs and other forms of traditional medicines for mitigation and cure of various ailments. Phytopharmaceuticals are pharmaceuticals using traditional compounds derived from botanicals instead of chemicals. One important class of phytochemicals widely spread throughout the plant kingdom include phenolic compounds. Phenolic compounds are essential for the growth and reproduction and are produced as a response for defending pathogens of injured plant parts (Rao *et al*, 2011).

Antioxidant activity is closely related to the phenolic content of plants (Braca *et al.,* 2002). Normally free radical formation is controlled naturally by various beneficial compounds known as antioxidants. When there is deficiency of these antioxidants damage due to free radicals can become cumulative and debilitating. Antioxidants are capable of stabilizing, or deactivating, free radicals before they attack cells.Vitamin C, vitamin E, and beta carotene are among the most commonly studied dietary antioxidants. Crude extracts of fruits, herbs, vegetables, cereals, and other plant materials rich in phenolics are increasingly of interest in the food industry because they retard oxidative degradation of lipids and thereby improve the quality and nutritional value of food. 'Anthelmintic herbs'is the class of herbs that are able to destroy parasitic worms with in human body. The transmission of these parasitic worms is usually by contaminated water or food. Anthelmintic herbs work by stopping the parasitic worms from reproducing or preventing their growth. Anthelmintic effects of plants are generally described to secondary metabolites such as alkaloids, terpenoids, or polyphenols such as proanthocyanidins, also known as condensed tannins (CT).The use of natural plant extracts as dewormers for humans and livestock has long been practiced.

Caesalpinia sappan L.(*Pathimukham*) (Family -Caesalpinaceae) is used in traditional Indian medicine as hemostatic and anti-inflammatory agent, as well as for the treatment of contusion and thrombosis. The heartwood of *C. sappan* has also been reported for its varied biological activities such as antioxidative, anti-inflamatory, immuno stimulant , anticomplementary , cytotoxic , hypoglycemic, antimicrobial ,antifungal, analgesic and hepatoprotective properties, which are attributed to the presence of phenolic compounds etc. The *Caesalpinia sappan* heartwoods have been used as a red dye for a long time. Several members of the species of *Caesalpinia* are being used traditionally for a wide variety of ethnomedical properties. Several flavonoids, phenols, triterpenoids and steroids have been isolated from the heartwood .In the present study an attempt is made to study the phytochemical constituents and anthelminthic activity of hot water extract of *Caesalpinia sappan* L(Heartwood).

The dried ground plant powder (2gm) was soaked in hot water (100ml) for 1 week separately. The soaked material was stirred and heated to boiling point and final extracts were filtered and concentrated by keeping in the hot water bath. The extraction yield is expressed as the percentage of total mass of extracts (*Mext*) with respect to the mass of material used (*Mo*). $Y\% = (Mext / Mo) \times 100$. The plant extract was diluted with distilled water for phytochemical analysis of primary and secondary metabolites (Kokate,2009). The concentration of phenolics in plant extracts was determined using spectrophotometric method (Bray and Thorpe, 1954). Based on the measured absorbance, the concentration of phenolics was read (µg/µl) from the calibration line; then the content of phenolics in extracts was expressed in terms of catechol equivalent (µg of CE/µg of extract). The ability of the plant extracts to scavenge 2,2-diphenyl-1-picrylhydrazyl (DPPH)-free radical activity by modified method (Braca *et al.,* 2002). The stock solution of extracts were prepared in water to achieve the concentration of 1 mg/ml. Dilutions were made to obtain concentrations of 5, 2.5, 1µg/ml. Diluted solutions (1 ml each) were mixed with 1 ml of methanolic solution of .002% DPPH . After 30 min incubation in darkness at room temperature (23^{o}C), the absorbance was recorded at 517 nm using Labtronics NT 290 Spectrophotometer. Control sample contained all the reagents except the extract. Percentage inhibition was calculated using equation (Bors *et al*., 1992). The optical density was recorded and percentage inhibition was calculated using the formula (A-B/A)*100 Where, A = optical density of the Control and B = optical density of the sample.

The anthelmintic assay was carried out as per the method of (*Ajaiyeoba et al.,2001*). Earthworms *(Pheretima posthuma)* of 3-5 cm in length and 0.1-0.2 cm in width (same type) were collected from Kerala Agricultural University, Mannuthy. Test samples of the extract was prepared at the concentrations, 25,50,75 mg/ml in distilled water and three worms ie, *Pheretima posthuma*, of approximately equal size were used for all the experimental protocol were placed in each nine cm Petri dish containing 25 ml of above test solution of extracts. Albendazole (25 mg/ml and 50mg/ml) was used as reference standard as advocated earlier. Observations were made for the time taken for paralysis was noted when no movement of any sort could be observed except when the worms were shaken vigorously. Time for death of worms were recorded after ascertaining that worms neither moved when shaken vigorously.

.

The plants are being used widely for a large number of traditional medicinal purposes. Although a diverse number of modern allopathic medicines are used for curing acute and severe illness, herbal medicines have maintained their importance (Shrishailappa *et al*,2012). Plant secondary metabolism produces a large number of specialized compounds (estimated 200.000) that do not aid in the growth and development of plants but are required for the plant to survive in its environment. In our study the plant active components or phytochemicals were extracted from herbs using water as solvent. The successful determination of biologically active compounds from plant material is largely dependent on the type of solvent used in the extraction procedure (*Prashant et al .2011*).The drying of extract was done to find the percentage yield of extracts in water in three herbs. The extraction yield of *Caesalpinia sappan* were 11.1 % (w/w) .

Plants have always been a rich source of phytochemicals such as phenolics, terpenoids, alkaloids and also possess several biological activities (Aanata *et al* , 2016). Phytochemical studies by Harjit *et al* , 2016 on *Caesalpinia sappan* leaf extract revealed the presence of carbohydrates, flavonoids, glycosides, phenols, tannins, amino acids and proteins but absence of phytosterols, alkaloids and saponins in the crude drug. Shobowale *et al*, 2013 studies the biological activities reported to have been associated with plants and plant derived compounds can be categorized according to the disease area which include anticancer activity, Nervous system activation/suppression, cardiovascular metabolic, antimicrobial activity immuno- modulating activity, anti-inflammatory activity etc. In the hot water extract of *Caesalpinia sappan* contains carbohydrate, protein, steroids, alkaloids saponins, phenol &tannins. Total phenols of hot water extracts of heart wood of *Caesalpinia sappan* is 342.4 µg catechol equivalent. Antioxidant activity of extracts were determined using DPPH assay. Table-1 shows the results of the free radical (DPPH) scavenging activity in % inhibition.

Table 1. Antioxidant activity of the Plant Extract

Plant Extract	**Concentration µg**	**O D Initial**	**OD Extract colour**	**Optical Density (Initial-Extract Colour)**	**Percentage of Inhibition**	**IC 50 µg/µl**
Caesalpinia sappan	Control	0.340				14
	5	0.081	0.029	0.052	84	
	2.5	0.162	0.081	0.081	76	
	1	0.210	0.005	0.199	39	

Development of resistance in helminthes against conventional anthelmintics is the foremost problem in treatment of helminthes diseases. Some serious side effects of drug like albendazole is that it causes giddiness, decreased urination, fever, chills, or sore throat tiredness etc. Henceforth it is important to look for alternative strategies against gastrointestinal nematodes, which have led to the proposal of screening medicinal plants for their anthelmintic activity (Sangh *et al*, 2012*)*.Aqueous extract of varying concentrations of *Caesalpinia sappan* (25,50, 75 mg/ml)were tested for anthelmintic activity (Fig 1) and compared with standard albendazole. The water extract showed promising anthelmintic activity.

Figure 1. Anthelmintic activity of hot water extract of *Caesalpinia sappan*

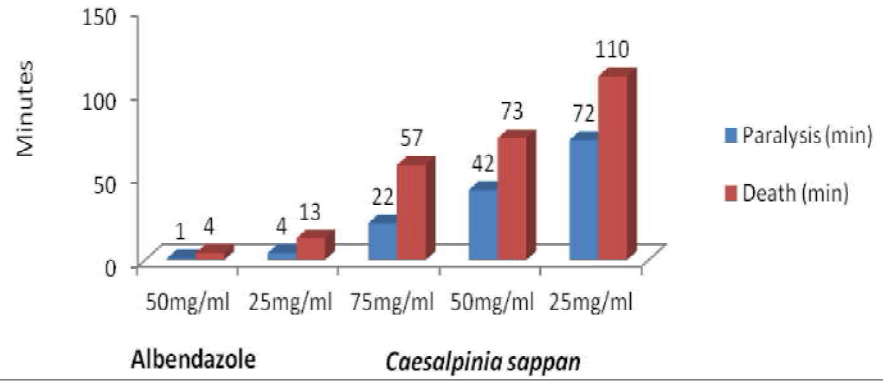

Hence it can be concluded that the hot water extracts of *Caesalpinia sappan* heart wood is a promising medicinal plant. It shows the presence of phytochemicals ,phenol content , anthelmintic and antioxidant property.There is also a need for further studies in order to isolate the active ingredients that are responsible for its potential anthelmintic activity and to elucidate the mechanism of action of these active ingredients to open the new door for natural anthelmintics.

References

1. Ayaiycoba E O ,Onocha P A, Olarenwaju O T.2001.Invitro anthelmintic properties of *Buchholzia coriaceae* and *Gynandropis gyandra* extract , Pharma bio 39:217-220.
2. AnantaSwargiary, Abhijita Daimari, ManitaDaimari, Noymi Basumatary, Ezekiel Narzary. 2016. Phytochemicals, antioxidant, and anthelmintic activity of selected traditional wild edible plants of lower Assam. Indian Journal of Pharmacology. 48(4): 418–423.
3. Braca A, Sortino C, Politi M .2002. Anti-oxidant activity of flavonoids from *Licania licaniaeflora*. J Ethnopharmacol 79: 379-381.
4. Bray H C and Thorpe W. 1954. Analysis of phenolic compounds of interest in metabolism; Meth.Biochem. Anal. **1** 27–52.
5. W. Bors M. SaranE. F. Elstner 1992 .Screening for Plant Antioxidants .Plant Toxin Analysis pp.277-295.

6. Harjit K, Amini M H, Suttee .2016. Evaluation of antioxidant and anthelmintic properties of *Caesalpinia sappan* L. Leaves .International Journal of Pharmacognosy and Phytochemical Research .8(2):362-368 .
7. Kokate C K 2009.Practical Pharmacognosy.New Gian Offset Printers, Delhi.
8. PrashantTiwari, Bimlesh Kumar, Manoj Kumar1, MandeepKaur, JibanDebnathPardeep Sharma.2011.Comparative study of anthelmintic activity of aqueous and ethanolic stem extract of *Tinospora cordifolia*, InternationalPharmaceutical Science, 3(1): 70-83.
9. SanghPartap, Saurabh Kumar, Amit Kumar, NeerajK,Sharma, Jha K K.2012. In-vitro anthelmintic activity of *Luffa cylindrica* leaves in Indian adult earthworm, Journal of Pharmacognosy and Phytochemistry, 2278- 4136.
10. Shrishailappa Badami, Sudheer Mookoth, Suresh B .2004. *Caesalpinia sappan* A medicinal and dye yielding plant Natural Product Radiance Vol 3(2) 75-82.
11. Shobowale, Ogbulie, Itoandon, Oresegun, Olatope . 2013 Phytochemical and antimicrobial evaluation of aqueous and organic extracts of *Calotropis proceraait* leaf and latex, Nigerian Food Journal.31(1):77–82.
12. Rao, L., K. Hayat, Y. Lv, E. Karangwa, S. Xia, C. Jia, F. Zhong and X.2011. Zhang, Effect of ultrafiltration and fining adsorbents on the clarification of green tea. J. Food Eng: 102(4), 321-326.

15.

BIOINFORMATICS AND PLANT SCIENCE

Nazmin Banu
University of Calicut

Abstract *Bioinfomatics is an interdisciplinary field that uses computation to extract knowledge from biological data. It mainly combines molecular biology, computer science, statistics and mathematics to manage, analyze and interpret biological data. One of the important applications of bioinformatics include drug designing which is used in discovering new drugs. In plant science bioinformatics tools are used in crop improvement to improve yield and quality of concerned crops, in phytochemistry for the improvement of traditional medicines and in pathology for diagnostics and disease management. In this article various applications of bioinformatics in the field of plants science are discussed.*

Introduction

Bioinformatics can be defined as application of computational techniques to understand and organize information associated with biological macromolecules. It's meant for analyzing, comparing, systemising, graphically displaying, modelling, storing and distributing biological information. Biological data can be DNA, RNA or protein sequences, macro molecular structures or three dimensional structures of protein and related infomations collected from various scientific literatures and research projects.

Frederick Sanger was the first to determine aminoacid sequence of insulin in 1950. After that sequences of thousands of organism's became available and their storage became essential which allow researchers to submit and retrieve datas related with their researches. Now, bioinformatics develops computational tools, data bases and Algorithms to support genomic, proteomic and metabolomic researches. There are many tools that can be implemented in plant research projects. Designing a proper algorithm make it meaningful. Identification of genes responsible for specific trait using bioinformatics tools make manipulation of such genes easier with biotechnology. Genomic comparison gives insight into various aspects that can be implemented in crop improvement. phytochemistry deals with the study of phytochemicals derived from plants and are produced by plants as a part of their defence mechanism against herbivores. Researchers have been trying to characterize the structures of secondary metabolic compounds, their genomic source and active components present in them mainly for it's use against human diseases as drugs. Bioinformatics help to tackle biological problems by collection, retrieving and submitting data, their analysis, integration and prediction from the data. Plant diseases caused due to both biotic as well as abiotic factors can be traced at genetic level with bioinformatics which aids in developing long term resistance and protection of economically important crops.

Bioinformatics

Bioinformatics is involved in development of database, softwares and algorithms for understanding biological data. It is a combination of molecular biology, computer science and statistics that analyse and interpret biological data. It is involved in collection, distribution and

analysis of biological data. Basic data of bioinformatics not only include nucleic acid and protein sequences and structures but also data of protein – protien and protein - nucleic acid interactions.

Major activities in bioinformatics include sequence comparison, analysis of nucleic acids and proteins, prediction of protein interactions and protein structures. Comparison of sequences in sequence data reveal evolutionary relationship among sequences in the sequence data. Thus it produce meaningful information from biological data using computational techniques. Database projects curate and annotate data that can be retrieved by key word seach. It uses artificial intelligence, soft computing, data mining, image processing and computer simulations to understand biological problems. Bioinformatics actually predict structure from sequence data and function from the structural data of protein.

Bioinformatics is also involved in drug - target identifications, screening and characterisation of side effects of a drug. With genetic sequence alignment it allow identification of novel genes and enable gene expression patterns studies. DNA microarray data analysis allows identification of novel genes and enables gene expression patterns studies. Genome mapping and comparison reveal function of target gene and it facilitate identification of agronomically important genes.

Some of the bioinformatics resources available for various applications in plant science include:

Nucleotide sequences	: Gen Bank, EMBL, DDBJ
Protein sequences (Primary)	: SWISS-PROT, PIR international
Protein sequences (Secondary)	: PROSITE, PRINTS, pfam,BLOCKS, S-BASE
Macromolecular structures	: PDB, NDB, PDBsum,CATH, SCOP, FSSP
Genome Sequence	: Entrez genomes, Ensembl Genomes
Sequence alignment	: BLAST, FASTA, CLUSTA L W, HMMR, PSI-BLAST
Phylogeny	: Phylogeny.fr, fast ME/Phylogene, BLASTO. Dentra UPGMA, PHYLIP
Genome Comparison	: miR Base, MP srch, TIGR, phylo-Vista, CMAP, FISH
Pathway databases	: KEGG, Biocarta, Metacyc
Structure prediction	: APSSP2, PROCLASS, PSA, Beta T pred
3D structure modeling	: Modeller, Mod Base, SWISS –MODEL, PROCHECK
Genefinding	: Genie, GeneFinder, Genscan,GLIMMER
Drug discovery	: BIOGRID, chEMBL, DINIES, DrugBank 3.0
Molecular marker db s	: SSRDB, CMAP, CMTV
Mapping and analysis	: PYPOP, PlabQTL, Blossoc
Protein-protein interaction	: MINT, BIND, DIP, Int Act

Applications of Bioinformatics in plant science

Crop Improvement

Feeding the growing population was a challenge to agriculture and plant biotechnology. Now Bioinformatics is also involved to find solution for this problem. Genomics is providing valuable information for crop improvement. Bioinformatics provides efficient resources of genome data for different plant species and microbes that are economically important. Comparative genomics

have been exploited to compare genome of target species and model organism to identify gene functions and conserved genetic sequences. Sequence alignment and comparison also reveal evolutionary relationship which is really valuable to trace evolution in specific agronomic traits. User friendly access and retrieval of macro molecular databases made its manipulation easier.

Identification of genes, involved in specific responses such as that during drought stress, in submergence tolerance and salt stress, with sequence comparison using software tools such as BLAST and CLUSTAL W help predict possible genes responsible for stress tolerance .Analysing evolutionary relationship provide information about conserved genetic sequences over species or gene families. Specific genes associated with agronomic traits thus identified can be manipulated with genetic engineering. In this way crop improvement for yield, resistance and quality can be achieved.

Gene expression data analysis such as that with microarray has been widely used for large scale genomic expression profiling. It can be applied for the identification of genes involved in specific response to discover genes responsible for specific trait and to find out mutation or evolutionary pattern. In microarray tissue samples are collected that are to be compared .mRNA from test sample and reference is isolated, reverse transcribed , labelled and scanned to identify extend of upregulation or down regulation and for finding genes involved in specific response .1000s of sequences can be analysed at a time. Detection of expression levels is done with the help of scanner which is connected to a computer .Image analysis is done by various bioinformatics tools such as Gene Traffic, Affymetrix"s Gene Chip Operating Software (GCOS), caARRAY (http://caarray.nci.nih.gov/) and Bioconductor (http://www.biconductor.org).

Instead of marker assisted selection (MAS) genomic selection can be proposed. It predict breeding values of lines in a population by analyzing their phenotypes and high density marker scores. It incorporates all marker information in the prediction model unlike that in MAS and avoid biased marker effect estimate.

Development of genetic maps with QT L and linkage dis-equilbrium (LD) mapping help in identification of DNA maikers linked to genes controlling qualitative and quantitative traits .QTL(quantitative trait locus) mapping for agronomically important traits such as yield, quality and resistance is done to identify the regions of genome that effect the trait of interest and to analyze the effect of QTL on the trait. After completion of sequences of Japonica rice genome, molecular marker and genomic resources accelerated researches in isolation of agronomiically important QTLs. Web QTL, Q gene, Rice Gene Thresher, QTL Match maker are some QTL mapping software tools.

NGS (next generation sequencing) technologies enable detailed study of crop genomics. Molecular marker generated by NGS analysis allows us to explore crop evolution. It is the latest method for genomic sequencing and it helps to identify gene related to agronomic traits.

Several genomic sequencing projects involving important crop species have been finished. For example Brassica rapa, eucalyptus, rice, maize, wheat, barley, soyabean, cotton, potato, tomato, cucumber, papaya, apple, date palm, cocoa.

Abiotic and biotic stresses, soil pollution and global climate changes are all threat to crop production. Emergence of bioinformatics and advancement in molecular biology has been contributing much to overcome constraints that limit crop productivity. These techniques revealed inheritance patterns and mechanisms of heterosis and epigenetics. Contextual manipulation of which improves crops yield and quality significantly.

In plants subjected to various stresses, regulatory response is induced, which involve miRNA silencing. Transcriptome analysis enables subsequent target gene identification. For all researches conducted these days bioinformatics is an essential part. Bioinformatics provide methods for mapping and identification of genes of interest. CSRDB (Cereal small RNADB) consist of maize and rice smRNA generated by high throughput pyrosequencing. Plant Omics Data Center is a database for interspecies gene expression networks.

Gramene (http://www.gramene.org) is a comparative genome mapping database for grasses. It comprises genomic data and expressed sequence tags sequences, genetic maps, molecular markers and proteins. UK Crop Net, the UK Crop plant bioinformatics Network provides databases and data mining tools, that are freely accessible through (http://ukcrop.net/) Legume information system (LIS) is a genomic database for the legume family. Blast 2 GO do function annotation and analysis of plant genomes to identify functional regions within DNA sequences.

AutoSNPdb allows Analysis of assembled EST sequence data to identify SNPs associated with functional genes.

Phytochemistry:

Plant extracts are used as remedies since ancient times. Nature is a great resource of medicine for most diseases. People of new generation are not aware of the medicinal plants and their medicinal properties. Likewise those who are aware of medicinal plants have no knowledge about the actual active component present in the plant extract that is responsible for its medicinal properties or its effect against particular disease and in the patient where is it exactly acting upon.

Identification of metabolites from many plant samples is a tedious process. It is important to collect, store and arrange data of phytochemical resources and bioactive compounds present in them and their properties and taxonomic information. Proper collection and access of scattered information about medicinal plants present in different corners of the world aids its proper utilisation. Data may also include genomic or molecular information. HerbMed is an evidence based categorisation of various medicinal plants. PubMed contain bibliography and literatures related to medicinal plants .PathDB store metabolic information and visualization methods

Closely related plant species may share similar biochemical properties and such plants can be identified using phylogenetic analysis and thus new plant resources also can be identified .Basic techniques involved in phytochemistry include collection and identification of plants and extraction of phytochemicals from it. It's qualitative and quantitative analysis involve chromatography which is a unique way of separation of required compound from 1000s of chemicals present in the extract. It also detects adulteration. For characterisation of isolated compounds spectroscopic methods are used. They provide metabolic fingerprints. NMR methods provide metabolic finger prints with good chemical specificity for compounds with elements having non zero magnetic moments such as 1H, 13C, 15N and 32P which are commonly found in most biological metabolites.

Metabolic data are used to construct metabolic correlation networks. Heirarchial cluster analysis is a method of grouping samples based on their similarity. It is done by progressive pairwise grouping of samples.

KEGG database is a collection of online databases dealing with genomes, enzymatic pathways and biological chemicals. KEGG ATLAS provides global map of cell or organism's

metabolism. KEGG genes is a collection of genes and genomes. KEGG pathway has pathway maps representing knowledge on molecular interaction and reaction networks. KEGG ligand contain chemical compound, drug , glycan reaction and enzymes.

KEGG Brite is a collection of heirarchical classification and has taxonomic data oriented collection. KEGG lists enzymes in a specific organism only if a sequence exists in GenBank that is annotated as coding for such an enzyme.

EMP (Enzymes and metabolic pathway db) contains many publications on enzymology and metabolism which are transformed into queriable database. Characterization of isolated compounds by mass spectrometry can be analysed through computer programs to relate structure and function. It has pictorial representation of metabolic pathways. Identification of genomic basis of production and function of plant secondary metabolism can be elucidated by integrated analysis of transcriptomes and metabolomes.

Flux Analyzer integrates metabolic pathway and its flux analysis. The Gene Ontology consortium provides concepts relating to gene function and relationships among them. It describes function with respect to molecular function, cellular component where the product is active and biological process .We can use CellDesigner (http://www.systems-biology.org) for drawing gene regulatory biochemical networks and perform analysis and stimulation.

Molecular docking analysis can be carried out to examine potential protein targets of plant derived secondary metabolites. Computer Aided Drug Design (CADD) uses computational approaches to discover, develope and anaylze drugs or biologically active molecules .The target will be a protein which may be a receptor or enzyme involved in a particular pathway associated with a disease.

With molecular mechanics and scoring function, binding affinity is predicted before a compound is synthesized and thus saves time and cost.

Various tools used in CADD include:

Databases	: PDB, chEMBL, PDB bind, Zinc Database
Homology modelling	: Modeller, SWISS-MODEL, LOMETS
Docking	: Autodock, DOCK, Swiss Dock
Screening	: Blaster, Swiss similarity
Target prediction	:Swiss target prediction, IXCHEL, patch search
QSAR	: Chem DB/Datasets,c QSAR
ADME Toxicity	:Swiss ADME, TOXNET, QikProp

QCAR model use machine learning Techniques to build models and their prediction accuracy is higher than QSAR model

Plant disease management

Plant pathology deals with biotic and abiotic conditions that cause diseases in plants and the mechanisms involved in, interaction between the casual agent and host and disease management. In pathology for disease management important factors that have been exploited include host pathogen interactions, Genetics of host and pathogen, disease genetics and host resistance.

Host-Pathogen interaction is complex process. With molecular biology and bioinformatics techniques the genetic basis underlying host pathogen interaction can be analyzed which aid in designing pesticides or antimicrobials that act accurately at specific sites. Plant pathogens

produce specific protein that enable It's entry and establishment in plant cell. Pathogen produce various enzymes and toxins for this purpose. As a response or before getting attacked plant also have some defence mechanisms that may be a mechanical defense or biochemical defence. Bioinformatics enable better understanding of molecular basis of host-pathogen interaction .It compare and analyze the genomic data and predict possible sites of genetic regulations and aid in better understanding of signalling pathways involved. Complete sequencing and mapping of genome such as that of arabidopsis and one of it's Pathogen Pseudomonas syringae pv tomato DC 3000 enabled improved understanding of genetic basis of interactions between them. Such advanced molecular analyses allow scientist to do their research at a broader level. Potential targets for analyses could be receptors of the host, key enzymes and effectors .The new pesticide or antimicrobial would be specific to target molecule or would interfere with disease cycle or epidemiology . It will minimize the use of many varieties of chemicals. such genetic level analyses also may lead to resistance against broad spectrum of pathogens.

Molecular analysis of host pathogen interaction reveal factors involved in host susceptibility and resistance. Genetic variation that influence disease susceptibility can be designed. Markers that are closer to the disease gene shows correlation with disease patterns. Likewise pathogenicity factors or genes involved in pathogenesis in the genome of a pathogen can be identified with genome comparison.

Identification of microbial virulence factors can be done using DNA microarray data analysis. Computational sources identify virulence factors from their sequence information alone. Pathogenicity is usually encoded by several genes (quantitative). The genetic variability that lead to formation of new races of pathogen is the limitation in creating disease resistant varieties .AnnoTALE- is a tool that allow analysis and annotation of TALE (Transcription activator like effectors) genes from Xanthomonas spp. genome. Comparing related TALEs help identification of mutations responsible for evolution of TALE specificities. As different strains of a pathogen cause different diseases and have different host specificities functional analysis of host specificity also reveal presence of genes involved in entry and establishment of that strain. Different strains can be compared with BLASTP and database for protein-protein interactions and NCBI tool kit scripts like "asn2all".

PPNEMA is a database resource of plant parasitic nematode ribosomal genes to analyze Plant parasitic ribosmal DNA. Microarray allows simultaneous analysis of various pathogens .Antigen based micrarrays can be used to learn host pathogen interactions. Softwares for microarray data analysis include, Flex array, Gene ARMADA, Bioconductor, Maanova & Expander. Other tools for gene expression data analysis include MA Explorer, geneXpress, JMPgenomics, SAM . Pathoplant is a database on plant pathogen interaction and signal transduction reactions prepared using microarray gene expression data from Arabidopsis thaliana subjected to pathogen infection and eliciitor treatment . (http://www . pathoplant .de)

Bioinformatics aid in precise diagnosis and development of small molecules that target virulence gene in pathogen.

(GWAS) Genome-wide association study has been a primary method for identifying genes responsible for diseases and other traits determining alleles associated with various SNPs and make statistical comparison. Association mapping software tools include DCell and EMMAX .

Next generation sequencing is DNA sequencing method by massively parallel processing. It involves generating DNA sequencing libraries, DNA sequencing by synthesis and spatially segregated amplified DNA templates are sequenced simultaneously. Roche 454, GSFLX Titanium, illuminaHiseq, illuminaGenome Analyzer IIX are some of the NGS Platforms. NGS applications in pathology include genome sequencing of pathogen, gene finding, identification and characterization of effectors of pathogens. Identification of genes involved in pathogenesis of broad range of pathogens by comparative genomic analysis aid in creating cultivars resistant to these identified genes.

Conclusion

This review is an attempt to describe some of the bioinformatics applications in plant science which include tools and databases for sequence alignment, sequence comparison, gene expression analysis, pathway analysis and drug designing. Many unresolved problems that exists in life science research can be tackled by data analysis and integration with bioinformatics. Bioinformatics is now an essential part of all scientific researches. It has a major role in reducing world's poverty and improvement in human and animal health.It decrease pollution by reduction of usage of pesticides and fertilizers. It design and discover novel drugs. It continue to change the way biologists do their researches. Thus it made researches fast, specific, accurate, broader and at deeper level.

References

1. Duran C et al (2009). AutoSNPdb: an annotated single nucleotide polymorphism database for crop plants. *Nucleic Acid Res* 37:D951-D953
2. Botero, David et al(.2018) "Network Analyses in Plant Pathogens" *Frontiers in microbiology* . 9 35.
3. Simhadri Vsdna, Nagesh et al.(2017) "Phytochemical analysis and docking study of compounds present in a polyherbal preparation used in the treatment of dermatophytosis" *Current medical mycology* 3(4) : 6-14.
4. Geromichalos, George. (2007). Importance of molecular computer modeling in anticancer drug development. 2nd seminar of the Balkan School of Oncology (BSO) , Suppl 1:S101-18
5. Pérez-de-Castro, A M et al.(2012) "Application of genomic tools in plant breeding" *Current genomics* vol. 13.,3 : 179-95.
6. Okii D, Chilagane LA, Tukamuhabwa P, Maphosa M (2014) Application of Bioinformatics in Crop Improvement: Annotating the Putative Soybean Rust resistance gene *Rpp3* for Enhancing Marker Assisted Selection. *J Proteomics Bioinform* 7:001-009.
7. Rhee SY et a(l 2006).. bioinformatics and its applications in plant biology. *Annu Rev Plant Biol*. 257:335-60
8. Kumar, Anil et al. (2015) "Systems Biology for Smart Crops and Agricultural Innovation: Filling the Gaps between Genotype and Phenotype for Complex Traits Linked with Robust Agricultural Productivity and Sustainability" *Omics : a journal of integrative biology* 19(10): 581-601.

9. King GJ, Bioinformatics: harvesting information for plant and crop science. *Semin Cell Dev Biol*. 2004 Dec;15(6):721-31.

10. Matthews DE, Lazo GR, Anderson OD (2009).Plant and crop databases.*Methods Mol Biol*. 513:243-62.

11. Mochida, Keiichi and Kazuo Shinozaki.(2010) "Genomics and bioinformatics resources for crop improvement" *Plant & cell physiology* . 51,4 : 497-523.

12. Dicks, J et al. (2000) "UK CropNet: a collection of databases and bioinformatics resources for crop plant genomics" *Nucleic acids research* . 28,1 : 104-7.

13.Ghosh A, Mehta A.(2017) Concept, Development, and Application of Computational Methods for the Analysis and Integration of Omics Data. *Plant Bioinformatics*, Springer.

14. Shah, Tariq et al.(2018) "Omics Approaches for Engineering Wheat Production under Abiotic Stresses" *International journal of molecular sciences* 19,8 2390 .

15. Hong, Jun et al.(2016) "Plant Metabolomics: An Indispensable System Biology Tool for Plant Science" *International journal of molecular sciences* 17:6 767.

16. Batley J, Edwards D (2016) The application of genomics and bioinformatics to accelerate crop improvement in a changing climate. *Curr Opin Plant Biol* 30:78-81

17. Nadella K D et al.(2012) Metabolomics in agriculture.OMICS. ;16(4):149-59.

18. Zang P, Foerster H, Tissier CP, Mueller L, Paley S, Karp PD, Rhee SY (2005) MetaCyc and AraCyc. Metabolic pathway databases for plant research Plant Physiol 138:27-37.

19. Winkel-Shirley B (2001) Flavonoid biosynthesis. A colorful model for genetics, biochemistry, cell biology and biotechnology. *Plant Physiol* 126:485-493.

20. Jha U.C, Bhat J.S, Patil B.S, Hossain F, Barh D. (2015) Functional Genomics: Applications in Plant Sceince. In: Barh D, Khan. M, Davies E. (eds) PlantOmics: The Omics of Plant Science. Springer.

22. Walls, Ramona L et al. (2012)"Ontologies as integrative tools for plant science" *American journal of botany* . 99(8) : 1263-75.

23. Sharma, Vivekanand and Indra Neil Sarkar.(2012) "Bioinformatics opportunities for identification and study of medicinal plants" *Briefings in bioinformatics* 14,2 : 238-50.

25. Techen N, Parveen I, Pan Z, Khan IA.(2014) Curr Opin Biotechnol. 25:103-10.

26 Rai A et al.(2017) integrated omics analysis of specialized metabolism in medicinal plants. *Plant J.* ;90(4):764-787.

27 Sharma S, Shrivastava N.(2016).Renaissance in phytomedicines: promising implications of NGS technologies. *244(1):19-38.*

28. Mendes Pedro(2002); Emerging bioinformatics for the metabolome, *Briefings in Bioinformatics*, 3 (2): 134–145.

29. Wittig,U. and De Beuckelaer,A. (2001) Analysis and comparison of metablic pathwaydatabases. *Briefings in Bioinformatics*, 2, 126– 142

30. International Human Genome Sequencing Consortium (2001) Initial sequencing and analysis of the human genome. *Nature*, 409, 860–921

31. Sharma V, Sarkar IN (2013) Bioinformatics opportunities for identification and study of medicinal. *Briefings in Bioinformatics* 14.2:238.

29. Rabbani, M Ashiq et al(2003). "Monitoring expression profiles of rice genes under cold, drought, and high-salinity stresses and abscisic acid application using cDNA microarray and RNA gel-blot analyses" *Plant physiology* . 133,4 : 1755-67.

30. *Brown PO, Botstein D (1999).Exploring the new world of the genome with DNA microarrays. Nat Genet. 21 (1): 33-37*

31. Wullschleger S D. and Difazio S P.(2003). Emerging use of gene expression microarrays in plant physiology *Comp FunctGenom.* 4: 216–224.

32. Xue, J., Zhao, S., Liang, Y., Hou, C. and Wang J. (2008) Bioinformatics and its Applications, *Computer and Computing Technologies in Agriculture* 2: 977–982.

33. Close TJ, Bhat PR, Lonardi S, Wu Y, Rostoks N, Ramsay L, et al.(2009). Development and implementation of high-throughput SNP genotyping in barley. *BMC Genomics*. 10:582.

34. Grau, Jan et al(2016). "AnnoTALE: bioinformatics tools for identification, annotation, and nomenclature of TALEs from Xanthomonas genomic sequences" *Scientific reports* . 6. 21077.

35. Mendes,P. et al. (2000) PathDB: a second generation metabolic database. In BTK 2000 (Minibook). pp. 207–21

36. Xenarios,I. et al. (2002) DIP, the database of interacting proteins: a research tool for studying cellular networks of protein interactions. *Nucleic Acids Res*., 30, 303–305.

37. Altschul,T.L. et al. (1997) Gapped blast and psi-blast: a new generation of protein database search programs. Nucleic Acids Res., 25, 3389–3402

38. Bork,P. et al. (1998) Predicting function: from genes to genomes and back. *J. Mol. Biol*., 283, 707–725

39. Van, K.; Rastogi, K.; Kim. K.H; Lee. S.H (2013) Next - Generation Sequencing Technology for Crop Improvment. *SABRAO Journal of Breeding & Genetics* 45(1):84-99

40. U Kushwaha et al.(2017) role of bioinformatics in crop improvement. *global journal of science frontiers research 17(1):13-23*

41. Klosterman S J, Rollins JR, Sudarshana M R, Vinatzer B A(2016) Disease Management in the Genomics Era—Summaries of Focus Issue Papers .*Focus Issue* 106(10): 1068-1070

42. Hagen JB (2000) The origins of bioinformatics.Nat Rev Genet;1(3):231-6.

43.Maudsley S,Chadwick W,Wang L, Zhou Y, Martin B, Park SS.(2011)Bioinformatics Approaches to Metabolic Pathways Analysis.In:Luttrell,Ferguson S,(eds) Signal Transduction Protocols. *Methods in Molecular Biology*(Methods and Protocols)756;99-130.

44. HeffnerE L et al,(2009).Genomic selection for crop improvement.*crop science* 49(1)1-12

45. Varshney R K,Graner A,Sorrels M E (2005).Genomics -assisted breeding for crop improvement.*Trends in plant science* 10(12):621-630

16.

ROLE OF PHYTASE IN THE PLANT BASED DIETS OF CATLA CATLA TO IMPROVE THE PROTEIN AND PHOSPHATE UTILIZATION

Savitha Nandanan* & Monisha.K.M
Department of Zoology, Sree Narayana College
Nattika, Thrissur - 680566, Kerala, India.
E-mail: savitha331@gmail.com

Abstract *Feed constitute one of the major input cost associated with aquaculture and is also the first source of pollutants released into the environment. The replacement of fish meal with plant derived diets supplemented with phytase will lead to cost effective solution for aquaculture feed. In this study Catla catla is taken as the experimental organism which is fed with plant based feed containing different concentrations of phytase. As the concentration of phytase increased, the protein content, protein digestibility and phosphate utilization of the fish found to be enhanced by releasing phosphate and proteins chelated to the phytate in the feed.*

Key words *Catla catla* , phytate, phytase, protein digestibility & phosphate excretion.

Introduction

Fishes are most fascinating and remarkable form of animal life in the world. The nutritive status of the fish is equal to or even higher than that of poultry, mutton and beef. Sustainability in aquaculture is constrained by various economic and environmental factors. Feed constitute one of the major input cost associated with aquaculture and is also the first source of pollutants released into the environment. Fish meal is one of the most important components of fish diet but its usage is restricted due to high cost (Baruah *et.al.,* 2004). Combination of rice bran and wheat is most preferable plant diet in aquaculture due to high phosphate and protein content. But major constraints that limit use of plant diet is the presence of anti-nutritional factor such as phytate or phytic acid (Jayant Ranjan 2014).

Phytate is the major phosphorous storage compound in plant derived feeds and can account for upto 80% of total phosphorus. Because of the high density phosphate group, phytate chelate with mineral cations like potassium, magnesium, calcium, zinc and iron. Apart from minerals, phytate also complexes with protein and amino acids. The phytate bound phosphorous limit the protein digestibility of fishes due to lack of intestinal phytase. Phytate phosphorous is excreted into the environment and acted upon by the micro organism that release phosphorus, causing eutrophication and algal blooming impairing water quality. Microbial phytase supplementation to the diet can overcome this problem. It make the chelated phosphate available to fish and hence there is less faecal phosphate excretion and there by reduces pollution. Since phytase release minerals and proteins chelated to the phytate, it enhances the utilization of proteins and minerals by fishes. Use of phystase in feed reduces the necessity of mineral supplementation, which also decrease the cost of feed. The replacement of fish meal with plant derived meals supplemented with phytase will lead to cost effective solution for aquaculture feed. In this study *Catla catla* is taken as the experimental organism which is an economically important south asian fresh water fish coming under carp family *Cyprinidae*.

Materials and Methods

Experimental diets were formulated using plant based ingredients such as wheat and rice bran. Different concentrations of phytase enzyme (.5,1,1.5&2g phytase per 100g wheat and rice bran mixture) are added to respective 4 bowls. The control diets were formulated with same ingredient of wheat and rice bran without phytase. *Catla catla* fingerlings were collected and fishes were divided into 5 groups. First group was labelled as control or T_0 diet and 2nd, 3rd, 4th and 5th groups are supplemented with phytase of different concentration (.5,1,1.5& 2g) were labelled as T_1, T_2 ,T_3, T_4 diets respectively.

One fish from each group were selected randomly for protein analysis. Then muscle tissue were collected carefully without including remnants of scales and skin. The homogenized tissue along with sucrose solution were subjected to centrifugation at 3000 rpm for 10 minutes. After centrifugation, supernatant is discarded and the sediment was dissolved in 0.1N NaOH solution. This solution is used as sample for the study. Then total amount of protein present in sample was estimated using Lowry method.

To calculate protein digestibility, fecal matters were collected after feeding trial and immediately transformed into bolting paper to remove water. Then homogenized and centrifuged at 3000 rpm for 10 minutes and the residue was taken for protein analysis. Similarly protein content of test diets were also determined by the Lowry method. Then protein digestibility can be determined by using the formula.

Apparent protein digestibility = Protein content in diet - Protein content in faecal matter

To estimate phosphate excretion standard solution was prepared by dissolving 136mg KH_2PO_4 in 100ml distilled water. Mixed reagent was prepared by mixing Ammonium molybdate solution, 5N Sulphuric acid, Ascorbic acid, Potassium antimonyl tartarate in the ratio 5:2:1:1. Label 3 test tubes as sample, standard and control. Then add 1ml water sample from rearing tub to sample, 1ml standard stock solution to standard and 1ml distilled water to control. Then add 1ml mixed regent to each test tubes mix well. After 15 minutes optical density of solution were measured in colorimeter at 690nm. By using this procedure phosphate content in each rearing tubs were estimated by following formula.

$$\text{Concentration of phosphate} = \frac{\text{OPTICAL DENSITY OF SAMPLE}}{\text{OPTICAL DENSITY OF STANDARD}} \text{ X Con. of std}$$

Result and Discussion

Phytase releases the phytate bound proteins and aminoacids hence phytase supplemented diets provide high protein availability. Protein content of *Catla catla* found to be increasing with increasing phytase concentration in the feed. Maximum protein found to be in T_4 diet is 6.15 mg/g and minimum protein observed in control diets T_0 without supplemented phytase is 1.56 mg/g. This shown that phytase enzyme increases the bioavailability of aminoacid from the diets. Variation in protein content due to phytase activity is 1.56 mg/g, 1.58 mg/g, 2.35 mg/g, 4 mg/g, 6.15 mg/g in T_0, T_1, T_2 ,T_3, T_4 diet fed fishes respectively (Graph-1).

Apparent protein digestibility of the diets were significantly improved by phytase supplementation. It found to be 12.27mg/g in T_4 diet supplemented with highest phytase supplementation, while without enzyme supplemented group showed a low

protein digestibility and is found to be in T_0 diet s 7.03mg/g. This is confirming the established properties of phytate to form phytate protein complexes that are resistant to proteolytic digestion. Phytase supplementation in plant based diets has been reported to increase protein digestibility with increasing concentration of phytase. These results shows that phytase has positive effect on protein digestibility. It found to be 7.03 mg/g, 9.92 mg/g, 10.32 mg/g, 11.49 mg/g, 12.27 mg/g in T_0, T_1, T_2, T_3, T_4 diet fed fishes respectively (Graph-2).

Phytase supplemented into the diet make chelated phosphate available to fish and there is less feceal phosphate excretion and reduce environmental pollution. In this study *Catla catla* had shown reduced phosphate excretion in T_4 diet. It found to be 1mg/L water, while increased excretion rate was reported in the control diet i.e 6.5mg/L water, without supplemented with phytase. Rate of phosphate excretion during phytase supplementation found to be decreased from 6.5 mg/L, 3 mg/L, 2.5 mg/L, 1.5 mg/L to 1 mg/L in T_0, T_1, T_2, T_3, T_4 diet fed fishes respectively (Graph-3).

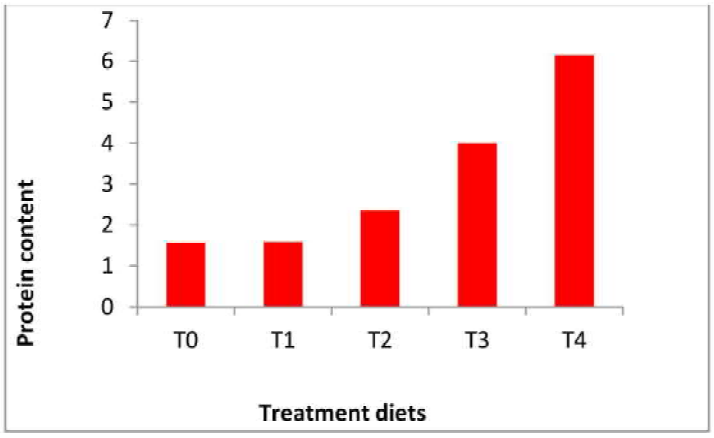

Graph-1 : Bar diagram showing the effect of phytase on protein content

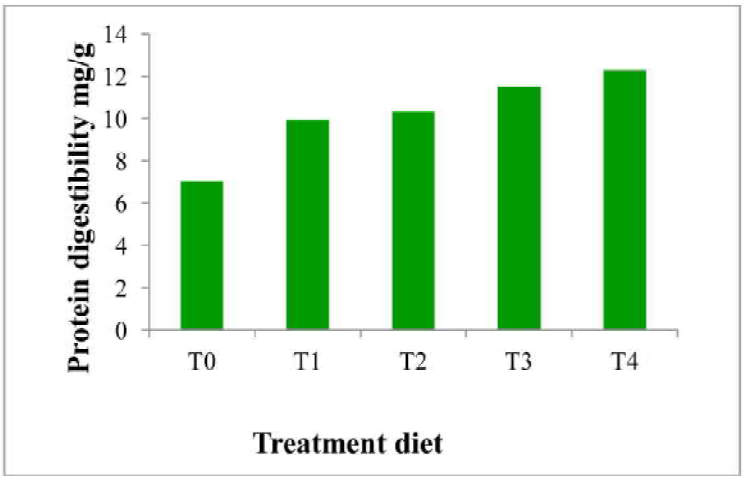

Graph-2 : Bar diagram showing fluctuation in protein digestibility during phytase supplementation

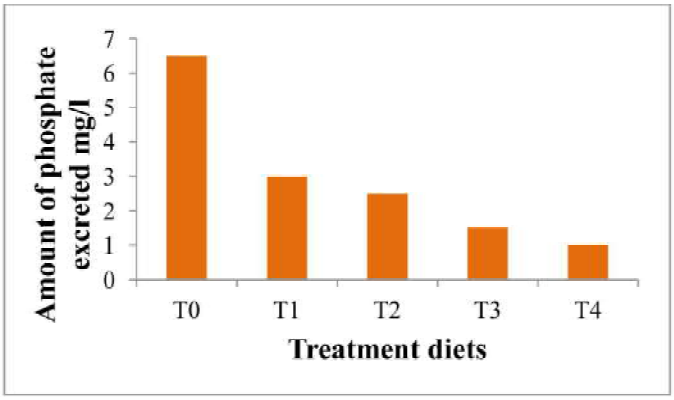

Graph-3 : Bar diagram showing rate of phosphate excretion during phytase supplementation

Protein content and protein digestibility of phytase fed *Catla catla* fingerlings were found to be increasing with increasing phytase concentration. This due to more phytase bound portein is available to fish during feeding trial because of activity of phytase. Similar findings were reported by many authors (Yan and Reigh, 2002; Portz and Liebert, 2009; Debnath *et.al.,*2005). Phosphorus loadings reduced in the rearing water with increase in phytase levels. This means that more phosphate was absorbed by the fish which consequently control pollution in fish culture systems. Sugiura, *et.al.,* (2001) and Jahan *et.al.,* (2003) reported that excretion of phosphorous in the faeces of fish fed plant based phystase contain meal was effectively reduced . The present study also revealed similar observations.

Conclusion

Expanded aquaculture production demand more fish feed which will require higher qualities of alternate protein sources to substitute fish meal. Demand of plant based meal in aquaculture is increasing due to their availability and comparatively lower cost, compared to fish meal. There is a need to boost awareness among the fish feed manufacturing industry and fish nutritionists on the use of phytase as an effective and efficient approach in the formulation of cost effective, growth promoting and low polluting fish feed based on plant protein sources, for profitable , and sustainable aquaculture production.

References

1. Baruah K.N, Sahu A.K, Paland, Debanath D, Dietary Phytase: An ideal approach for a cost effective and low-polluting aquafeed, *Naga*, 2004; 27(3):15-19.
2. Debnath D, Pal A.K, Narottam P.S, Jain K.K, Effect of dietary phytase supplementation on growth and nutrient digestibility of *Pangasius pangasius* fingerlings, *Aquaculture* 2005; *36:180-187.*
3. Jahan P, Watanbe T, Kiron, Satoh, Improved carp diets based on plants protein sources reduce environmental phosphorous loading, *Fisheries science*,Tokyo , 2003; 69:219-225.
4. Jayanth Ranjan, Dietary phytase an ideal approach for sustainable aquaculture, *Fishing Chimes* ,2014; 23:112-115.

5. Portz L and Liebert L, Growth nutrient utilization and parameter of mineral metabolism in nile thilapia *Oreochromis niloticus* fed plant diets with graded level of microbial phytase. *J. Anim. Physiol*, 2009; 88:311-320.
6. Sugiura S. H, Gabaudan J, Dongand F. M, Hardy R. W, Microbial phytase supplementation and utilization of phosphate minerals and protein by rainbow trout fed soyabean meal based diets. *Aquaculture*, 2001; 32:583-591
7. Yan W and Reigh R.C, Effect of fungal phytase on utilization of dietary protein, minerals and dephosphorylation of phytic acid in alimentary tract of channel catfish *Zctulurus puntutus* fed with plant protein diet *J.world aquaculture societies*,2002; 33:10-22.

PHYSICAL EDUCATION

17.

THE IMPACT OF BMI ON VO_2 MAX

Dr. Sujoy Birbanshi[1]
sujoybappa@gmail.com
[1]Govt. approved P.T.T. in Physical Education, Department of Physical Education
Vivekananda Satavarshiki Mahavidyalaya, Manikpara, Jhargram, West Bengal, India

Abstract: *The purpose of the present investigation was to determine the relation between BMI & maximum oxygen uptake or VO_2 max of house wives. A total of 70 house wives in between the age of 30 to 48 years were selected randomly from different region of different districts of West Bengal in this study group. Body mass index was measured as weight in kilograms divided by height in meters squared (kg/m^2). The maximum oxygen uptake or VO_2 max was assessed by using Queen' college step test. The collected data were calculated by using descriptive statistic and Coefficient of Correlation "r" and level of significance was set at 0.05 levels. Data was analysed using SPSS Version 20.0 (Statistical package for the social sciences, version 20.0, SPSS Inc, Chicago, IL, USA).There was a significant negative correlation between body mass index (BMI) and VO2max (ml/kg/min) ($r = -0.1672$, $p<0.05$). "Journal of Sports Medicine and Physical Fitness," high BMI measurements are linked to lowered VO_2 max values. The role BMI plays in reducing VO_2 max is related to changes in respiratory capacity and cardiovascular endurance. Increased BMI levels have also been associated with decreases in cardiovascular system capacity (Warren Rosenberg, 2017).*

Key words: - VO2 Max; Maximum Oxygen Uptake; House Wives; BMI

I. Introduction

`To determining fatness the most common method is calculating body mass index (BMI). Body mass index (BMI) is a measure of relative size based on the mass and height of an individual. BMI values are age-independent and the same for both sexes. However, BMI may not correspond to the same degree of fatness in different populations due to different body proportions. BMI is a simple, inexpensive and non-invasive surrogate measure of body fat.[1] BMI was designed to be used as a simple means of classifying average sedentary (physically inactive) populations, with an average body composition.[6] VO_2 max is a measure of the maximum amount of oxygen that your body can consume during maximum workload. The ability of your respiratory system to take in large volumes of air and the ability of your heart and blood vessels to transport oxygen from your lungs to your muscles both contribute to your VO_2 max.[8] According to "Journal of Sports Medicine and Physical Fitness," high BMI measurements are linked to lowered VO_2 max values. The role BMI plays in reducing VO_2 max is related to changes in respiratory capacity and cardiovascular endurance.[8]

Objective of the study: The objective of this study was to determine the relationship between maximum oxygen uptake or VO_2 max and body mass index of house wives.

II. Materials and Methods

Subjects: The study was conducted on 70 house wives, ranging the age between 30 and 48 years.
Study Area: The subjects were chosen from different districts namely, Birbhum, Bardhaman and West-Medinipur of West-Bengal, India.

Criterion Measures: The measurements of the weight and height were done with digital weighting scale (Pounds and kg) and stadiometer (cm). BMI was calculated from body weight and body height (kg/m^2). The maximum oxygen uptake or VO_2 max was assessed by using Queen' college step test (ml/Kg/min).

Statistical Technique: For determining the relationship of VO_2 Max and BMI of house wives descriptive statistics and Pearson's product moment correlation test was used, the data analysed with the help of SPSS (20.0 version) software and the level of significance was set at 0.05.

III. Findings and Result

The descriptive statistics of personal data and selected parameters of mid-age subjects is presented in Table I:

Table- I
Descriptive Statistics of Selected Parameters

Parameters	Mean	Std. Deviation
Age (Years)	36.86	5.04
Height (cm)	153.94	6.36
Weight (kg)	58.55	10.27
VO2max (ml/Kg/min)	35.33	1.75
BMI (kg/m^2)	24.69	4.03

Figure 1
Graphical representation of Selected Parameters

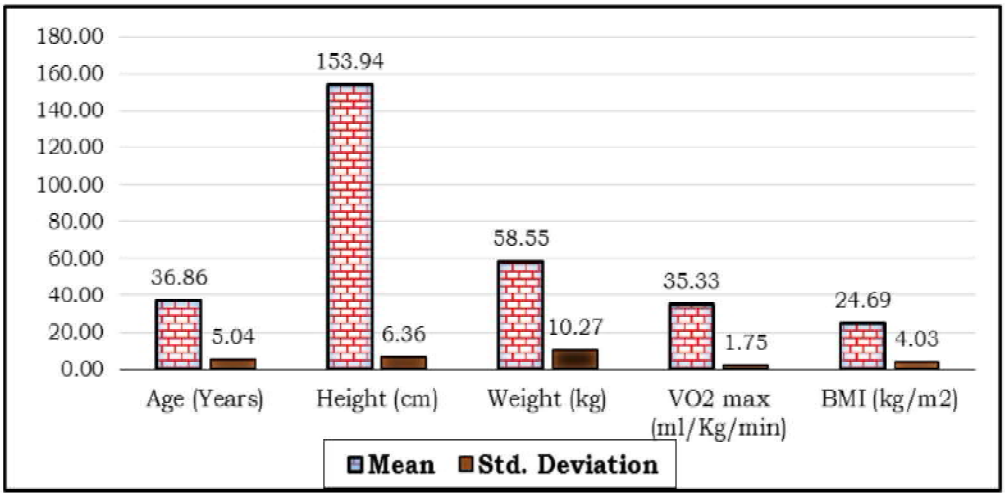

Table-I and Figure-1depicts that the mean and standard deviation of scores in selected parameters height, weight, VO_2 max and BMI of house wives subjects were 153.94±6.36 centimetres, 58.55±10.27 kilograms, 35.33±1.75 ml/Kg/min and 24.69±4.03 kg/m^2 respectively.

Table- 2

Histogram

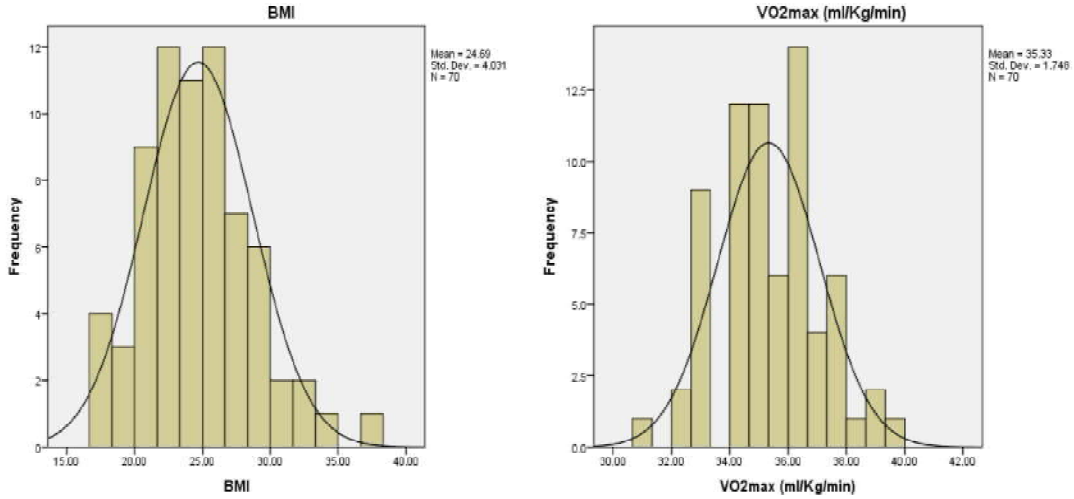

Table- 3
Relationship between Selected Parameters

Parameters	Mean	Standard Deviation	Coefficient of Correlation 'r'
BMI ($kg.mt^2$)	24.69	4.03	-0.1672
VO2max (ml/Kg/min)	35.33	1.75	

The value of R is -0.1672. Although technically a negative correlation, the relationship between parameters is only weak.

V. Conclusion:

Within the limitation of the present study and on the basis of findings of the result of the study, it may be concluded that there is a significant negative correlation found between BMI and VO_2 max (ml/kg/min) suggesting the possibility of effect or body fat on cardiorespiratory function.

Reference

1. By The MNT Editorial Team Last updated Tue 5 January 2016 https://www.medicalnewstoday.com/info/obesity/what-is-bmi.php
2. Blackburn H, Jacobs D (June 2014). "Commentary: Origins and evolution of body mass index (BMI): continuing saga" (PDF). International Journal of Epidemiology. 43 (3): 665–9. doi:10.1093/ije/dyu061 Freely accessible. PMID 24691955.
3. Jeremy Singer-Vine (July 20, 2009). "Beyond BMI: Why doctors won't stop using an outdated measure for obesity". Slate.com. Archived from the original on 7 September 2011. Retrieved 15 December 2013.
4. Keys A, Fidanza F, Karvonen MJ, Kimura N, Taylor HL (July 1972). "Indices of relative weight and obesity". Journal of Chronic Diseases. 25 (6): 329–43. doi:10.1016/0021-9681(72)90027-6. PMID 4650929.
5. Warren Rosenberg , How Does BMI Affect VO2 Max? Last Updated: Jul 18, 2017 https://www.livestrong.com/article/356265-how-does-bmi-affect-vo2-max/
6. "Physical status: the use and interpretation of anthropometry. Report of a WHO Expert Committee" (PDF). World Health Organization Technical Report Series. World Health Organization. 854: 1–452. 1995. PMID 8594834. Archived (PDF) from the original on 2007-02-10.
7. https://en.wikipedia.org/wiki/Body_mass_index
8. https://www.livestrong.com/article/356265-how-does-bmi-affect-vo2-max/#

Mampad College P. O., Malappuram Dist., Kerala, India - 676 542
mesmacconferences@gmail.com | info@mesmampad.org
www.mesmampad.org